

A STUDY ON THE EFFECTS OF LEAKAGE
FOR SCALED-DOWN BRAKEPIPE MODEL



Andrew Kwong-cheung Ho

A Research Thesis

in

The Faculty

of

Engineering

Presented in Partial Fulfillment of the Requirements
for the Degree of Master of Engineering at
Concordia University
Montréal, Québec, Canada

© Andrew K.C. Ho, 1982

ABSTRACT

Andrew Kwong-cheung Ho

A STUDY ON THE EFFECTS OF LEAKAGE
FOR SCALED-DOWN BRAKEPIPE MODEL

Experimental investigation and theoretical analysis of a scaled-down brakepipe model are presented in this research thesis. Two analytical methods (the method of characteristics and the method of lumped analog component) have been proposed to study the effects of leakage for the brakepipe model. The major field of work is to study the relation between signal propagation velocity and brakepipe leakage. Detailed mathematical models with computer simulation for generating pressure distribution along the brakepipes were developed for both methods. The method of lumped analog component (lumped modeling) was easier to apply than the method of characteristics. It was proved that the modified approach of using a pressure chamber instead of a pneumatic pressure relay valve was in close agreement and could therefore simplify the testing procedures. Simple experiments on the brakepipe model were performed to compare with the analytical methods. It was shown that the effects of leakage on the pressure gradient, distribution and propagation speed depended on the locations and sizes of the leaks. We found that during the transient response of a pressure signal in a brake pipe the propagation factor affected the output magnitude such that a longer time delay and lower propagation speed were shown.

ACKNOWLEDGEMENT

The author is very grateful to his supervisors, Dr.S. Katz and Dr.R.M.H. Cheng for their excellent guidance, suggestions and moral support throughout this research and the writing of this thesis..

He would like to acknowledge Concordia University for the facilities provided through the Fluid Control Research Centre, where this work was conducted.

Many thanks are due to Mr. John Elliot and Mr. Rock Lee for their assistance during the experimentation.

Thank you, God, for the many blessings You give me.

Also, thanks to my parents and sisters, and my friends for their encouragement and support throughout my graduate studies.

TABLE OF CONTENTS

	Page
ABSTRACT	iii
ACKNOWLEDGEMENT	iv
TABLE OF CONTENTS	v
LIST OF FIGURES	viii
LIST OF TABLES	xii
NOMENCLATURE	xiii
CHAPTER 1 INTRODUCTION	
1.1 ROLE OF THE BRAKEPIPE IN THE OPERATION OF THE AUTOMATIC BRAKE SYSTEM OF A FREIGHT TRAIN	1
1.1.1 PRINCIPLE OF AIR BRAKE OPERATION OF A FREIGHT TRAIN	2
1.1.2 DESCRIPTION OF THE BRAKEPIPE	6
1.2 USE OF PRESSURE CHAMBER TO REPRESENT THE RELAY VALVE	10
1.3 REVIEW OF PREVIOUS WORKS	18
1.4 SCOPE OF THESIS	20
CHAPTER 2 FORMULATION OF EQUATIONS FOR THE BRAKEPIPE MODEL BY THE METHOD OF CHARACTERISTICS	
2.1 INTRODUCTION	23
2.2 MATHEMATICAL MODEL	24
2.2.1 MODIFIED APPROACH- WITH PRESSURE CHAMBER	24
2.2.2 BRAKEPIPE LEAKAGE	34
CHAPTER 3 FORMULATION OF EQUATIONS FOR THE BRAKEPIPE MODEL BY LUMPED MODELING	
3.1 INTRODUCTION	37
3.2 MATHEMATICAL MODEL	37
3.2.1 COMPONENTS	37
3.2.2 TRANSIENT RESPONSE	42

	Page
CHAPTER 4	EXPERIMENTAL INVESTIGATION AND DISCUSSION
4.1	INTRODUCTION
4.2	PRESSURE-FLOW CHARACTERISTICS ON THE PIPE-BEND COMBINATIONS
4.2.1	PIPE TEST SET-UP
4.2.2	PIPE-BEND COMBINATION TEST AND RESULT
4.3	PRESSURE-FLOW CHARACTERISTICS ON ORIFICE
4.3.1	ORIFICE TEST SET-UP
4.3.2	ORIFICE TEST AND RESULT
4.4	SCALED-DOWN BRAKEPIPE MODEL
4.4.1	MODEL TEST SET-UP
4.4.2	BRAKEPIPE MODEL TESTS AND RESULTS
4.4.2.1	PRESSURE GRADIENT TEST AND RESULT
4.4.2.2	PRESSURE REDUCTION TEST AND RESULT
4.4.2.3	DISCHARGE TEST AND RESULT
4.4.2.4	CHARGE TEST AND RESULT
4.4.2.5	EVALUATION OF TIME DELAY
4.5	DISCUSSION
4.5.1	COMPARATIVE STUDIES ON BRAKEPIPE MODEL
4.5.1.1	PRESSURE REDUCTION
4.5.1.2	DISCHARGE WITH LEAKAGE ORIFICES
4.5.2	EFFICIENCY OF METHODS
4.5.2.1	MESH SIZE
4.5.2.2	EFFECT OF LUMPING
4.6	SUMMARY

	Page
CHAPTER 5	SIGNAL PROPAGATION VELOCITY
5.1	INTRODUCTION 102
5.2	EVALUATION OF PROPAGATION SPEED IN BRAKEPIPE MODEL 105
5.3	TRANSIENT RESPONSE OF THE BRAKE PIPE MODEL 115
5.4	EFFECT OF LEAKAGE ON THE PROPAGATION SPEED 120
CHAPTER 6	CONCLUSION
6.1	SUMMARY 126
6.2	SUGGESTION FOR FURTHER WORK 128
REFERENCES	130
APPENDIX A	DERIVATION OF EQUATIONS 134
APPENDIX B	COMPUTER PROGRAMS 141
APPENDIX C	DYNAMIC CHARACTERISTIC OF THE RELAY VALVE 185
APPENDIX D	PREDICTION OF BRAKEPIPE PERFORMANCE OF A FREIGHT TRAIN 192

LIST OF FIGURES

Figure		Page
1.1	Schematic illustration of the air brakepipe system	3
1.2	Sectional view of a relay valve	11
1.3a	Schematic drawing of the relay valve in the experiment of displacement of diaphragm due to pressure force . .	13
1.3b	Characteristic of a relay valve: exhaust valve area vs. pressure difference . .	15
1.4	Characteristic of a relay valve: effective combined area vs. pressure difference	17
2.1	Modified configuration of brakepipe . . .	25
2.2	Characteristic grid for large-amplitude signals	28
3.1a	Simplified brakepipe model	38
3.1b	Lumped parameter model	38
4.1a	Test set-up for calibration	49
4.1b	Result of transducer calibration	49
4.2	Set-up for pressure-flow characteristic on pipe-bend combination	50
4.3	Mass-flow characteristics of the pipe- bend combination	53
4.4	Data distribution chart	54
4.5	Set-up for the orifice test	56
4.6	Pressure-flow characteristics of the orifices	58

Figure	Page
4.7a A photo of brakepipe model	59
4.7b Schematic drawing of brakepipe model . .	60
4.8 Piping diagram	63
4.9 Steady state pressure gradient curves .	67
4.10 Steady state pressure vs. leak location curves	70
4.11 Pressure reduction on first pipe with plumbing leakage and different d_e	72
4.12 Pressure reduction for brakepipe model with plumbing leakage and $d_e/d=0.22$	73
4.13 Discharge curves due to 15 leakage orifices of 0.33mm in diameter	75
4.14 Discharge to tank with $d_e/d=0.22$ from 75 pipe-bend combinations with 15 leakage orifices along the brakepipe	76
4.15 Pressure drop at first pipe with brake- pipe leakage and different tank orifice d_e	78
4.16 Discharging time vs. leak location curves	79
4.17 Air flow into an 1737cc tank from the pipes with plumbing leakage	80
4.18 Air flow into an 1737cc tank from the pipes with 15 leakage orifices along brakepipes	82
4.19 Brakepipes are recharged with plumbing leakage	84

Figure		Page
4.20	Brakepipes are recharged with 15 leakage orifices	85
4.21a	Time delay in pressure reduction	87
4.21b	Time delay curves	89
4.22	Time delay vs. leak location curves	90
4.23	Total time taken for the last pipe at steady state with different mesh sizes	95
4.24	CPU times for method of characteristics	96
4.25	Total time taken for the last pipe at steady state with different number of lumps	98
4.26	CPU times for lumped modeling	99
5.1	One-dimensional linearized brakepipe model	106
5.2a	Speed of propagation in the brakepipe model	110
5.2b	Effect of leakage on propagation speed	111
5.3a	Attenuation-phase ratio in brakepipe model	113
5.3b	Normalized attenuation vs. frequency with leakage as a parameter	114
5.4	Transient response of a semi-infinite brakepipe	129
5.5	Propagation speed curves	122
5.6	Propagation speed vs. leak position	124
A1	Show the characteristic lines and points	134
A2	Pipe flow	137

Figure	Page
C1 Nonlinear system-- charging process	188
C2 Nonlinear system-- discharging process	191
D1 Brakepipe pressure with B.P.=552kPa during 41kPa B.P. reduction, 150-car train	193
D2 Brakepipe pressure with B.P.=552kPa during 41kPa B.P. reduction, 150-car train by lumped modeling	194
D3 Brakepipe pressure with B.P.=552kPa during 103kPa B.P. reduction, 150-car train by method of characteristics	195
D4 Brakepipe pressure with B.P.=552kPa during 103kPa B.P. reduction, 150-car train by lumped modeling	196
D5 Pressure change in the chamber	198

LIST OF TABLES

Table	Page
4.1 Specification for brakepipe model	61
4.2 Tubing connection	64
4.3 Model condition for plumbing	66
4.4 Time delay vs. leakage orifice size	88
5.1 Young's modulus & Poisson's ratio for pipe materials	108
5.2 Propagation speed vs. leakage size	121

NOMENCLATURE

a	Local speed of sound, m/s
a_f	Reference sonic velocity, m/s
a_p	Normalized signal variable
A_E	Effective exhaust area, mm^2
A_e	Exhaust orifice area between chamber and first pipe, mm^2
A_1	Cross section area of brakepipe, mm^2
A_{oi}	Orifice area at i^{th} pipe, mm^2
B_j	Pressure ratio
C	Arbitrary constant
C_d	Discharge coefficient
c_0	Fluid sonic speed, m/s
d	Diameter of brakepipe model, mm
d_{oi}	Diameter of leakage orifice at i^{th} pipe, mm
d_e	Diameter of exhaust orifice between chamber and first pipe, mm
d_e/d	Non-dimensional diameter of leakage orifice
E	Young's modulus of material, kPa
e	Wall thickness of brakepipe, mm
f	Friction factor
G	Line leakance, $\text{m}^2\text{-kg/kN-s}$
g_c	Gravitational constant, kg-m/N-s^2
K'	Friction number, $f1/2d$
K_a	Bulk modulus of air, kPa(abs.)

K_i	Linearized resistance constant, $\text{kN}\cdot\text{s}/\text{m}^2\cdot\text{kg}$
K_2	Resistance constant for turbulent-compressible $\text{kN}^2\cdot\text{s}^2/\text{m}^4\cdot\text{kg}^2$
l	Length of a brakepipe, m
L	Line inertance, kg/m^5
\dot{m}_L	Leakage flow rate, kg/s
M_L	Mass of air in the brakepipe, kg
\dot{m}_{lc}	Mass flow rate in the brakepipe no.1, kg/s
N	Ratio factor
p_i	Brakepipe pressure at pipe <u>ith</u> , kPa
\bar{p}_i	Mean pressure value in brakepipe <u>ith</u> , kPa
p_d	Pressure in brakepipe after reduction, kPa
p_L	Brakepipe pressure for 1 <u>st</u> pipe, kPa
p_M	Brakepipe pressure for 25 <u>th</u> pipe, kPa
p_R	Brakepipe pressure for 75 <u>th</u> pipe, kPa
q	Volume flow, cc/s
R	Gas constant, N-m/kg-K
R_i	Linear leakage resistance in <u>ith</u> pipe, $\text{kN}\cdot\text{s}/\text{m}^2\cdot\text{kg}$
R_{si}	Series resistance in <u>ith</u> pipe, $\text{kN}\cdot\text{s}^2/\text{m}^2\cdot\text{kg}^2$
t_{di}	Delay time at <u>ith</u> pipe section, s
\bar{t}_d	Ideal time delay, $(1/c_0)$, s
T_d	Total time delay, s
T_r	Response time, s
T, T_f	Brakepipe absolute temperature, K
u_p	Normalized signal variable, non-dimension
u	Axial velocity of air flow, m/s

V_c	Volume of the pressure chamber, cc
V_l	Volume of the brakepipe, cc
w	Characteristic frequency of the wave, rad/s
Y	Shunt admittance, Ω^{-1}
Z_c	Characteristic impedance, ohm (Ω)
ρ	Density of air, kg/m^3
τ	Shear force, N
τ', t'	Normalized time
α	(i/n), where i is pipe no. & n is no. of pipes
γ	Specific heat ratio
θ	Mesh ratio
μ	Poisson's ratio
Δp	Pressure difference, kPa
x	Distance or displacement, mm

Subscript: P_{ij} -- Nodal point with coordinates of i & j
in the characteristic grid

f -- Reference level or value.

CHAPTER 1

INTRODUCTION

1.1 ROLE OF THE BRAKEPIPE IN THE OPERATION OF THE AUTOMATIC BRAKE SYSTEM OF A FREIGHT TRAIN

Brakepipe functions as a signal conduit as well as a power supply for the brake assemblies in each car of a freight train.

Brakepipe leakage is an unavoidable feature in train operation and train handling. Excessive leakage affects the safety of the train by transmitting false signals to the brake cylinder as well as overloading the compressor units in the locomotives. Because of the leakage resulting from broken pipes which had formed fractures in the threaded area, threadless fitting employing a rubber compression grip and seal were used. Although this virtually eliminated pipe breakage, it created leakage problems. Leakage was more serious in winter due to insufficient tightening of gland nuts. This has led to the application of welded brakepipe and welded flanged fittings which has reduced leakage to some extent. However, leakage in practice cannot be

totally eliminated. Instead it is controlled within safe operating limits.

1.1.1 PRINCIPLE OF AIR BRAKE OPERATION OF A FREIGHT TRAIN

Referring to Figure 1.1, a schematic illustration of the automatic brake system of a typical freight train is shown. This system consists of a locomotive control unit (L.C.U.) placed at the head-end of the train, and a car control unit (C.C.U.) situated at each single car. The L.C.U. in turn contains the compressor which supplies air at a suitable pressure as the ambient medium of the entire brake system, a brake valve assembly incorporating the control lever, and the brake cylinders which are responsible for actuating the brake rigging and shoes at the locomotive only. The C.C.U., similarly, consists of the ABD type brake valve, with its combined emergency and auxiliary reservoir, as well as the brake cylinders which actuate the brake rigging and shoes of that particular car only. The L.C.U. and C.C.U. are connected together in a chain-like manner by the brakepipe which therefore runs the full length of the car (1,2).

NOTE: * Underlined number(s) in parenthesis designate the reference(s) at the end of thesis.

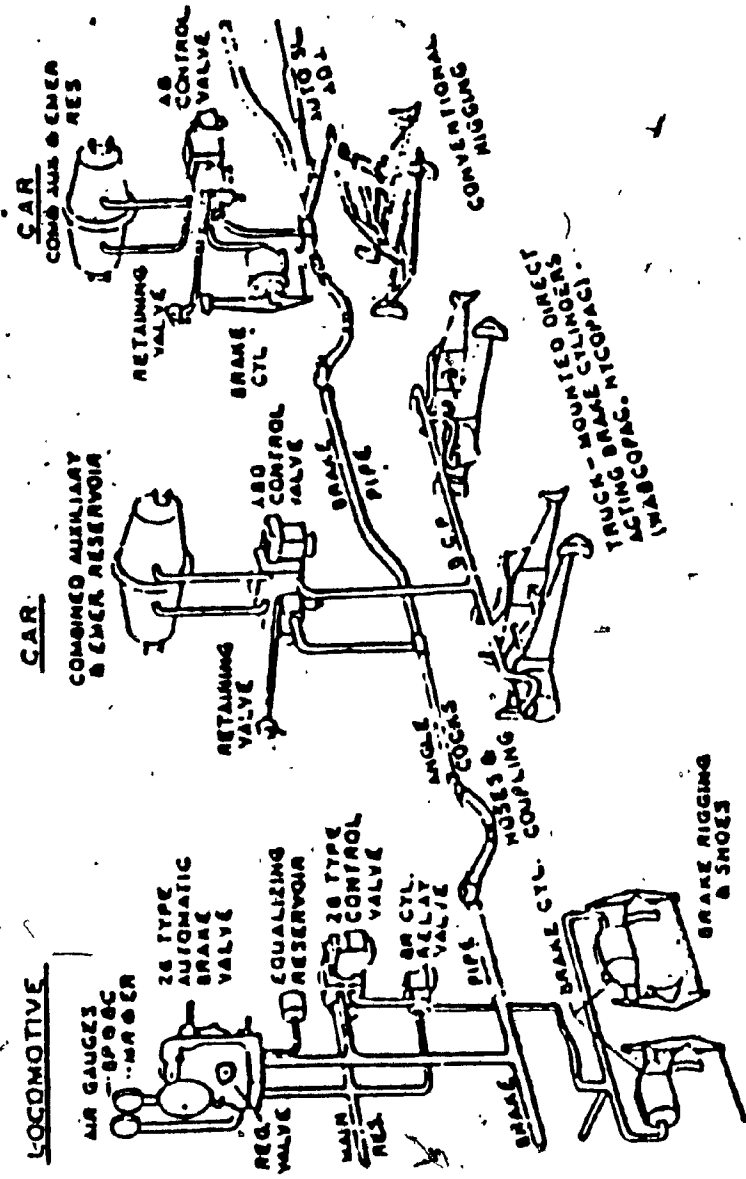


FIG.1.1* SCHEMATIC OF THE AIR BRAKEPIPE SYSTEM

*From References (2) and (24).

The primary source for slowing and stopping trains is the compressed air stored in the auxiliary reservoir on each car as directed by the control valve in each car. This air is transmitted to the brake cylinder, translated to a mechanical force acting on the brake shoes against the wheels of the train to retard their rotation. The air brake is actuated by the engineman through a 26-LUM automatic brake valve which provides for a fixed minimum reduction. This valve permits the charging and discharging of the brakepipe. When the brakepipe is fully charged between 483kPag (70psig) and 758kPag (110psig), the engineman may brake by lowering the brakepipe pressure with the valve which is positioned to connect the locomotive end of the brakepipe to a bleed orifice. The amount of braking is controlled by the reduction of brakepipe pressure, as determined by the brake valve handle position in the locomotive. This brakepipe reduction throughout the train causes the control valve at each car to respond. The control valve then meters the stored air in the brake cylinders in proportion to the amount of drop in brakepipe pressure (1).

When the automatic brake valve handle is moved to the release position, this causes the brake valve to readmit air to the brakepipe. The increasing brakepipe

pressure then causes the equipment at each car to move to release, thereby exhausting the brake cylinder pressure and recharging the auxiliary reservoir. The time required to achieve release of the brakes on the last car of a train is longer as train length increases. The release time becomes longer as train brakepipe leakage increases regardless of train length. The degree of increase is most noticeable on the minimum reductions because the pressure head to restore brakepipe pressure is low and results in longer times to achieve release. The time to initiate the release of the brakes on the last car in a train is also dependent on the type of brake valves (1).

The use of a split service reduction or graduated application is widely used for applying train brakes. This type of application is achieved by making a 41 to 48kPag (6 to 7 psig) initial reduction, waiting for about 20 seconds, then continuing the reduction to the desired brakepipe pressure. This has the advantage that, as the train comes to a stop, the slack will gather and starting of the train following the stop is made easier.

When the car auxiliary reservoir pressure and the brake cylinder pressure are equal in value, it is noted that brakepipe pressure increase only about 10.5kPag at

each car location to cause the valve on that car to move to release. If overreduction has occurred, that is, brakepipe pressure reduced below that required to produce equalization, a release of the brakes on any car cannot be accomplished until brakepipe pressure has been slowly increased to the equalization pressure plus the 10.5kPag. This is of importance particularly with long trains where the time to obtain release is materially lengthened by an overreduction (1,24).

1.1.2 DESCRIPTION OF THE BRAKEPIPE

The brakepipe of the automatic brake system of a train is defined as the system of piping including branch pipes, angle cocks, cutout cocks, dirt collectors, hose couplings and flexible hoses, used for connecting locomotive and all cars for the passage of air to control the locomotive and car brakes (1).

This brakepipe is not straight and has at least one cross-over in each car. The brakepipes of adjoining cars are connected together by flexible hoses and hose couplings. Thus, the brakepipe extends throughout the entire length of the train. Each brakepipe and hose is usually connected to an angle cock. Referring to the schematic freight car illustrated in Figure 1.1, there

are tee-branch pipes from the brakepipe over to the control valves, reduction relay valves, and quick service valves. Brakepipe air flows to and from the control valves through a combined dirt collector and branch pipe cutout cock which allows the brake equipment on the car to be cut out in case of trouble without affecting the brakepipe pressure control to other cars (1,2).

An important feature of the brakepipe is that it functions as a signal conduit as well as a power supply for the brake assemblies in each car.

For a typical freight car, there exists some 100 joints and seals in the various control valves and brake-cylinder arrangement as potential sources of air leakage. As a result brakepipe leakage becomes an unavoidable feature in train operation and train-handling. It creates a considerable difference between locomotive pressure and last car pressure. This pressure difference is often referred to as brakepipe gradient. With leakage it takes a longer time to fully charge or recharge the system, and tends to reduce brakepipe exhaust time. True brakepipe gradient is dependent on the train length and the distribution of leakage within any given train length. In general, longer trains and higher pressures lead to an

increase in the pressure gradient. When leakage is highly concentrated in the rear cars of a long train, it produces the largest pressure gradient. This may result in loss of braking function or in undesired braking application.

However, since leakage is unavoidable, standards of acceptable leakage have been provided. The acceptable amount of leakage has been specified for long trains in terms of brakepipe gradient. These standards are the results of practical experience, and they have served as good indications of brakepipe performance (1,2,3).

There is a need for a quick and efficient method to locate excessive leakage when and where it exists based on a good analytical understanding of the interplay between pressure gradient in a brakepipe and leakage along the brakepipe. It should be noted that when checking trains for leakage, correction of leakage at the rear of the train will produce greater improvement in brakepipe gradient than correction of comparable leakage at the head end of the train (2).

After the engineman has initiated the braking action by moving the brake valve handle from the release position, the following sequence of events will occur:-

- (a) the locomotive equalizing reservoir pressure reduces;
- (b) this causes the train brakepipe pressure at the loco-

motive to reduce; (c) this pressure drop is then transmitted through the brakepipe of the train until it reaches the control valve on the ith car; (d) the control valve then meters the supply of air from the auxiliary reservoir to the brake cylinder of the ith car. The overall time delay T_d which occurs between events (a) and (d) is known to be of the form (4):-

$$T_d = T_r + 1/c |L_i(t) - L_1(t)| \quad \dots \dots (1-1)$$

where symbols are defined as follows:

T_r = response time of the automatic brake valve and equalizing reservoir, i.e. events (a) and (b).

c = transmission speed of the pressure drop signal in the brakepipe of the train.

L = distance between two locations.

subscript: 1 = the car number of the locomotive nearest ith car which is capable of effecting a reduction in brakepipe pressure.

Note: Typical values for T_r and c are 2 seconds and 153 m/s (500 ft/sec) respectively (4).

The reduction in brakepipe pressure at the ith car, $r_i(t)$ is therefore designated as $r(t-T_d)$. Thus, the auxiliary reservoir supply pressure to the brake cylinder pipe can be represented as $k.r(t-T_d)$, where T_d is defined by equation(1-1) and k is a constant of proportionality.

between the time delayed equalizing reservoir pressure drop appearing at the control valve of the ith car and the supply pressure of that car's auxiliary reservoir (4). In the remainder of this thesis, time delay t_d is referred to ($T_d - T_r$), that is, events (c) and (d).

1.2 THE USE OF PRESSURE CHAMBER TO REPRESENT THE RELAY VALVE

The function of the relay valve is to control the time rate of change of the brakepipe pressure in response to change in equalizing reservoir pressure. Consequently, it is possible to reduce the stopping distance of the train by shortening the propagation time and the time required to exhaust the compressed air from the brakepipe to achieve the desired pressure reduction.

The relay valve shown in Figure 1.2 consists of a supply unit and an exhaust unit, both being controlled by a diaphragm assembly. During transient operation, any excess increase of pressure p_R in the inner diaphragm chamber(I), causes air to flow back into the brakepipe chamber(H) where it is then vented through the exhaust poppet valve(Y). When the pressure balance in the diaphragm chambers and the brakepipe chamber is attained, the relay valve assumes 'lap position'. In this position,

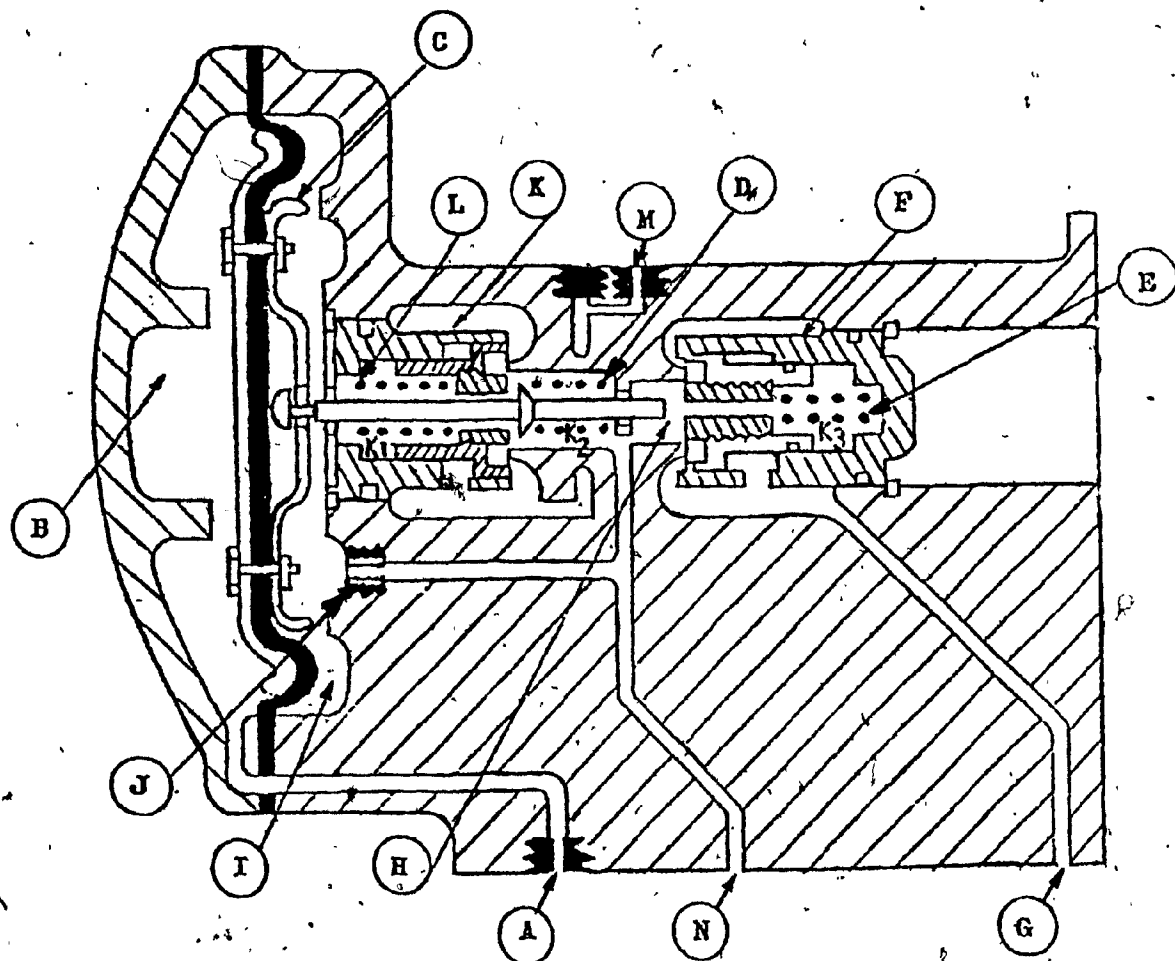


Figure 1.2* Sectional view of a relay valve

(A)	INPUT ORIFICE	(H)	BRAKE PIPE CHAMBER
(B)	OUTER DIAPHRAGM CHAMBER	(I)	INNER DIAPHRAGM CHAMBER
(C)	DIAPHRAGM ASSEMBLY	(J)	FEEDBACK ORIFICE
(D)	DIAPHRAGM ASSEMBLY SPRING	(K)	EXHAUST POPPET VALVE
(E)	SUPPLY VALVE SPRING	(L)	EXHAUST VALVE SPRING
(F)	SUPPLY POPPET VALVE	(M)	EXHAUST PORT
(G)	SUPPLY PORT	(N)	OUTPUT PORT

* From Reference (24).

the diaphragm assembly is in a state of static equilibrium indeed. Both supply valve and exhaust valve are being closed, since the self-lapping feature of the relay valve automatically maintains the brakepipe pressure against overcharge and leakage. If this state is disturbed, either the supply valve or the exhaust valve is opened in an effort to restore static equilibrium (24).

The experimental set-up employed in the investigation of the relationship between the pressure difference across diaphragm ($p_R - p_L$) and the displacement of the diaphragm (X), is shown in Figure 1.3a. The relay supply and output port are blocked so that there is no flow derived from them, that is, no load condition. Referring to Figure 1.3a again, the pressure p_R is the input pressure which is measured by a pressure gauge at the input port. The pressure p_L is the outer diaphragm pressure which is kept to be atmospheric. The diaphragm displacement due to the pressure difference across the diaphragm is measured by a displacement transducer. This experiment is conducted for input pressure of 0.69kPag to 103kPag in increments of 0.69kPa, at no load condition.

In the case of flat poppet valves such as the exhaust valve which is modulated by the diaphragm displac-

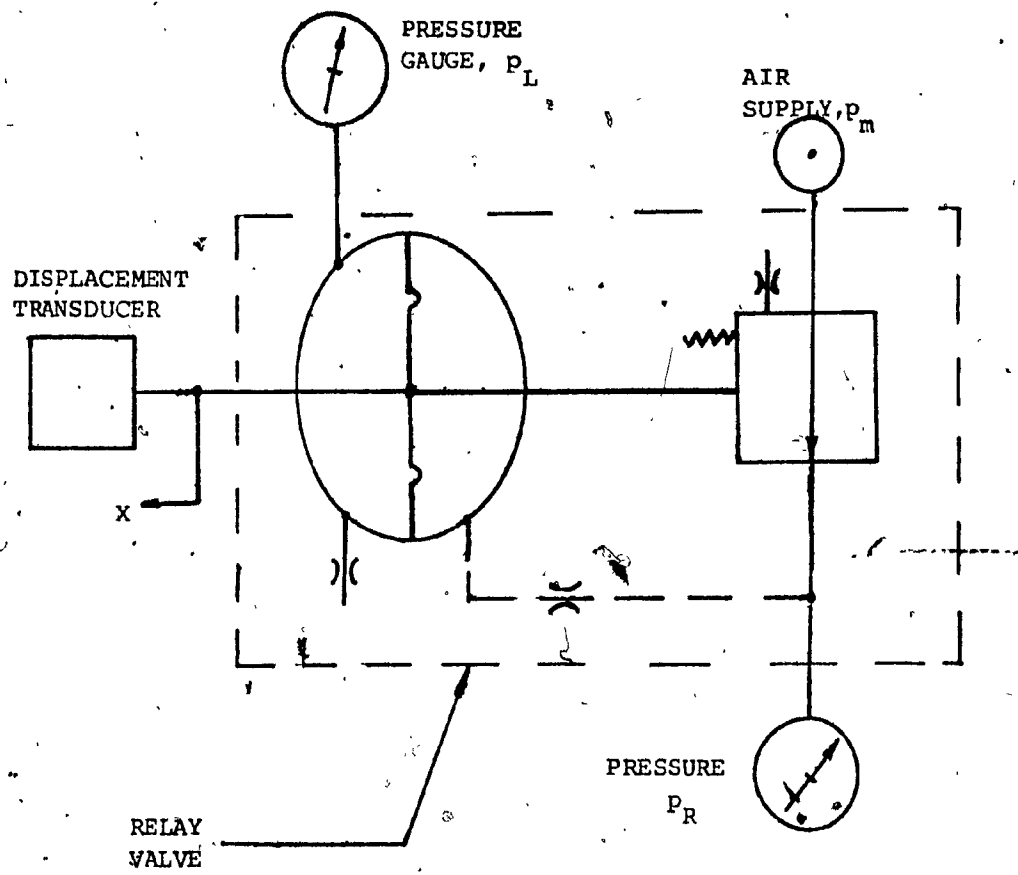


FIG. 1.3a SCHEMATIC DRAWING OF RELAY VALVE
IN THE EXPERIMENT OF DISPLACEMENT
OF DIAPHRAGM DUE TO PRESSURE FORCE

ement, it has been shown in Reference (23) that the coefficient of discharge varied with downstream to upstream pressure ratio as well as valve lift. However, for simplicity, a single constant coefficient of discharge $C_d = 0.80$ is adequate. Thus, the effective area A_4 of the exhaust valve as shown in Figure 1.3b, is given as follows (23):-

$$A_4 = C_d \pi d_4 (X_1 - X); \quad 0 < X < X_1 \quad \dots \dots \quad (1-2)$$

where d_4 = diameter of supply valve seat

X_1 = displacement to close exhaust valve

The equivalent effective exhaust area A_E can be calculated as follows:

Consider the same mass flow rate and temperature in both cases, that is,

$$A_E N_{Rf} = A_4 N_{RL} \quad \dots \dots \quad (1-3)$$

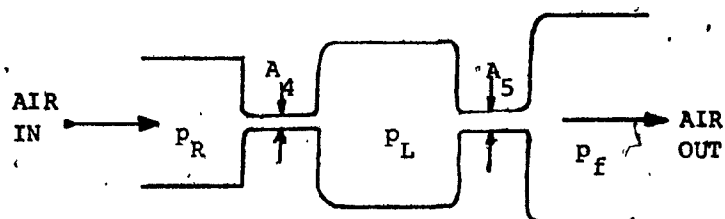
where A_4 is given from Figure 1.3b,

N_{RL} is given from Ref.(23), RL refers to ij,

N_{Rf} is always 1 since p_f/p_R is less than 0.5283

Note: When A_4/A_5 is less than 0.5283 (for air), A_4 is sonic; otherwise, A_4 is subsonic, then to find N , use Table A.2 from Ref.(23).

The result obtained from the above experiment and combined with the relation given from equation(1-2) is shown in Figure 1.3b. It shows that when the pressure



NOTE: $A_5 = \text{FIXED EXHAUST PORT AREA} = C_d^2 d_{5v}^2 / 4$

$A_4' = \text{VARIABLE EXHAUST VALVE AREA}$

$$= C_d^2 d_4 (x_1 - x)$$

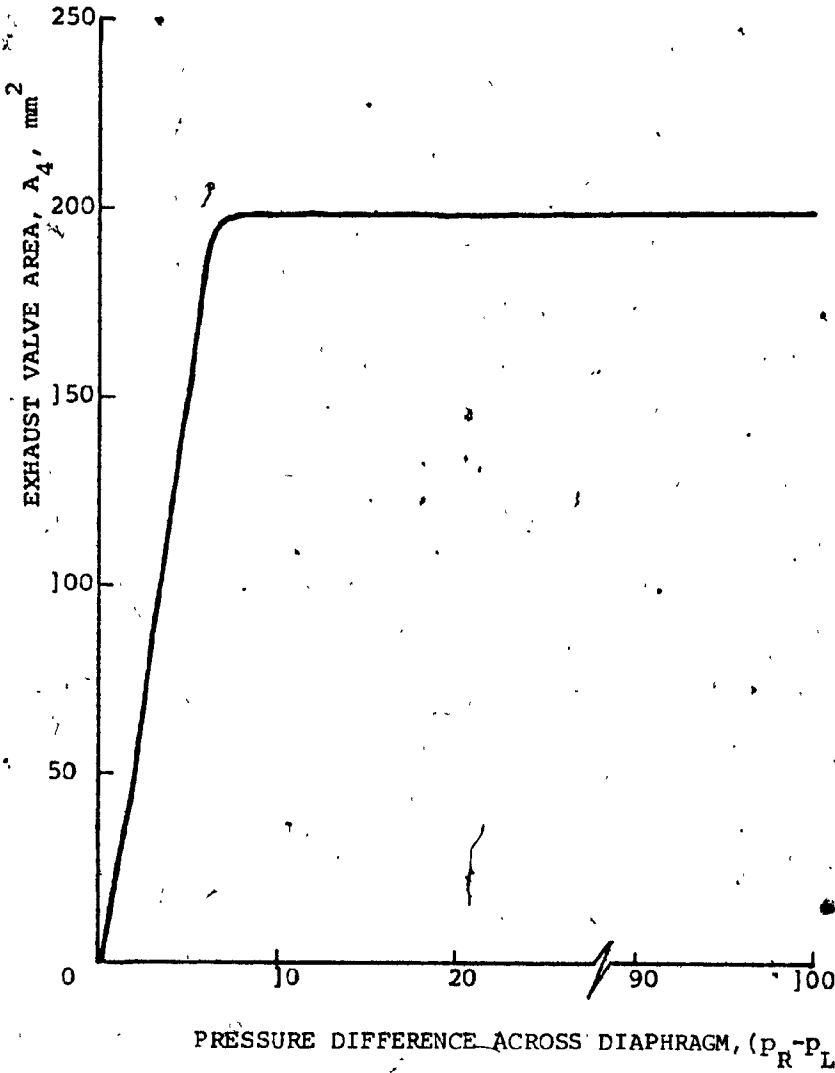


FIG. 1.3b CHARACTERISTIC OF A RELAY VALVE:
EXHAUST VALVE AREA VS. PRESSURE DIFFERENCE

difference across diaphragm is greater than 7.6kPa, the exhaust valve area is fully opened. This means that the exhaust area can be approximately assumed to be a constant with respect to pressure change. One can replace the relay valve by a fixed volume pressure chamber with an orifice having an equivalent effective exhaust area A_E .

In Figure 1.4, it shows the relationship between $(p_R - p_L)$ and A_E . It is worthy to note that when $(p_R - p_L)$ is greater than 7.6kPa, the effective exhaust area A_E is close to the effective exhaust port area A_5 . Also, when $(p_R - p_L)$ is less than 2.8kPa, the slope of the curve is very steep of about $9.25(10)^{-6} \text{ m}^2/\text{kPa}$. This implies that in the beginning, the rate of the pressure drop is very fast but after the pressure difference is less than 7.6kPa it will take a longer time to be in a state of static equilibrium.

Note: In appendix D, a brakepipe reduction of 41kPa and 103kPa with relay valve and pressure chamber had been shown in graphical forms. It was found analytically that they were matched closely within $\pm 5\%$ difference. We concluded that the application of the pressure chamber to represent the relay valve was satisfied. Also, in appendix C, dynamic characteristic of the relay valve is presented analytically and graphically.

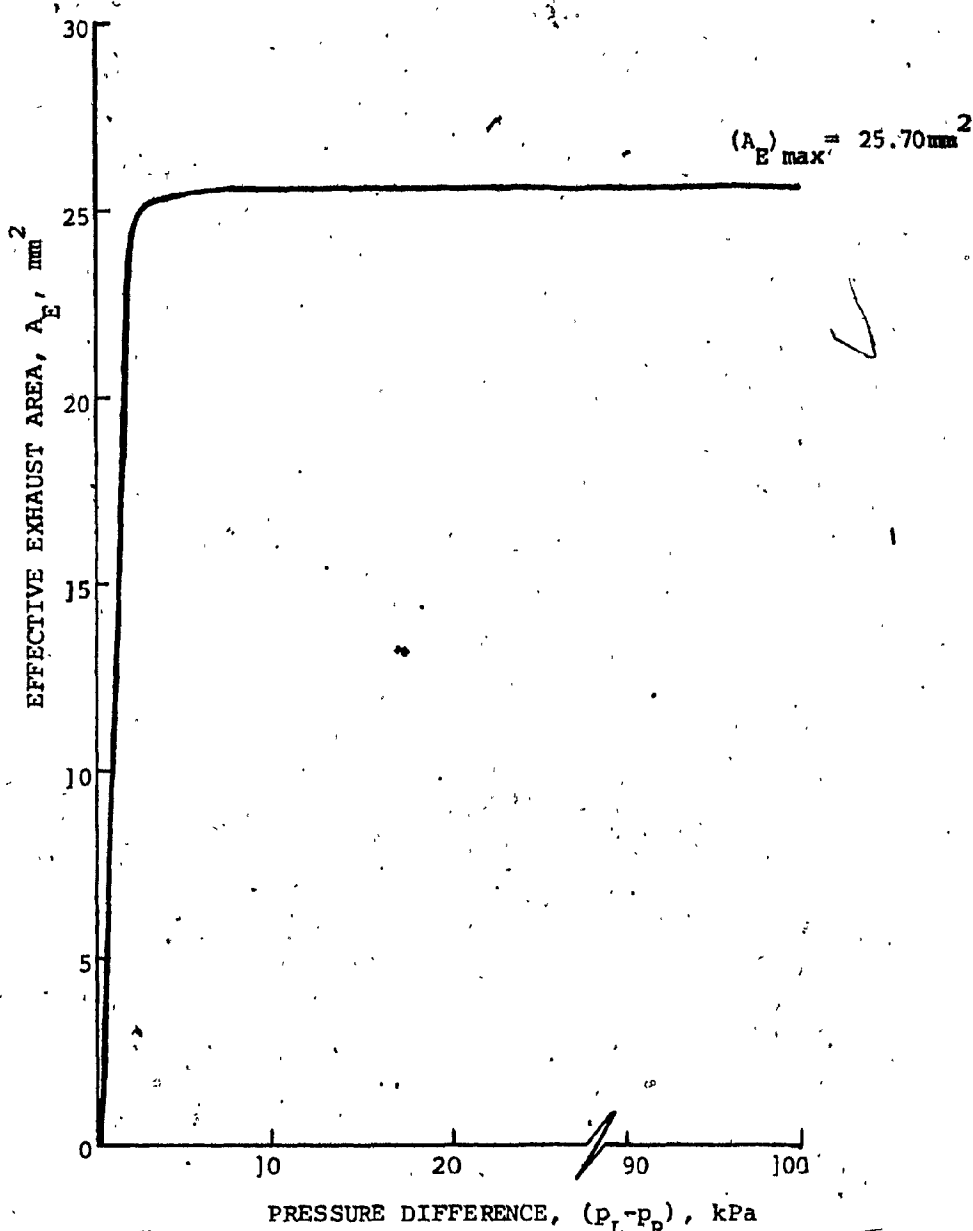


FIG. I.4 CHARACTERISTIC OF A RELAY VALVE:
EFFECTIVE COMBINED AREA VS. PRESSURE DIFFERENCE

1.3 REVIEW OF PREVIOUS WORKS

The earliest work on fluid transmission line models was based on acoustic theory. Iberall(5) provided a formulation for the acoustical impedance of cylindrical enclosure with the effects of both distributed friction and heat transfer. However, his analysis was cumbersome and avoided the use of static friction factor data, but appeared to be unsatisfactory for large damping. Moise(6) investigated the dynamic characteristics of dead-ended and volume-terminated pneumatic transmission lines. The agreement between theory and experiment was quite good for the dead-ended tube except at very low pressure amplitudes. The reason for the poorer results at low amplitudes was that laminar flow friction factors were used. Iberall's discussion of the approximate solution obtained by Rohmann and Gorgan(7) presented the complete solution based on a system of evenly distributed fixed parameters. An equation was derived by Schauder and Binder(8) which described the pressure-time relationship that occurs at the end of a dead-ended or volume-terminated pneumatic transmission line following a sudden pressure change at its input. The derivation was based on a one-dimensional uniformly distributed system, small, reversible, adiabatic-pressure changes, and laminar flow. Nicohols(9) derived Iberall's

solution and interpreted it in the form of an equivalent circuit. The work is performed in the frequency domain and includes both high- and low-frequency approximations.

Karam and Franke(10) used Nichols' approach to obtain an improved high-frequency approximation. Franke, Malanowski and Martin(11) obtained the frequency response of pneumatic circular line including the effects of temperature, end-conditions, flow & branching. The state-of-the-art in circular fluid lines is summarized by Goodson and Leonard(12). They suggested that further research be conducted in complex systems through the use of computer programs or the development of models for such application as large signals with turbulence.

All the work cited above applies to propagation models for circular fluid lines without leakage. Katz and Cheng(13) have proposed a network approach to study the effects of leakages in brakepipe models and formulated mathematical model for generating pressure distribution for this model. This provides the possibility of using network theory to detect leaks in brakepipes. Kwan(3) suggested network models for brakepipe leakage under several cases of leakage flow. He proved that the effects of leakage on pressure gradient and brakepipe taper depended on the position of the fault and that leakage at the rear had larger effect on the pressure gradient.

than leakage at front. Aula, Cheng and Katz(14) have confirmed the validity of experiments on a scaled-down brakepipe model. Subsequently, their proposed methods would have to be tested extensively on actual brakepipes of a freight train.

1.4 SCOPE OF THESIS

This research is concerned with the experimental investigation and theoretical analysis of a scaled-down brakepipe model. The two analytical methods used are based on fluid mechanics theory and verified by experimentation on the brakepipe model. A detailed mathematical model (with computer simulation on each method) for generating the pressure distribution along the brakepipes is formed. The partial differential equations of motion are solved by finite difference technique through the minicomputer PDP-11 at the Fluid Control Research Laboratory, Concordia University. Also, different boundary conditions for the brakepipe are discussed. It was shown analytically that the modified approach of using a fixed-volume tank instead of a relay valve was satisfactorily applied to the testing procedure of train-operation and train-handling for the engineman, and to simplify the experimental set-up for the engineer. Simple experimental tests on the brakepipe model

are demonstrated so as to measure the pressure distribution along the pipes as a function of time, to find the effect of brakepipe leakage, and to evaluate the time delay t_d , that is, $(T_d - T_r)$ which is explained in section 1.1.2. The lumped modeling method was found to be much easier to apply but less accurate than the method of characteristics for large-amplitude signals. Subsequently, the proposed methods would have to be tested extensively on actual brakepipes. A preliminary prediction for actual brakepipe is given in Appendix D. This thesis is confined mainly to developing and verifying the proposed methods on a scaled-down brakepipe model.

This research thesis is divided into six chapters. The first chapter briefly introduces the role of the brakepipe in the operation of the automatic brake system of a freight train and reviews the previous work that has been related to this area.

The second chapter gives a formulation of the brakepipe model by the method of characteristics for large-amplitude signals. This method is applied to a brakepipe without leakage along the length. The third chapter deals with formulation of the nonlinear model of the brakepipes by the lumped modeling, developing a set of equations for generating pressure distribution

along the brakepipe with leakage.

In the fourth chapter, the experimental investigation conducted on the laboratory brakepipe model is given. Larger and more pipes are restricted due to the lack of enough space and facilities in the research laboratory. Discussion on and comparison between experimental and analytical results are introduced also in chapter 4. Chapter five discusses the effect of leakage on the transmission speed of air propagation. The last chapter briefly summarizes the previous chapters, concludes the discussion and presents some suggestions for further work in this field.

CHAPTER 2

FORMULATION OF EQUATIONS FOR THE BRAKEPIPE MODEL BY THE METHOD OF CHARACTERISTICS

2.1 INTRODUCTION

The method of characteristics has been used in a variety of numerical, analytical and graphical ways as a powerful tool in the solution of hyperbolic partial differential equations. Steady and unsteady compressible flow problems have been solved by this method for many years. Computational simulation has been given by Benson et al.(15), Manning(16), and Trikha(17) for compressible flow problems. All the foregoing treatments neglect frequency-dependent effects. Zielke(18) introduced the concept of a historetic weighting function which related the wall shear stress in transient laminar pipe flow to the instantaneous mean velocity and the weighted past velocity changes. Brown(19) developed a quasi-method of characteristics which considered both frequency-dependent friction and heat transfer effects. Brown's method was conceived as a consequence of his reformulation of the results of Zielke and extended the scope of the method.

of characteristics. The availability of high-speed digital computers has allowed the general method to be applied to a greatly extended class of problems represented by semi-hyperbolic equations. Streeter(20) has compared the characteristic method, typifying explicit method and the centered implicit method. He emphasized that complex problems with large-amplitude signals handled by applying the computerized method of characteristics would be time-consuming but this method could still be an excellent tool to solve the hyperbolic equations.

2.2 MATHEMATICAL MODEL

2.2.1 MODIFIED APPROACH — WITH PRESSURE CHAMBER

For compressible flow in a long brakepipe which is shown in Figure 2.1, we consider two dependent signal variables u and a , where ' u ' is the velocity of air flow (one-dimensional) and ' a ' local speed of sound. The simplified method of characteristics for large-amplitude signals considers the effects of time-dependent friction and omits heat transfer effects. The basic characteristic equations for the u and a variables are developed by first relating the local speed of sound, a , to the static brakepipe pressure, p . From $a = (\gamma p/\rho)^{1/2}$ and $d\rho/\rho = dp/\gamma p$, we may relate p and a as:

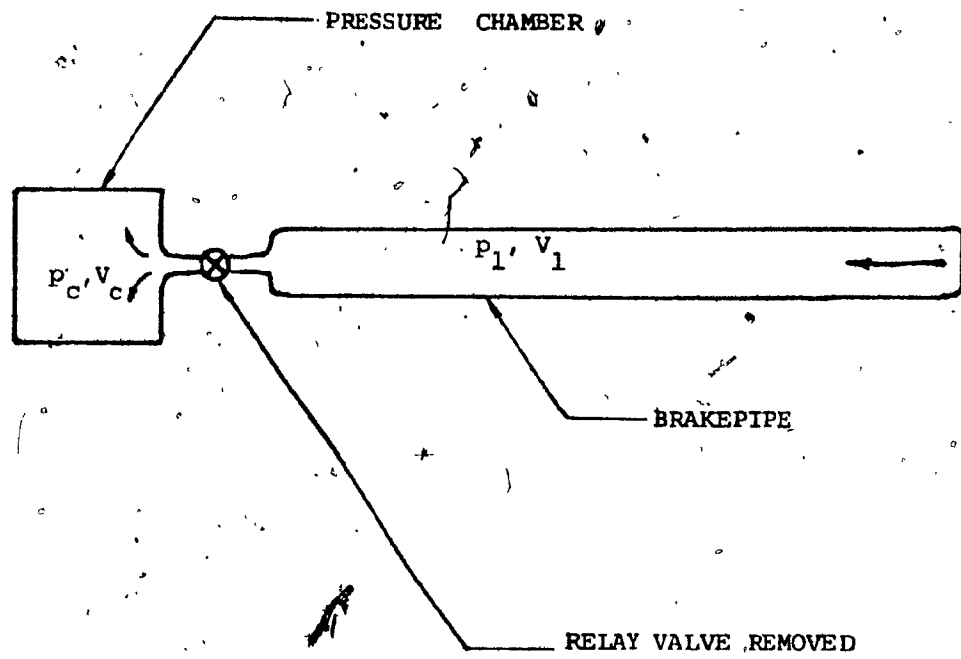


FIG. 2.1 MODIFIED CONFIGURATION OF BRAKEPIPE.

$$\frac{dp}{p} = \left(\frac{2\gamma}{\gamma-1}\right) \cdot \frac{da}{a} \quad \dots \dots \quad (2-1)$$

where ρ = density of air

γ = ratio of specific heats

For one-dimensional flow with friction, the momentum equation and continuity equations are given from Ref. (21) as follows:

$$\frac{\rho \partial q}{A \partial t} + \frac{u \rho \partial q}{A \partial x} + \frac{\partial p}{\partial x} = \left(\frac{\partial \bar{\tau}}{\partial y} \right) \quad \dots \dots \quad (2-2)$$

$$\frac{1}{\gamma p} \left(\frac{\partial p}{\partial t} + u \frac{\partial p}{\partial x} \right) + \frac{\partial q}{A \partial x} = 0 \quad \dots \dots \quad (2-3)$$

where q = volume flow of air = uA

$\left(\frac{\partial \bar{\tau}}{\partial y} \right) = - \frac{\rho f u^2}{2d}$ = average frictional force/unit volume

x = linear distance

A = cross sectional area

d = diameter of pipe

y = radial distance

To simplify the equations (2-2) and (2-3), we obtain from Ref. (21):

$$\frac{\partial u}{\partial t} + u \frac{\partial u}{\partial x} + \left(\frac{2}{\gamma-1} \right) a \frac{\partial a}{\partial x} = - \frac{f u^2}{2d} \quad \dots \dots \quad (2-4)$$

$$\left(\frac{2}{\gamma-1} \right) \left(\frac{\partial a}{a \partial t} + \frac{u \partial a}{a \partial x} \right) + \frac{\partial u}{\partial x} = 0 \quad \dots \dots \quad (2-5)$$

The multiplication of equation (2-5) by an arbitrary constant K , and subsequent addition to equation (2-4) leads to:

$$\frac{2K}{(\gamma-1)a} \left[\frac{\partial a}{\partial t} + (u+\frac{a^2}{K}) \frac{\partial a}{\partial x} \right] + \left[\frac{\partial u}{\partial t} + (u+K) \frac{\partial u}{\partial x} \right] = - \frac{fu^2}{2d} \quad \dots \dots \quad (2-6a)$$

Since u and a are functions of both time and distance, total derivatives of these variables have the form of:

$$\frac{d}{dt} = \frac{\partial}{\partial t} + \frac{dx}{dt} \frac{\partial}{\partial x} \quad \dots \dots \quad (2-6b)$$

When $K = \pm a$, equation(2-6a) transforms to the characteristic equation sets:-

$$\frac{du}{dt} + (\frac{2}{\gamma-1}) \frac{da}{dt} = - \frac{fu^2}{2d} \text{ only when } (\frac{dx}{dt}) = u \pm a \quad \dots \dots \quad (2-7a)$$

while

$$\frac{du}{dt} - (\frac{2}{\gamma-1}) \frac{da}{dt} = - \frac{fu^2}{2d} \text{ only when } (\frac{dx}{dt}) = u - a \quad \dots \dots \quad (2-7b)$$

Now, we normalize equation(2-7) with $x' = x/l$, $a' = a/a_f$, $u' = u/a_f$ and $t' = ta_f/l$, then

$$\frac{du'}{dt'} + (\frac{2}{\gamma-1}) \frac{da'}{dt'} = - K' u'^2 \quad \text{for } (\frac{dx'}{dt'}) = u' + a' \quad \dots \dots \quad (2-8a)$$

while

$$\frac{du'}{dt'} - (\frac{2}{\gamma-1}) \frac{da'}{dt'} = - K' u'^2 \quad \text{for } (\frac{dx'}{dt'}) = u' - a' \quad \dots \dots \quad (2-8b)$$

where $K' = \frac{f_1}{2d}$ and $(\frac{dx'}{dt'}) = \text{slope of characteristic line}$

l = length of brakepipe, a_f = reference sonic speed.

Figure 2.2 shows the rectangular grid with fixed time intervals and positions that is used to calculate the variables in equation sets(2-8). The nodal points

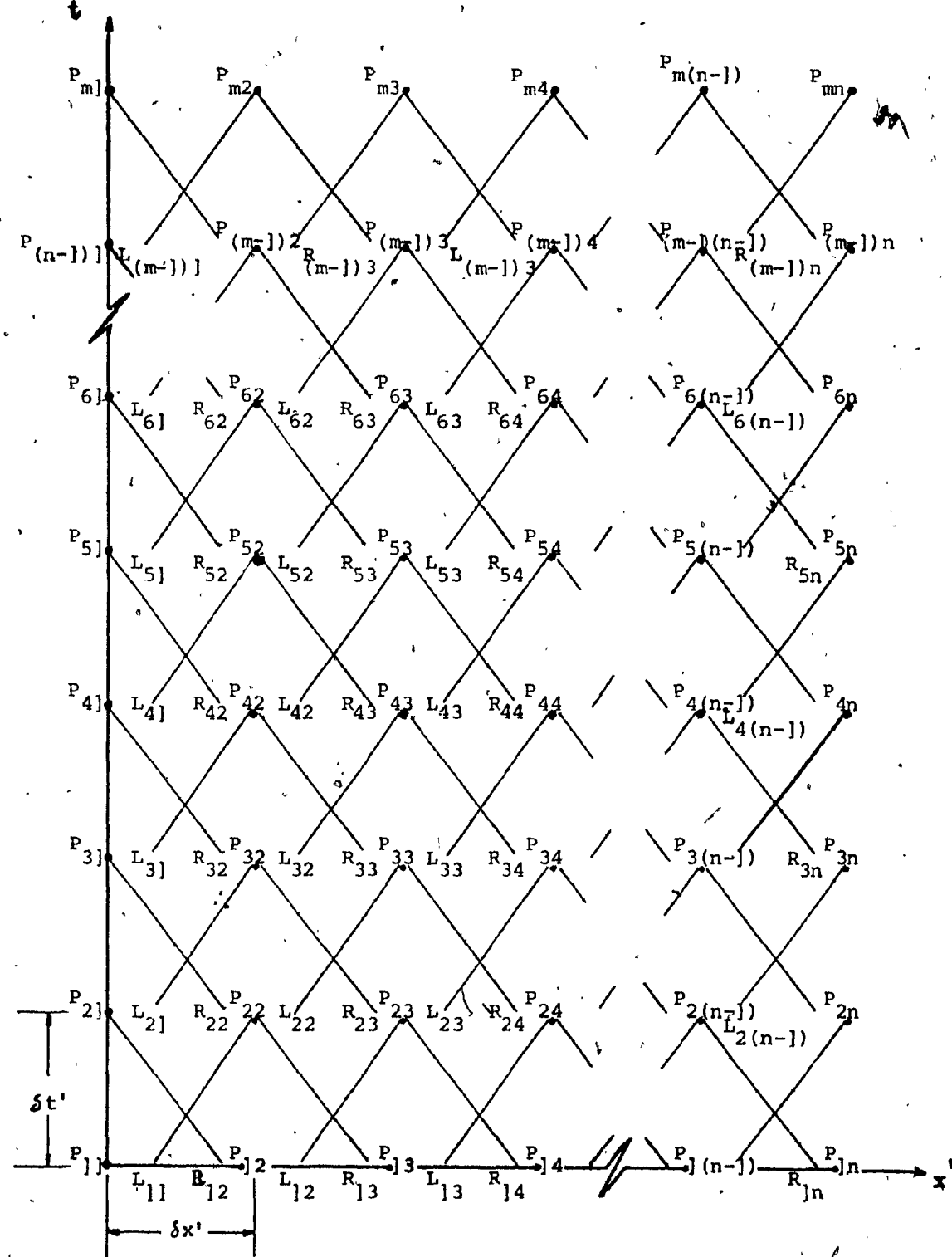


FIG. 2.2 CHARACTERISTIC GRID FOR LARGE-AMPLITUDE SIGNALS.

P are represented by solid dots and the variables are only computed for these points. The characteristic lines that pass through the local or nodal points do not emanate from the nodal points of a previous time step when there is the appreciable magnitude of the velocity u' . As a result the signal variables corresponding to the characteristic lines must be obtained by interpolation between the previous time nodal points. For example, to calculate the variables at point P_{32} requires the variables at points L_{21} and R_{23} . These in turn, are obtained by linear interpolation between P_{21} and P_{22} , and P_{22} & P_{23} respectively as shown in Figure 2.2.

Applying a first-order finite difference approximation to equation sets(2-8), we can get the signal variables at the interior points, the right boundary nodal point, and the left boundary nodal point in the following sub-sections.

A. Right Boundary — closed end

For the right boundary nodal point, the boundary conditions for $\gamma=1.4$ are as follows:-

$$u'_{P_{jn}} = 0 \quad \dots \quad (2-9)$$

$$5a'_{P_{jn}} = \bar{u}'_{L(j-1)(n-1)} + 5a'_{L(j-1)(n-1)} - K'u'_{L(j-1)(n-1)} \\ |u'_{L(j-1)(n-1)}| \delta t \quad \dots \quad (2-10)$$

where $u' L_{(j-1)(n-1)} = \frac{(u' P_{(j-1)n} + \theta Y' L_{(j-1)(n-1)})}{(1 - \theta V' L_{(j-1)(n-1)})}$

$$a' L_{(j-1)(n-1)} = \frac{(a' P_{(j-1)n} - \theta Y' L_{(j-1)(n-1)})}{(1 - \theta V' L_{(j-1)(n-1)})}$$

$$Y' L_{(j-1)(n-1)} = u' P_{(j-1)(n-1)} * a' P_{(j-1)n} \\ u' P_{(j-1)n} * a' P_{(j-1)(n-1)}$$

$$V' L_{(j-1)(n-1)} = u' P_{(j-1)(n-1)} + a' P_{(j-1)(n-1)} \\ u' P_{(j-1)n} - a' P_{(j-1)n}$$

$$\theta = \frac{\delta t'}{\delta x'} = \text{mesh ratio}$$

Note: (i) Since our interpolation procedure implies that for instance, the points R_{13} and L_{11} are between P_{11} and P_{13} , we must choose θ to be less than the smallest value of $\frac{1}{u' + a'}$, the interpolation will fall outside the range of the closest previous points, then this solution becomes unstable (21).

(ii) For further mathematical explanation, it can be found in Appendix A.

B. Interior Points — without brakepipe leakage

After simplification, the equation set(2-8)

becomes:-

$$u' P_{ji} + 5a' P_{ji} = u' L_{(j-1)(i-1)} + 5a' L_{(j-1)(i-1)} - \\ K' u' L_{(j-1)(i-1)} | u' L_{(j-1)(i-1)} | \delta t' \\ \dots \quad (2-11)$$

$$u' P_{ji} - 5a' P_{ji} = u' R_{(j-1)(i+1)} - 5a' R_{(j-1)(i+1)} - K' u' R_{(j-1)(i+1)} |u' R_{(j-1)(i+1)}| \delta t \\ \dots \dots \quad (2-12)$$

where subscripts $j = 2, 3, \dots, m$ and

$$i = 2, 3, \dots, (n-1).$$

$$u' L_{(j-1)(i-1)} = \frac{(u' P_{(j-1)i} + \theta Y' L_{(j-1)(i-1)})}{(1 - \theta V' L_{(j-1)(i-1)})}$$

$$u^R_{(j-1)(i+1)} = \frac{(u^P_{(j-1)i} + \theta Y^R_{(j-1)(i+1)})}{(1 + \theta V^R_{(j-1)(i+1)})}$$

$$a'_{L(j-1)(i-1)} = \frac{(a'_{P(j-1)i} - \theta Y'_{L(j-1)(i-1)})}{(1 - \theta V'_{L(j-1)(i-1)})}$$

$$a' R_{(j-1)(i+1)} = \frac{(a' P_{(j-1)i} + \theta Y' R_{(j-1)(i+1)})}{(1 + \theta v' R_{(j-1)(i+1)})}$$

$$Y' L_{(j-1)(i-1)} = u' P_{(j-1)(i-1)} * a' P_{(j-1)i} - \\ u' P_{(j-1)i} * a' P_{(j-1)(i-1)}$$

$$Y' R_{(j-1)(i+1)} = u' P_{(j-1)(i+1)} + a' P_{(j-1)i}$$

$$u' P_{(j-1)i} + a' P_{(j-1)(i+1)}$$

$$V' L_{(j-1)(i-1)} = u' P_{(j-1)(i-1)} - a' P_{(j-1)i}$$

$$u' P_{(j-1)i} + a' P_{(j-1)(i-1)}$$

$$V' R_{(j-1)(i+1)} = u' P_{(j-1)(i+1)} - a' P_{(j-1)(i+1)}$$

$$u' P_{(j-1)i} + a' P_{(j-1)i}$$

C. Left Boundary — with pressure chamber

To simplify the determination of the dynamic characteristics of a long brakepipe, we propose an artificial left-boundary condition. Instead of connecting the relay valve at the left-end, we put in a pressure chamber shown in Fig.2.1 with a known volume of air according to a particular brakepipe reduction.

We consider the following boundary equations:

$$u' P_{j1} = B_5 N_{lc} a' P_{j1}^2 \quad \dots \dots \quad (2-13)$$

$$u' P_{j1} - 5a' P_{j1} = u' R_{(j-1)2} - 5a' R_{(j-1)2} \quad \dots \dots \quad (2-14)$$

$$K' u' R_{(j-1)2} | u' R_{(j-1)2} | \delta t \quad \dots \dots \quad (2-14)$$

$$\text{where } B_5 = \frac{B_1 B_4}{B_3}$$

$$B_1 = \frac{C_d K A_e}{T^{1/2}}$$

$$B_3 = A_1 = \frac{\pi d^2}{4}$$

$$B_4 = \frac{P_f}{\rho_f c}$$

$$N_{lc} = \left[\frac{\left(\frac{P_c}{P_1} \right)^{2/\gamma} - \left(\frac{P_c}{P_1} \right)^{(\gamma+1)/\gamma}}{\left(\frac{\gamma-1}{2} \right) \left(\frac{2}{\gamma+1} \right)^{(\gamma+1)/(\gamma-1)}} \right]^{1/2}$$

$\frac{P_c}{P_1} > 0.5283$

$$= 1.0$$

$\frac{P_c}{P_1} \leq 0.5283$

c = transmission speed of air propagation

T = absolute temperature

Subscripts: c = chamber

1 = brakepipe

e = exhaust orifice

Substituting equation(2-13) to (2-14), we can get

$a'_{p_{j1}}$. We use the relation of $a'_1 = (p'_1)^{1/7}$ to find the
brakepipe pressure at the left-end.

The increment of chamber pressure is

$$p_c = \frac{nRT M_{lc} \delta t}{V_c} \quad \dots \dots (2-15)$$

where M_{lc} = mass flow rate

$$= C_d A_{lc} p_1 K N_{lc} / T^{1/2}$$

Thus, $p_c(t + \delta t) = p_c(t) + \delta p_c$ (2-16)

From equation(2-16) we can get the value of N_{lc} .

Note: Evaluation of chamber volume V_c and derivation of equation(2-13) are given in Appendix A.

D. Initial Conditions

The initial values of the signal variables are:

$$u' P_{1i} = 0 \quad \text{where } i = 2, 3, \dots, n. \quad \dots \dots \quad (2-17)$$

$$u' P_{11} = B_5 N_{lc} a' P_{j1}^2 \quad \dots \dots \quad (2-18)$$

$$a' P_{1r} = \left(\frac{p_1}{p_f}\right)^{1/7} \quad \text{where } r = 1, 2, \dots, n. \quad \dots \dots \quad (2-19)$$

2.2.2 BRAKEPIPE LEAKAGE

It is assumed that leakage occurs only at the last pipe of the brakepipe model. If we use a linear leakage resistance and a turbulent-compressible pipe resistance, the head-rear pressure relation is:

$$p_L^2 - p_R^2 = K_2^2 \quad \dots \dots \quad (2-20)$$

$$p_R = Rh \quad \dots \dots \quad (2-21)$$

where $K_2 = \frac{16f_1RT}{\pi^2 d^5 g_c}$ and $R = \frac{T^{1/2}}{KNA_0}$

Since initial pressures $p_L(0^+)$, leakage orifice area A_o , friction factor f , pipe length l and diameter or brakepipe d are known, $p_R(0^+)$ and initial mass flow rate $\dot{m}(0^+)$ can be obtained from the above equations. For each nodal point i , where $i = 2, 3, \dots, (M+1)$; $p_i(0^+)$ is equal $(p_L^2(0^+) - (K_2/l)(i-1)\dot{m}^2(0^+))^{1/2}$, where M is number of mesh size. Hence,

$$u' p_{1i}(0^+) = \left(\frac{p_L}{p_i}\right)^{5/7} u' p_{11}(0^+)$$

$$\text{where } u' p_{11}(0^+) = \frac{\dot{m}(0^+)}{c \beta_l A_1}$$

We then modify the boundary conditions as follows:
for right boundary condition,

$$u' p_{jn} = (0.5283)^{5/7} A_o a' p_{jn} / A_1 \quad \dots \dots (2-22)$$

$$u' p_{jn} + 5a' p_{jn} = u' L_{(j-1)(n-1)} + 5a' L_{(j-1)(n-1)} - \\ K' u' L_{(j-1)(n-1)} | u' L_{(j-1)(n-1)} | \delta t \quad \dots \dots (2-23)$$

for left boundary condition,

$$u' p_{j1} = \frac{\dot{m}(t)}{A_1 \beta_f a' \frac{5}{P_{j1}} c} \quad \text{since } a' p_{j1} \text{ is known.}$$

Note: The usual method of characteristics is used in calculating transient pressure distribution along the brakepipe. It is restricted to a brakepipe

without leakage along the length. However, if leakage is restricted to the ends of the pipe, we can do the calculation by modifying the boundary conditions. Since the formulation of equations for leakage along the brakepipe is cumbersome, further study on this case is necessary. In Appendix B, two computer programs using this method are presented.

CHAPTER 3

FORMULATION OF EQUATIONS FOR THE BRAKEPIPE MODEL BY LUMPED MODELING

3.1 INTRODUCTION

Since the formulation of equations for leakage along the brakepipes by the method of characteristics for large-amplitude signal was cumbersome, it needed to apply the method of lumped modeling. An excellent description of this method is given in Reference (21).

Simplified brakepipe model shown in Fig.3.1(a)&(b) is used to represent the brakepipe by a circuit with a series of volumes (capacitance) and fluid resistances. In a more exact model, fluid inertance will be included. At present, however, inertance is omitted. In appendix B, two computer programs using this method are presented.

3.2 MATHEMATICAL MODEL

3.2.1 COMPONENTS

In formulating the equations that describe a physical circuit model, it is important to specify the characteristics of the elements expressed as the relation between the through variable and the across variable.

- 38 -

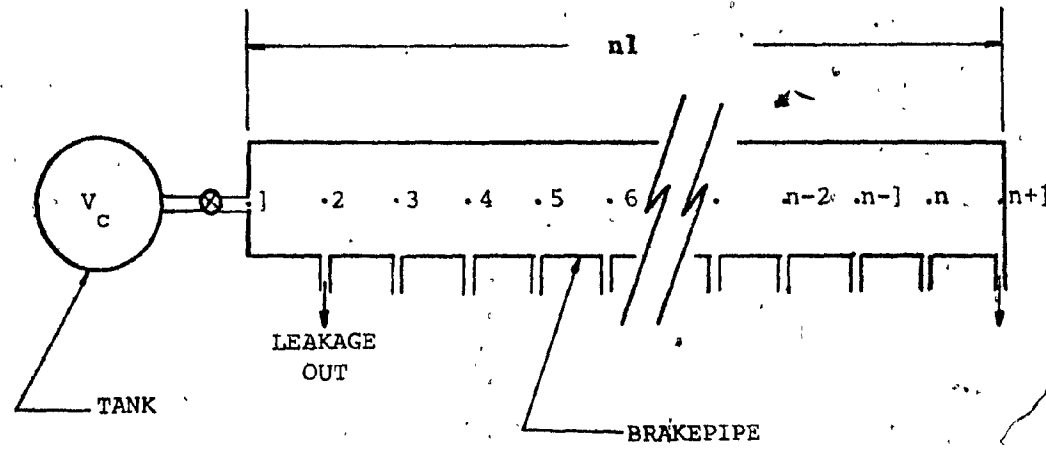


FIG. 3.]a SIMPLIFIED BRAKEPIPE MODEL

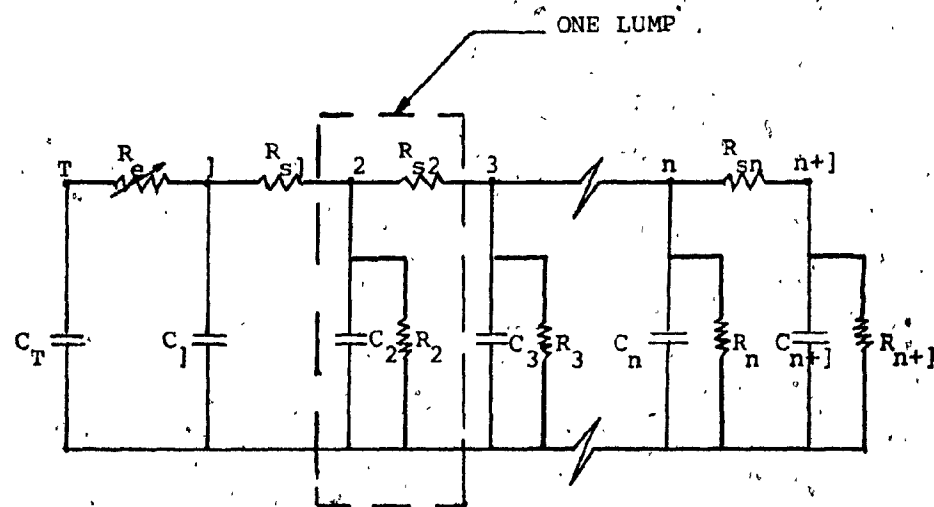


FIG. 3.]b LUMPED PARAMETER MODEL

The fundamental elements are restricted to resistive type components and capacitance only. This model, for fluid components, is complicated by the behaviour of turbulent and compressible flow through the pipes. Kwan(3) concluded that linear resistive leakage and a turbulent-compressible in-line flow component was the best model to be used for the resistances.

The components are:

A. Series Resistance R_{si}

The nonlinear relation, of the mass flow rate \dot{m}_i and pressure difference between i^{th} and $i+1^{\text{th}}$ pipes, is presented in Refs.(2,3,13) as:-

$$\dot{m}_i^2 = \frac{|p_{i+1}^2 - p_i^2|}{K_2} \quad \dots \dots (3-1)$$

where K_2 = constant characterizing flow resistance

$$= \frac{16f l \bar{R} T}{\pi^2 d^5 g_c} \quad \dots \dots (3-2)$$

f = friction factor

l = length between i^{th} and $i+1^{\text{th}}$ pipes

\bar{R} = gas constant

T = absolute temperature

d = diameter of pipe

g_c = gravitational constant

Simplifying equation(3-1) if $|p_{i+1} - p_i| \leq 20\text{kPa}$ (3psi), where $i = 1, 2, \dots, n$. Thus,

$$p_{i+1}^2 - p_i^2 \approx 2\bar{p}_i(p_{i+1} - p_i) \quad \dots \dots \quad (3-3a)$$

$$\text{or } \approx 2\bar{p}_{i+1}(p_{i+1} - p_i) \quad \dots \dots \quad (3-3b)$$

where \bar{p}_i = mean pressure value in brakepipe within
ith pipe

$$\text{Hence, } \dot{m}_i^2 = \frac{|p_{i+1} - p_i|}{R_{si}} \quad \dots \dots \quad (3-4)$$

$$\text{where } R_{si} \approx \frac{K_2}{2\bar{p}_{i+1}} = \frac{K_2}{\bar{p}_i + \bar{p}_{i+1}} \quad \dots \dots \quad (3-5)$$

To linearize the nonlinear equation(3-4), thus

$$\delta \dot{m}_i = \frac{\partial \dot{m}_i}{\partial (\Delta p_i)} \delta(\Delta p_i) \quad \dots \dots \quad (3-6)$$

$$\text{where } \Delta p_i = |p_{i+1} - p_i|$$

$$\Delta p_i = |\bar{p}_{i+1} - \bar{p}_i|$$

$$\text{Hence } K_i(\dot{m}_i - \bar{m}_i) = \Delta p_i - \Delta p_i \quad \dots \dots \quad (3-7)$$

where K_i = linearized resistance constant

$$= 2 \left(\frac{K_2 |\bar{p}_i - \bar{p}_{i+1}|}{\bar{p}_{i+1} + \bar{p}_i} \right)^{1/2} \quad \dots \dots \quad (3-8)$$

B. Shunt Capacitance C_i

This component is related to compressibility of fluid. Mass flow through the capacitance \dot{m}_{ci} is:

$$\dot{m}_{ci} = C_i \frac{dp_i}{dt} \quad \dots \dots \quad (3-9)$$

$$\text{where } C_i = \frac{V_i}{RT} = \frac{\pi d^2 l}{4RT}, \text{ from Ref.(22)} \quad \dots \dots \quad (3-10)$$

V_i = air volume of brakepipe per lump

l = length of a lump

C. Shunt Leakage Resistance R_L

This is a linear type resistance. It is based on the fact that when the pressure ratio of the brakepipe pressure and atmosphere, (p_i/p_f) is greater than 2, the leakage behaves as a choked orifice. The relation between brakepipe pressure and leakage flow is linear.

Leakage resistance R_i is:

$$R_{\frac{1}{k}} = \frac{\sqrt{RT}}{A_{oi}} \left/ \sqrt{y_E c \left(\frac{2}{y+1} \right)^{(y+1)/(y-1)}} \right. \quad \dots \dots \quad (3-11a)$$

For air, $\gamma = 1.4$, the shunt leakage resistance will be:

$$R_i = \frac{4\sqrt{T}}{0.5318\pi C_d d_{oi}^2 N} \quad \dots \dots (3-11b)$$

where p_f = atmospheric pressure

$$A_{oi} = \text{leakage area} = \pi d_{oi}^2 / 4$$

d_{oi} = diameter of leakage orifice

C_d = discharge coefficient

γ = ratio of specific heats

$$N = \left[\frac{\left(\frac{p_f}{p_i}\right)^{2/3} - \left(\frac{p_f}{p_i}\right)^{(3+1)/3}}{\left(\frac{3-1}{2}\right) \left(\frac{2}{3+1}\right)^{(3+1)/(3-1)}} \right]^{1/2}; \frac{p_f}{p_i} > 0.5283$$

$$= 1; \frac{p_f}{p_i} \leq 0.5283$$

Leakage flow through such a resistance is:

$$\dot{m}_{Li} = \frac{p_i}{R_i} \quad \dots \dots \quad (3-12)$$

3.2.2 TRANSIENT RESPONSE

A. Initial Condition during discharge:-

Since the circuit presentation of the model as shown in Figure 3.1(b) was nonlinear, it was very difficult to obtain a direct and exact relationship between supply source p_o and the pressure in the last pipe p_n with intermediate pressure terms not appearing. Hence a recursive formula was set up from which normalized pressures at each of the nodes (that is, the pressure distribution) could be found.

The pressure source p_o was constant. As air was released from the head-end to the rear-end, brakepipe pressure decreased due to plumbing leakage and resistance of the brakepipe.

The mass flow m_i is the sum of all leakage flow occurring after i th pipe, that is:

$$m_i = \sum_{j=1}^{n-i+1} \frac{p_{j+i}}{R_{j+i}} \quad \text{where } i = 1, 2, \dots, n \quad \dots \dots \quad (3-13)$$

Substituting equation(3-13) into equation(3-4), after some factoring, the result is :-

$$p_i = p_{i+1} \left[1 + \frac{K_2}{2R_{i+1}}^2 \left(1 + \sum_{j=1}^{n-i} \frac{p_{i+j+1} R_{i+1}}{p_{i+1} R_{i+j+1}} \right)^2 \right] \quad \dots \dots \quad (3-14)$$

as a shorthand notation, B_{i+1} is defined as follows:-

$$B_{i+1} = \frac{p_i}{p_{i+1}} \quad \dots \dots \quad (3-15)$$

Equation(3-15) can be used to express the ratios of non-adjacent pipe pressure as the products of terms. For example:-

$$\frac{p_{i+j+1}}{p_{i+1}} = \prod_{k=1}^j \left(\frac{1}{B_{i+k+1}} \right) \quad \dots \dots \quad (3-16)$$

Applying equation(3-15) and (3-16) to equation(3-14), one gets:

$$B_{i+1} = 1 + \frac{K_2}{2R_{i+1}} \left[1 + \sum_{j=1}^{n-i+1} \left(\prod_{k=1}^j \frac{1}{B_{i+k+1}} \right) \frac{R_{i+1}}{R_{i+j+1}} \right]^2 \quad \dots \dots \quad (3-17)$$

The value of B_i can be calculated from B_n to B_1 if one specializes R_i from R_i to R_n . For example, from eqn.(3-17) one gets:-

$$B_n = 1 + \frac{K_2}{2R_n} \quad \dots \dots \quad (3-18a)$$

$$B_{n-1} = 1 + \frac{K_2}{2R_{n-1}} \left[1 + \frac{R_{n-1}}{B_n R_n} \right]^2 \quad \dots \dots \quad (3-18b)$$

$$B_{n-2} = 1 + \frac{K_2}{2R_{n-2}} \left[1 + \frac{R_{n-2}}{B_{n-1} R_{n-1}} + \frac{R_{n-2}}{B_{n-1} B_n R_n} \right]^2 \quad \dots \dots \quad (3-18c)$$

Then the pressure at any pipe p_i can be related to the initial pressure p_0 as:-

$$\frac{p_i}{p_0} = \prod_{k=1}^i \frac{1}{B_k} \quad \dots \dots (3-19)$$

From the known values of series resistance K_2 and the shunt resistance R_i , B_i can be calculated from B_n to B_1 .

Then the pressure distribution along the pipes can be computed by applying equation (3-17) to (3-19). If one specifies the value of R_i these equations can also be applied to the case of uneven leakage distribution. In general, the ratio $K_2/2R_i^2$ will be very small, and as a result, the powers of $K_2/2R_i^2$ will be second order small. If this approximation is made, equations (3-17) and (3-18) can be reduced to a simplified function particularly in the case of uniform leakage distribution.

If $K_2/2R_i^2 \approx 0$, and $R_1=R_2=\dots=R_n$, substituting them into equation (3-18), thus:

$$B_n = 1 + \frac{K_2}{2R_n^2} \quad \dots \dots (3-20a)$$

$$B_{n-1} = 1 + \frac{K_2}{2R_n^2} (2)^2 \quad \dots \dots (3-20b)$$

$$B_{n-2} = 1 + \frac{K_2}{2R_n^2} (3)^2 \quad \dots \dots (3-20c)$$

Substituting equation (3-20) into (3-16) and relating the ith pipe and 1st pipe to the last pipe, one gets:

$$\frac{p_i}{p_n} = \frac{1}{\left[1 + \frac{K_2}{2R_n^2}\right] \left[1 + \frac{K_2}{2R_n^2}(2)^2\right] \dots \left[1 + \frac{K_2}{2R_n^2}(i)^2\right]} \dots \dots \quad (3-21)$$

$$\frac{p_o}{p_n} = \frac{1}{\left[1 + \frac{K_2}{2R_n^2}\right] \left[1 + \frac{K_2}{2R_n^2}(2)^2\right] \dots \left[1 + \frac{K_2}{2R_n^2}(n)^2\right]} \dots \dots \quad (3-22)$$

Again, the same approximation is applied, and equations (3-21) & (3-22) are combined. Thus,

$$\frac{p_i}{p_o} = \frac{1 + \frac{K_2}{2R_n^2} \left[(n-i)(n-i+1)(2n-2i+1)/6 \right]}{1 + \frac{K_2}{2R_n^2} \left[n(n+1)(2n+1)/6 \right]} \dots \dots \quad (3-23)$$

An approximate normalized form of this equation is given from Ref.(3) as follows:-

$$\frac{\frac{p_o - p_i}{K_2}}{p_o \left(\frac{K_2}{2R_n^2} \right) (n)^3} = \frac{1 - (1-\alpha)^3}{3} \dots \dots \quad (3-24)$$

where $i = 1, 2, \dots, n$ and $\alpha = \frac{i}{n}$

Since p_o is defined as supply pressure, p_i can be found accordingly.

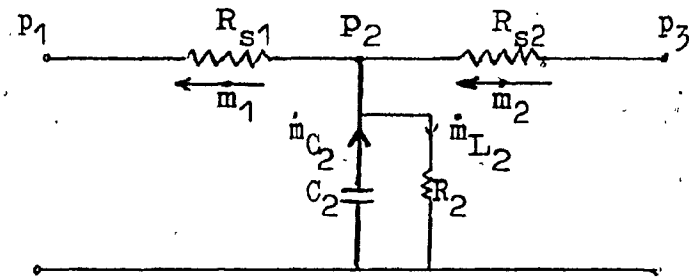
During discharging process, boundary conditions for our brakepipe model will be:

\dot{m}_o = mass flow rate at the locomotive = 0

\dot{m}_{n+1} = mass flow rate at the $n+1^{th}$ pipe = 0

Note: As the leakage is concentrated in the rear of the pipes, rate of pressure drop in the front becomes smaller. This is a consequence of the fact that the total leakage flow becomes smaller. For further explanation of the above equations, one can refer to Aula's thesis(2) and/or Kwan's thesis(3).

B. Transient state of this model will be:-



The sign conventions of the 4 mass-flows are arbitrary though consistent with what is happening during service or discharge. Mass-flow balance is:

$$\dot{m}_{C2} = -\dot{m}_2 + \dot{m}_1 + \dot{m}_{L2} \quad \dots \dots (3-25)$$

According to equation(3-9), one gets:

$$\dot{p}_2 = \frac{1}{C_2} (-\dot{m}_2 + \dot{m}_1 + \dot{m}_{L2}), \text{ where } \dot{p}_2 = \frac{dp_2}{dt} \quad \dots \dots (3-26a)$$

From equations(3-4),(3-10) and (3-12), one modifies equation(3-26a) by substitution. Hence,

$$\dot{p}_2 = \frac{R_T}{V_2} \left(-\sqrt{\frac{(p_3 - p_2)}{R_{s2}}} + \sqrt{\frac{(p_2 - p_1)}{R_{s1}}} + \frac{p_2}{R_2} \right) \quad \dots \dots (3-26b)$$

After time increment δt , the pressure p_2 will be:

$$p_2(t + \delta t) = p_2(t) - p_2(t) \cdot \delta t \quad \dots \dots (3-27)$$

In general,

$$\begin{aligned}\dot{p}_i &= \frac{1}{C_i} (-\dot{m}_i + \dot{m}_{i-1} + \dot{m}_{L_i}) \\ &= \frac{1}{C_i} \left(-\sqrt{\frac{(p_{i+1}-p_i)}{R_{s1}}} + \sqrt{\frac{(p_i-p_{i-1})}{R_{s(i-1)}}} + \frac{p_i}{R_i} \right) \dots \dots (3-28)\end{aligned}$$

$$p_i(t+\delta t) = p_i(t) + \dot{p}_i(t) \cdot \delta t \dots \dots (3-29)$$

where $i = 2, 3, \dots, n$

The rate of pressure drop \dot{p}_1 & \dot{p}_{n+1} at the left- and right-boundary, respectively, is:

$$\dot{p}_1 = \frac{1}{C_1} \left(-\sqrt{\frac{p_2-p_1}{R_{s1}}} \right) \dots \dots (3-30)$$

$$\text{where } C_1 = C_i/2 \quad \text{and} \quad R_{s1} = \frac{16f_1RT}{\pi^2 d^5 g_c (p_1+p_2)}$$

$$\dot{p}_{n+1} = \frac{1}{C_{n+1}} \left(\sqrt{\frac{p_{n+1}-p_n}{R_{sn}}} + \frac{p_{n+1}}{R_{n+1}} \right) \dots \dots (3-31)$$

where $C_{n+1} = C_i/2$ = shunt capacitance

R_{sn} = in-line resistance

$$= \frac{16f_1RT}{\pi^2 d^5 g_c (p_{n+1}+p_n)}$$

R_{n+1} = leakage resistance = R

$$= \frac{4T^{1/2}}{0.5318\pi d_{oi}^2}$$

CHAPTER 4

EXPERIMENTAL INVESTIGATION AND DISCUSSION

4.1 INTRODUCTION

At first, diaphragm-type electrical pressure transducer was calibrated against a manometer (accuracy within $\pm 0.1\%$) and a digital multimeter was set to provide 0-10 volt reading to govern the working range of the transducer in later experiments. The schematic drawing of the calibration set-up and result of this calibration are shown in Fig.4.1(a)&(b) respectively.

Before the assembly of the complete test set-up, two types of preliminary experiment were done. These compared the pressure-flow characteristics on pipe-bend combination and orifices in accordance with the mathematical description given in the previous chapters. The test set-up and results for brakepipe model will be given separately in the following sections. Comparisons between the experimental and theoretical results will then be discussed.

Main objective of the investigation is to find the effects of leakage on the time delay so as to check

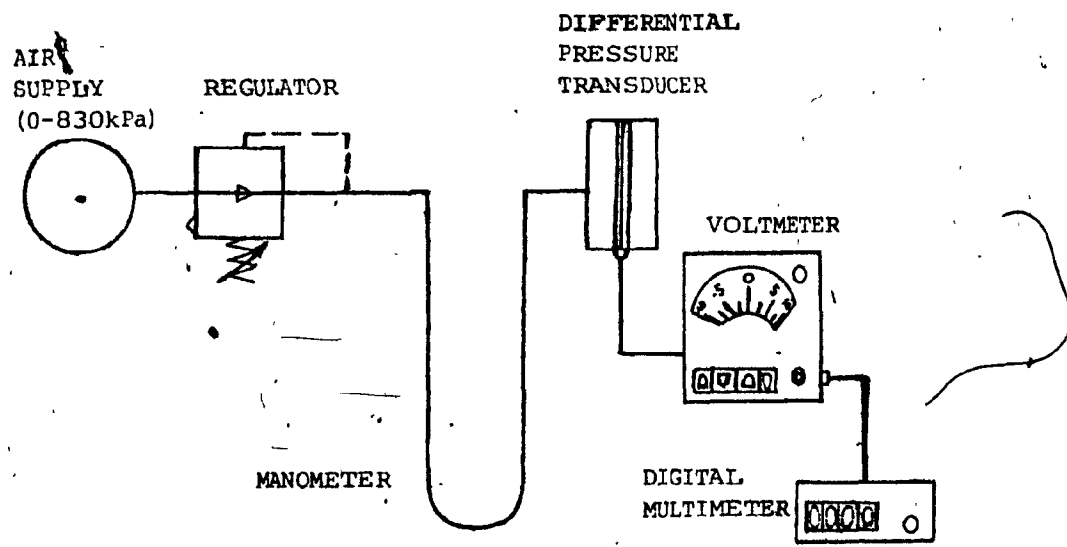


FIG.4.]a TEST SET-UP FOR CALIBRATION

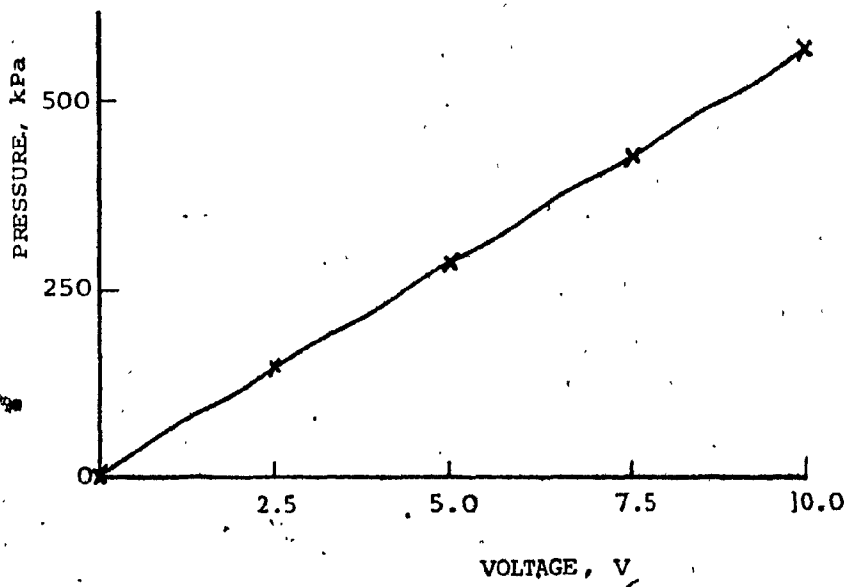


FIG.4.]b RESULT OF TRANSDUCER CALIBRATION

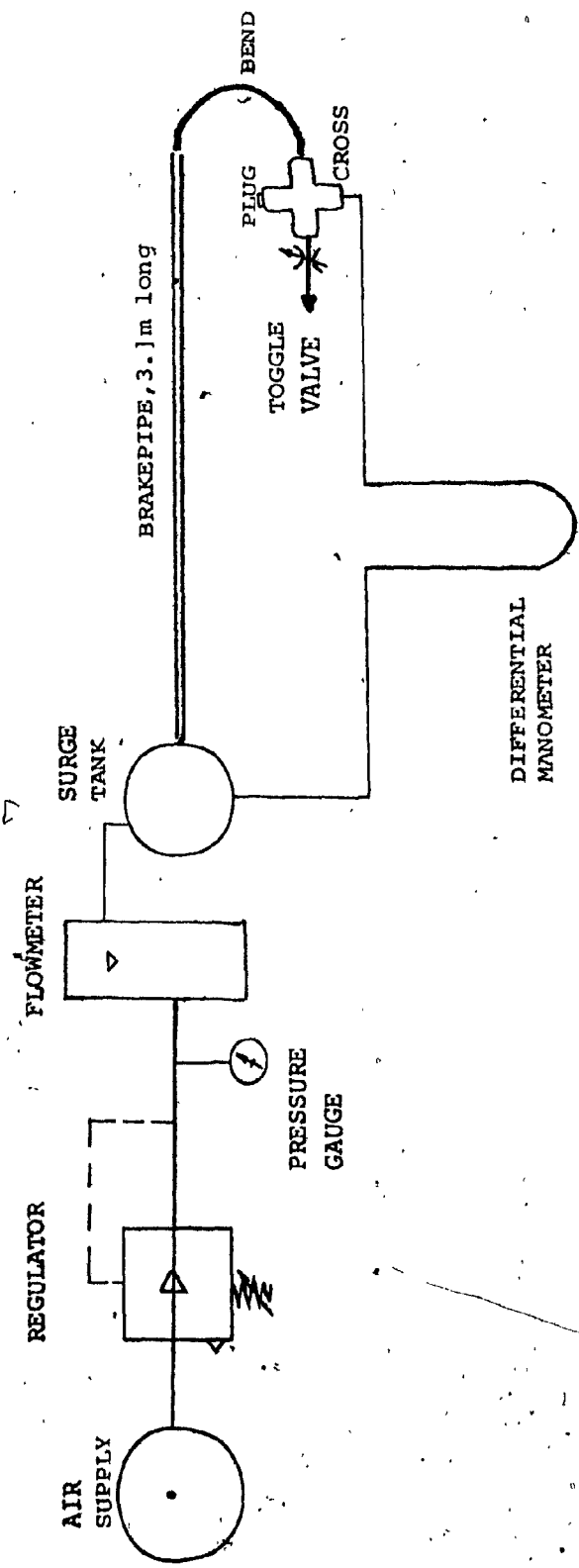


FIG. 4.2 SET-UP FOR PRESSURE-FLOW CHARACTERISTIC ON PIPE-BEND COMBINATION

the propagation speed of air wave in the brakepipe model.

4.2 PRESSURE-FLOW CHARACTERISTIC ON THE PIPE-BEND COMBINATIONS

4.2.1 PIPE TEST SET-UP

Figure 4.2 shows the schematic drawing of the set-up. In this experiment, a regulated supply of air 552kPa (80 psig), was passed through a FP-1/4-20 flowmeter and then to an individual pipe-bend combination. The pipe-bend combination basically consisted of a galvanized pipe and a flexible plastic tubing with a cross. The galvanized pipe was 3.1m (10ft.) long and 6.35×10^{-3} m (0.25in.) inside diameter. This arrangement gave an approximate scale down ratio of 5:1. The pipes were connected by 0.254m (10in.) length of plastic tubing in an U-bend with a cross placed downstream of the bend. The flow through the pipe-bend was varied by a toggle valve placed at the end of the whole unit. The volume flow measurement was read by the flowmeter and was subsequently converted to mass flow by the manufacturer's flow-conversion chart. The pressure drop between the head end and the cross was measured by a differential manometer.

4.2.2 PIPE-BEND COMBINATION TEST AND RESULTS

During this experiment, the head end pressure was maintained at 552kPag. Air flow through the combination was controlled by a valve. The pressure change in the rear end due to different flow could be read on the water manometer. Figure 4.3 shows the difference in the square of non-dimensional pressure between the head end (L) and the rear end (R) of the pipe-bend combination, that is, $(p_L^2 - p_R^2)/p_f^2$ against the mass-flow, \dot{m} . The experimental data varied from one pipe-bend combination to another. The lowest experimental value of K_2 was $1.70 \times 10^{13} \text{ kPa}^2 \cdot \text{s}^2 / \text{kg}^2$ ($8.1 \times 10^6 \text{ lbf}^2 \cdot \text{sec}^2 / \text{in}^4 \cdot \text{lbfm}^2$) and the highest value was about $3.78 \times 10^{13} \text{ kPa}^2 \cdot \text{s}^2 / \text{kg}^2$ ($18.0 \times 10^6 \text{ lbf}^2 \cdot \text{sec}^2 / \text{in}^4 \cdot \text{lbfm}^2$). The mean curve was drawn by using the equation(3-2) with mean K_2 .

Data obtained from 83 different bend pipe-sections are shown in a form of data distribution chart in Fig.4.4, which is drawn according to the number of data fell on a small range of pressure difference. It was found that most of data fell to region number 2.

With the geometric parameters of the pipe, friction factor f is equal to 0.06, and neglecting the curvature of the bend, resistance constant for the turbulent-compressible flow in the pipe, K_2 ,which is calculated from the equation(3-2),is $2.52 \times 10^{13} \text{ kPa}^2 \cdot \text{s}^2 / \text{kg}^2$ ($12.0 \times 10^6 \text{ lbf}^2 \cdot \text{sec}^2 / \text{in}^4 \cdot \text{lbfm}^2$). Calculated K_2 was agreed well with mean K_2 .

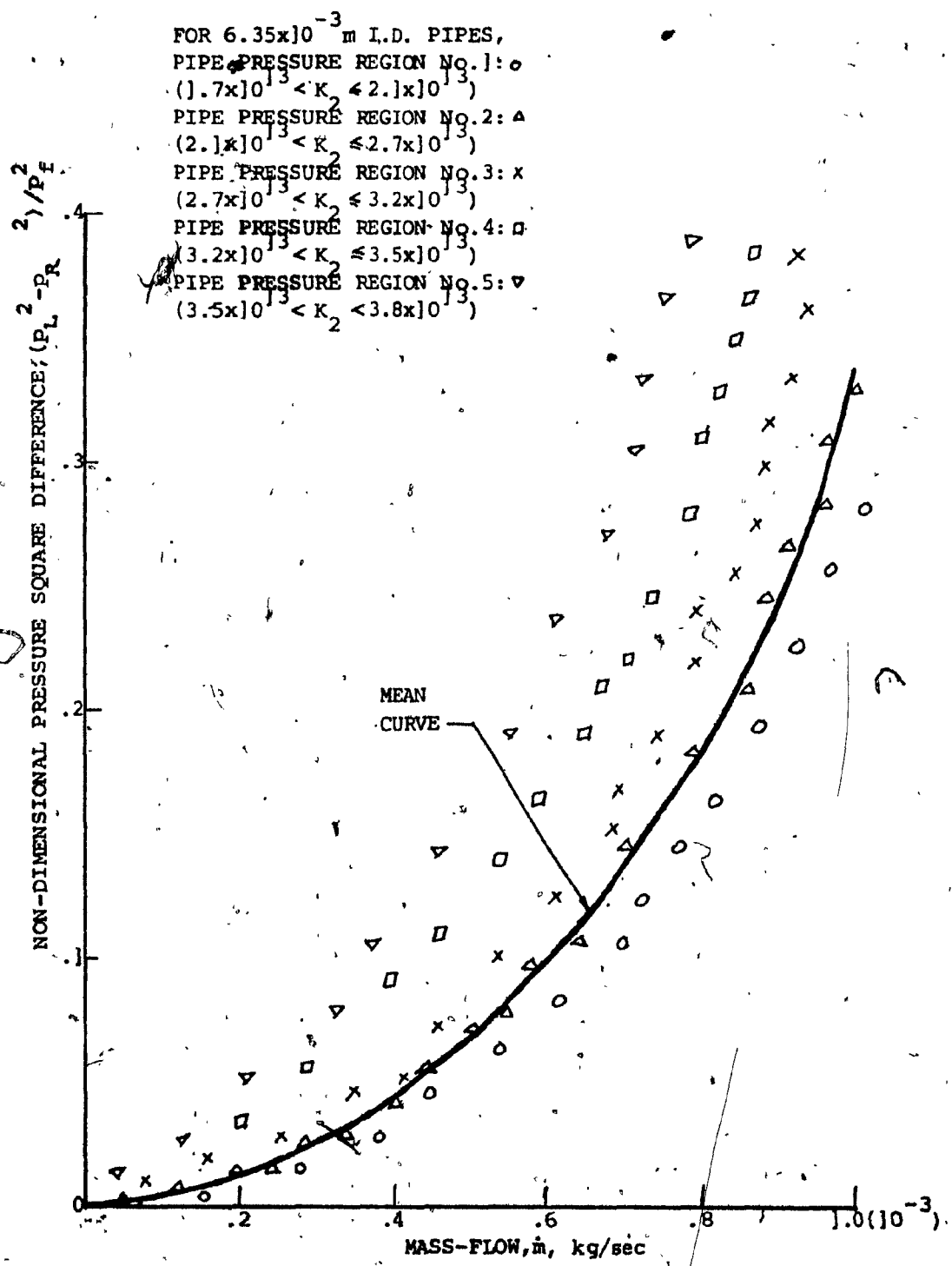


FIG. 4.3 MASS-FLOW CHARACTERISTIC OF THE PIPE-BEND COMBINATION

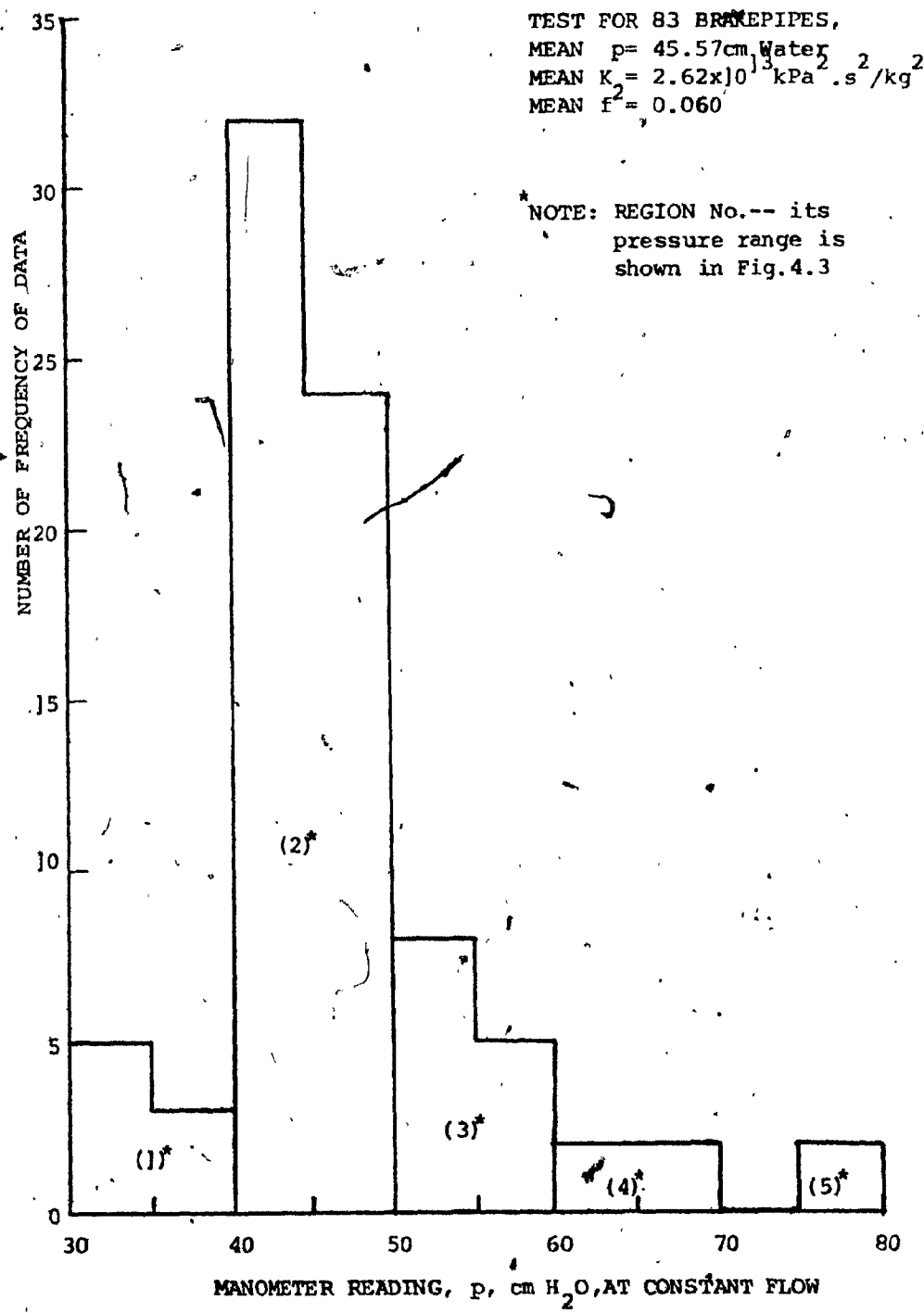


FIG. 4.4 DATA DISTRIBUTION CHART

4.3 PRESSURE-FLOW CHARACTERISTIC ON THE ORIFICE

4.3.1 ORIFICE TEST SET-UP

Figure 4.5 shows the schematic drawing of this set-up. During the test, the air supplied from the air pressure regulator was passed through a flowmeter and a cross. The openings of the cross, perpendicular to the flow direction were used to mount a pressure gauge and a toggle valve. At the exhaust port of the valve, a pipe-plug was mounted, and a 'leakage' orifice was formed by drilling a thin hole through the centre of the plug. The opening facing to the flow direction was blocked by a hexagonal plug. The flow into the set-up could be varied with a regulator and the pressure inside the cross was indicated on the pressure gauge. Five types of the orifice ($d_o = 0.330\text{mm}, 0.584\text{mm}, 0.787\text{mm}, 1.397\text{mm}, 1.854\text{mm}$ inside diameter) which were used to model the leakage resistance were examined in the following section.

4.3.2 ORIFICE TEST AND RESULTS

During the orifice test, the ~~and~~ pressure could be changed by the regulator, and the leakage flow from the orifice was indicated on the flowmeter. In the case of the resistance leakage experiment; all orifices of the same diameter yielded pressure-flow characteristics within

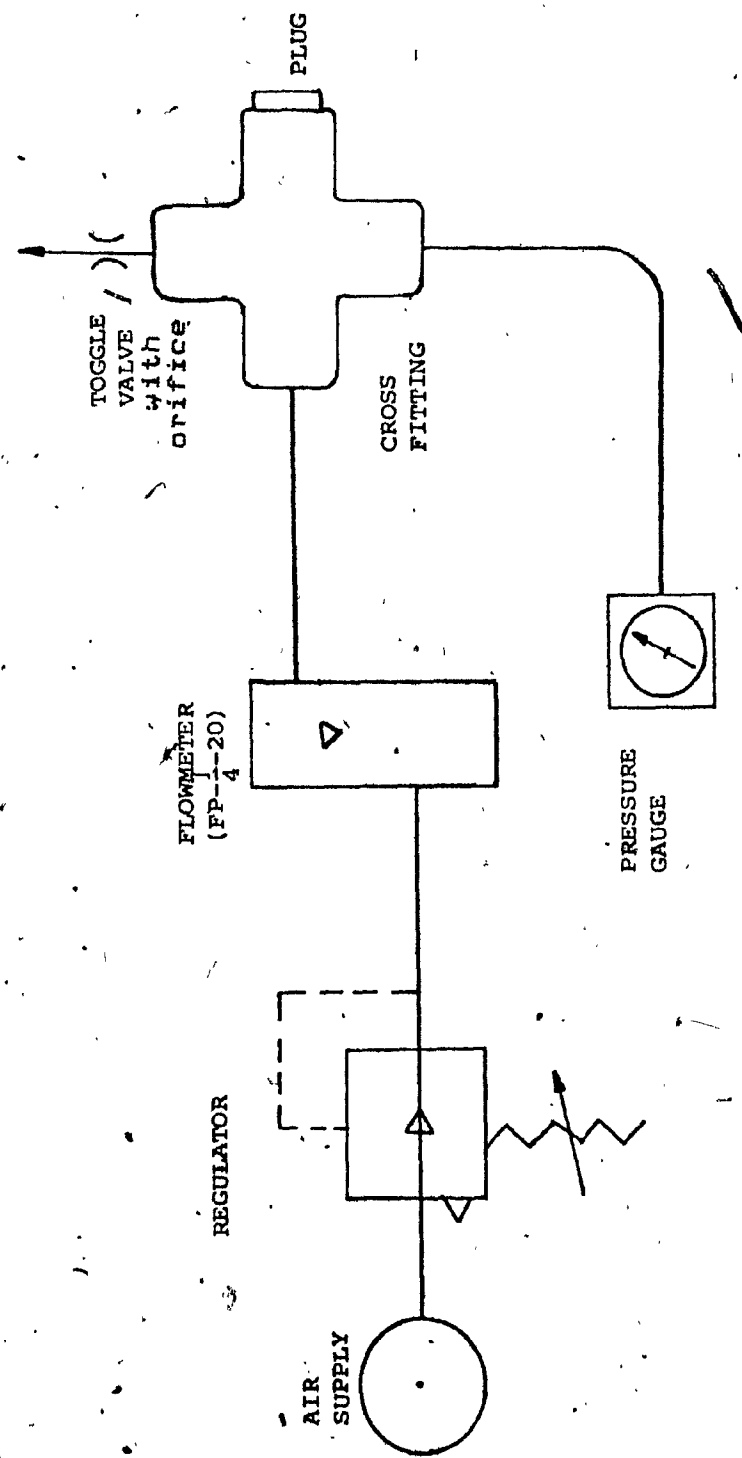


FIG. 4.5 SET-UP FOR THE ORIFICE TEST

$\pm 5\%$. Some typical experimental pressure-flow characteristics of the orifices are given in Figure 4.6. The theoretical characteristic calculated from equation(3-11b) with $C_d = 0.82$ are superimposed on the above figure. Theory and experiment were in good agreement in this case. Thus, the linear leakage resistance, R_i , of the orifice with the normalized diameter $d_o/d = 0.052$ was $56.1 \times 10^5 \text{ kPa-s/kg}$ or $36.5 \times 10^4 \text{ lbf-sec/in}^2\text{-lbm}$ and of the orifice with $d_o/d = .292$ was $1.94 \times 10^5 \text{ kPa-s/kg}$ or $1.26 \times 10^4 \text{ lbf-sec/in}^2\text{-lbm}$.

4.4 SCALED-DOWN BRAKEPIPE MODEL

4.4.1 MODEL TEST SET-UP

Figure 4.7(a) is a picture of our brakepipe model along with some measuring equipment and Figure 4.7(b) is the schematic drawing. Table of specification is presented in Table 4.1. The model connected of 75 pipe-bend combinations. They were connected and mounted parallel to one another 12.5mm apart. Pressure gauge was used to monitor the supply pressure. Surge tank was connected to reduce pressure fluctuation at the supply. The transducers have an accuracy of 0.5% and a digital multimeter of 0.04% accuracy were used to provide easy read out.

Figure 4.8 and Table 4.2 show how 75 pipe-bend combinations were connected. Two openings in each cross,

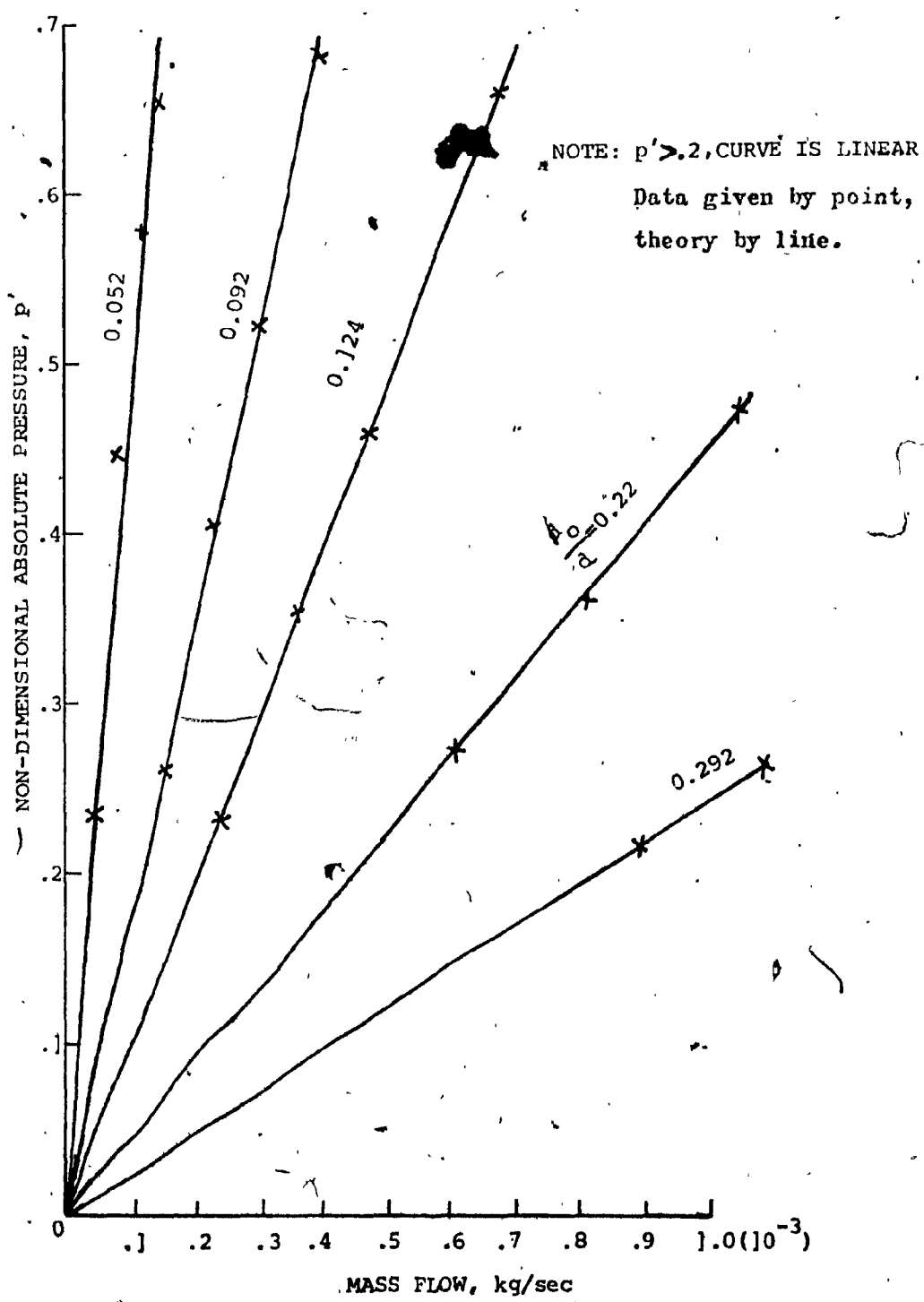


FIG. 4.6 PRESSURE-FLOW CHARACTERISTICS OF THE ORIFICES

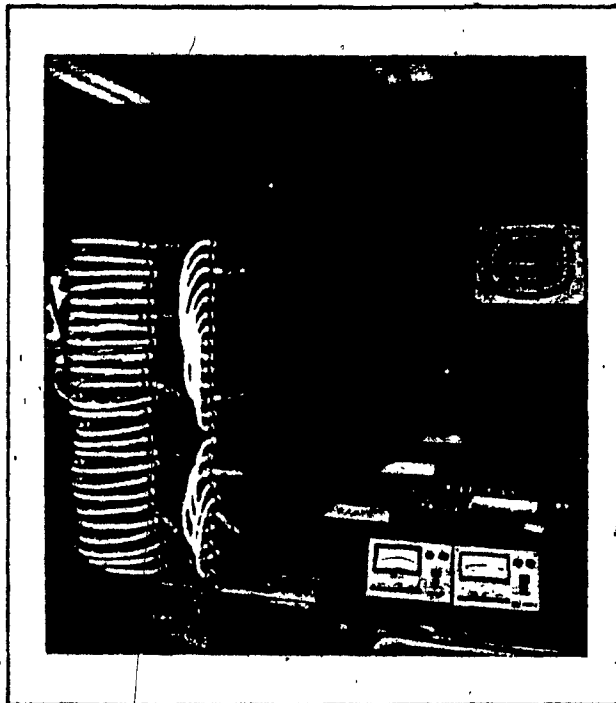


FIG. 4.7a A PHOTO OF BRAKEPIPE MODEL

NOTE: THIS EXPERIMENTAL MODEL WAS
SET-UP AND DEMONSTRATED IN
FLUID CONTROL RESEARCH LAB.
CONCORDIA UNIVERSITY.

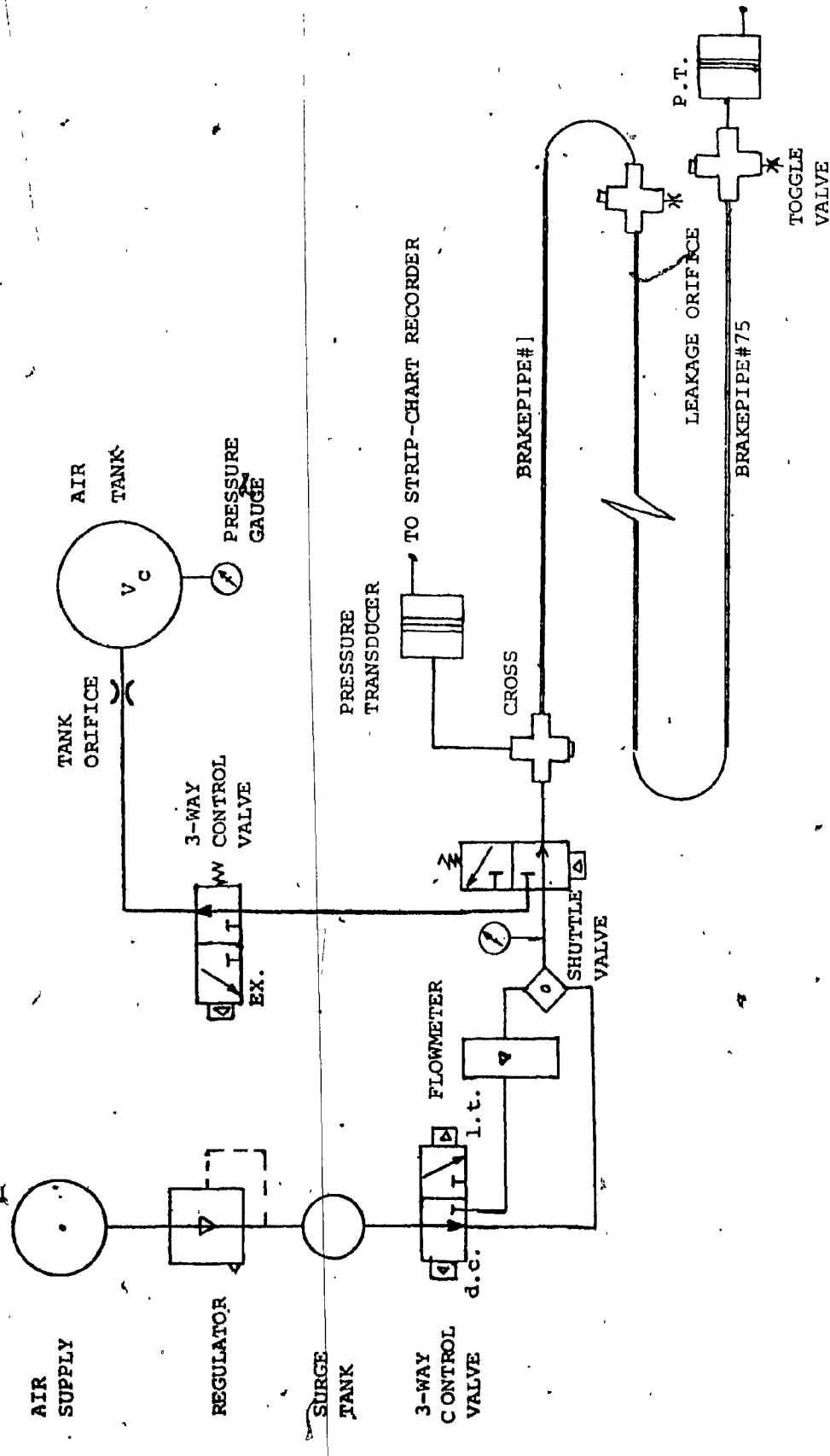


FIG. 4.7b SCHEMATIC DRAWING OF BRAKEPIPE MODEL.

TABLE 4.1 SPECIFICATION FOR BRAKEPIPE MODEL

PIPES

Number of brakepipes	75
Material	Cast Iron
Length of a pipe	3.05m
Inside diameter	6.35×10^{-3} m
Outside diameter	9.52×10^{-3} m
Friction factor	0.06

FITTINGS

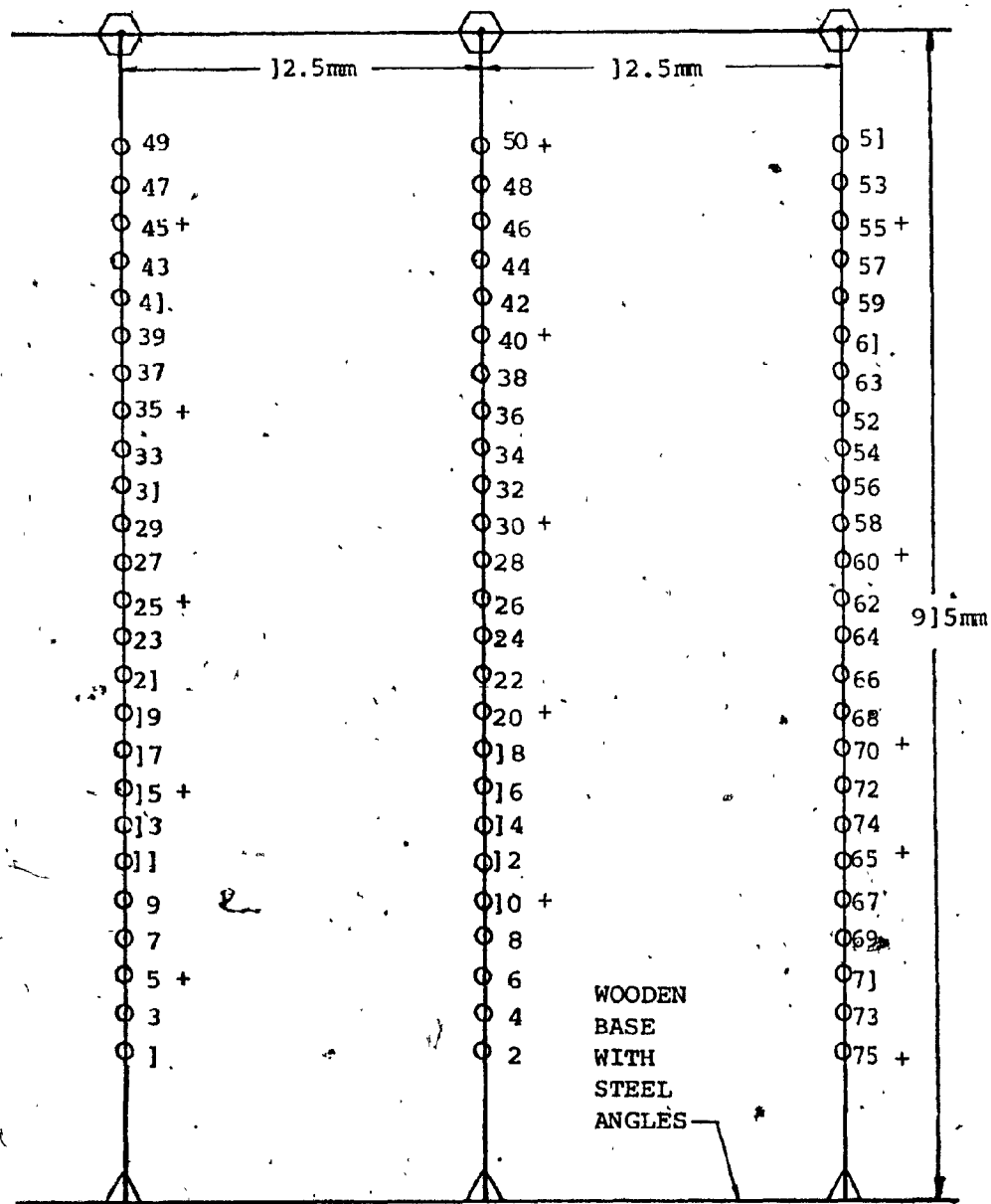
75 Plastic tubes	230mm each
15 Crosses	
15 Toggle valves	
15 Hexagonal plugs with orifices	
150 Male and female connectors	

OTHER APPARATUS

1 Differential manometer	0-80cm H ₂ O
3 Pressure transducers	electrical type
3 three-way control valves & one shuttle valve	
1 Pressure source	0-830kPa
1 Surge tank(steel)	700 c c
1 Pressure chamber(steel)	1737 g c
1 Strip-chart recorder	4-channel
1 Regulator	0-690kPa
1 Flowmeter	0-12.5c c /sec
1 Digital multimeter	0-10 volts
2 Pressure gauges	0-690kPa
3 Wooden stands with 25 holes each	

perpendicular to the flow direction, were connected with a toggle valve on which an orifice was used to simulate flow leakage, and a plug to prevent air exhausting from this opening. On the 1st, 25th and 75th pipes, there was a differential pressure transducer mounted. Pipe pressure was measured and recorded by 4-channel strip-chart recorder. For uniform resistance-leakage distribution, 15 same-size orifices were used (in every 5 pipe-bend combinations). If no leakage is desired, the toggle valve can be shut off in order to block the air flow through the orifice. An 1737 cc(106 cu.in.) air tank was located at the front end of the 1st pipe and was used to store mass of air during discharging process or pressure reduction. The air flow into the tank was controlled by a 3-way control valve.

It should be noted that, besides the physical configuration, there are some differences between the actual brakepipe and the experimental set-up:- In the analytical and experimental models, brakepipe leakage is concentrated at one point while the leakage in an actual freight car is distributed at random; the flow through the connecting hose of a freight car has more restriction than the experimental pipe fitting; the brakepipe in a freight car has some degree of curvature depending on location of other devices equipped on the



NOTE: SYMBOLS -- ○ FOR HORIZONTAL PIPE
 + FOR CROSS FITTING

FIG. 4.8 PIPING DIAGRAM FOR BRAKEPIPE MODEL

TABLE 4.2 TUBING CONNECTION

LEFT-ENDS(L)		RIGHT-ENDS(R)	
INPUT	- 1L	38L - 39L	1R - 2R 39R - 40R
2L	- 3L	40L - 41L	3R - 4R 41R - 42R
4L	- 5L	42L - 43L	5R - 6R 43R - 44R
6L	- 7L	44L - 45L	7R - 8R 45R - 46R
8L	- 9L	46L - 47L	9R - 10R 47R - 48R
10L	- 11L	48L - 49L	11R - 12R 49R - 50R
12L	- 13L	50L - 51L	13R - 14R 51R - 52R
14L	- 15L	52L - 53L	15R - 16R 53R - 54R
16L	- 17L	54L - 55L	17R - 18R 55R - 56R
18L	- 19L	56L - 57L	19R - 20R 57R - 58R
20L	- 21L	58L - 59L	21R - 22R 59R - 60R
22L	- 23L	60L - 61L	23R - 24R 61R - 62R
24L	- 25L	62L - 63L	25R - 26R 63R - 64R
26L	- 27L	64L - 65L	27R - 28R 65R - 66R
28L	- 29L	66L - 67L	29R - 30R 67R - 68R
30L	- 31L	68L - 69L	31R - 32R 69R - 70R
32L	- 33L	70L - 71L	33R - 34R 71R - 72R
34L	- 35L	72L - 73L	35R - 36R 73R - 74R
36L	- 37L	74L - 75L	37R - 38R 75R - CLOSED

NOTE: EACH PLASTIC TUBE IS 230mm - 250mm LONG.

car; and the use of brake cylinder and relay valve in a real car has been replaced by 'artificial' pressure tank and orifices in the experimental model.

Before performing the experiment, all fittings were checked carefully for plumbing leakage. Once tested integrity of the test rig, several parameters such as brakepipe gradient, plumbing leakage flow rate and rate of "plumbing leakage" pressure drop were considered. One regulated the pressure source from 345kPa to 759kPa, then measured the pressure difference between the head-end and rear-end, air flow rate and plumbing leakage rate. Hence, Table 4.3 show a set of acceptable criteria on this model. Since the brakepipe gradient was within 5% of the supply pressure, and the leakage rate was low, one could continue to perform the following experiments.

4.4.2 BRAKEPIPE MODEL TESTS AND RESULTS

4.4.2.1 Pressure Gradient Test and Result

In the set-up for flow resistance leakage, a small orifice of 0.33mm in diameter was placed in each cross-fitting with the toggle valve. The head-end pressure was maintained at 552kPas by the regulator. Pressure differential measurements at every 5 pipe-bend combinations were measured with pressure transducers. Figure 4.9 shows the result of the steady state pressure gradient

TABLE 4.3 MODEL CONDITION FOR PLUMBING

SUPPLY PRESSURE (kPa)	BRAKEPIPE GRADIENT (kPa)	PLUMBING LEAKAGE FLOW RATE (c c /sec)	PLUMBING LEAKAGE RATE (kPa/sec)
345	11.7	4.24	0.020
414	15.2	4.61	0.028
483	19.3	4.92	0.033
552	23.5	5.23	0.040
621	26.9	5.54	0.046
690	30.4	5.84	0.052
759	34.5	6.15	0.059

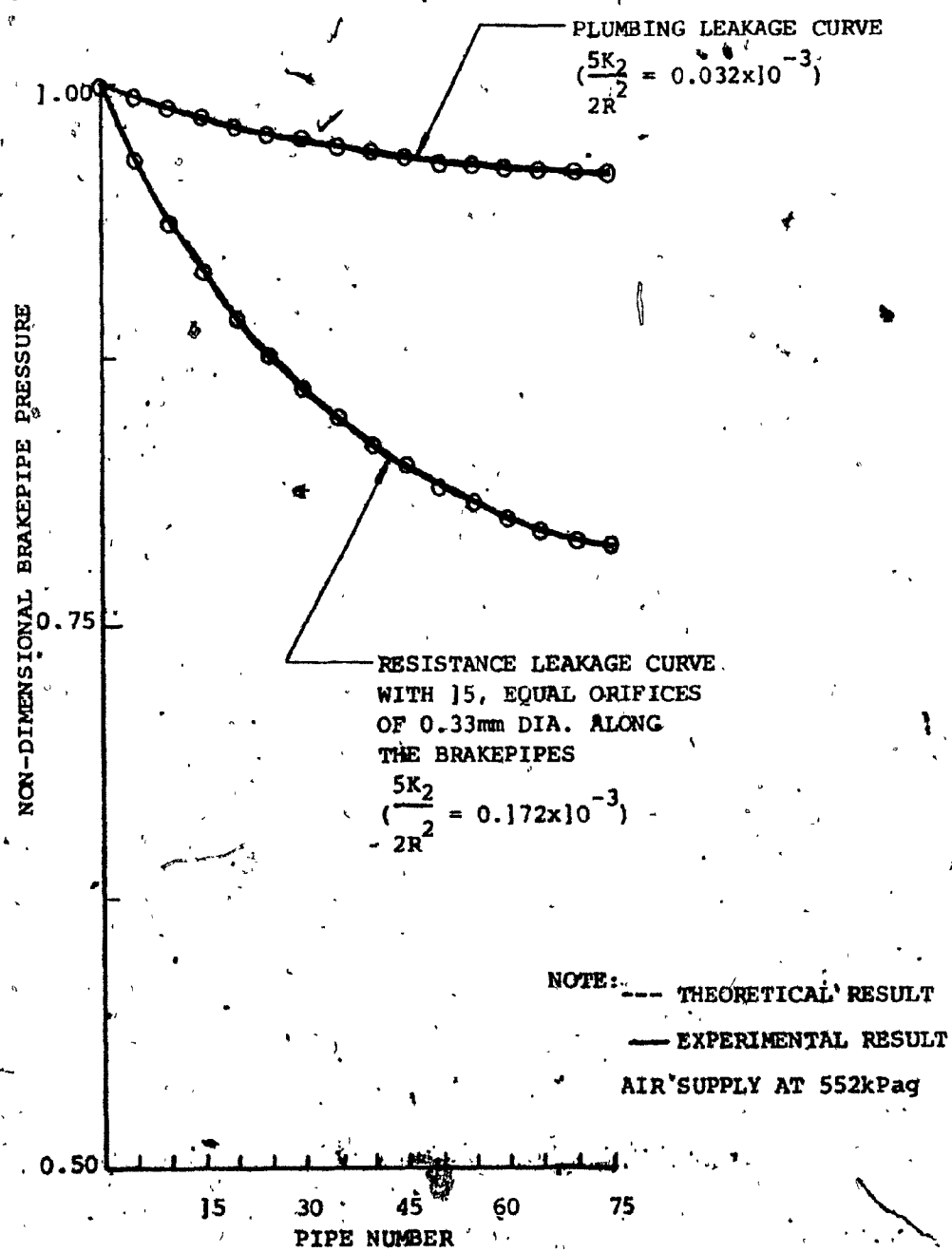


FIG.4.9 STEADY STATE PRESSURE GRADIENT CURVES

test in this case.

Kwan(3) mentioned that towards the rear of the composite pipe the weighting factor of rear pipes becomes significant. A rear pipe error in the pipe resistance constant K_2 , or leakage resistance R_i was weighted and therefore its effect was magnified. Any truncation error would show up more pronounced in the rear. The data and model diverge gradually as the pipe position was further from the head end as shown in Ref.(3). In addition, one must recognize that the model was initially calculated with equal values of R_i and K_2 for each pipe. The data from Figures 4.3 and 4.6 show that this is not the case. Therefore, one applied equation(3-19) with the individual values measured for R_i and K_2 on each pipe and orifice. From Figure 4.9, "resistance leakage" pressure gradient curve was drawn according to "plumbing leakage" pressure gradient curve. Superimposed on the experimental curves was the result obtained from the analytical model. It was found that much closer agreement between experiment and theory was achieved.

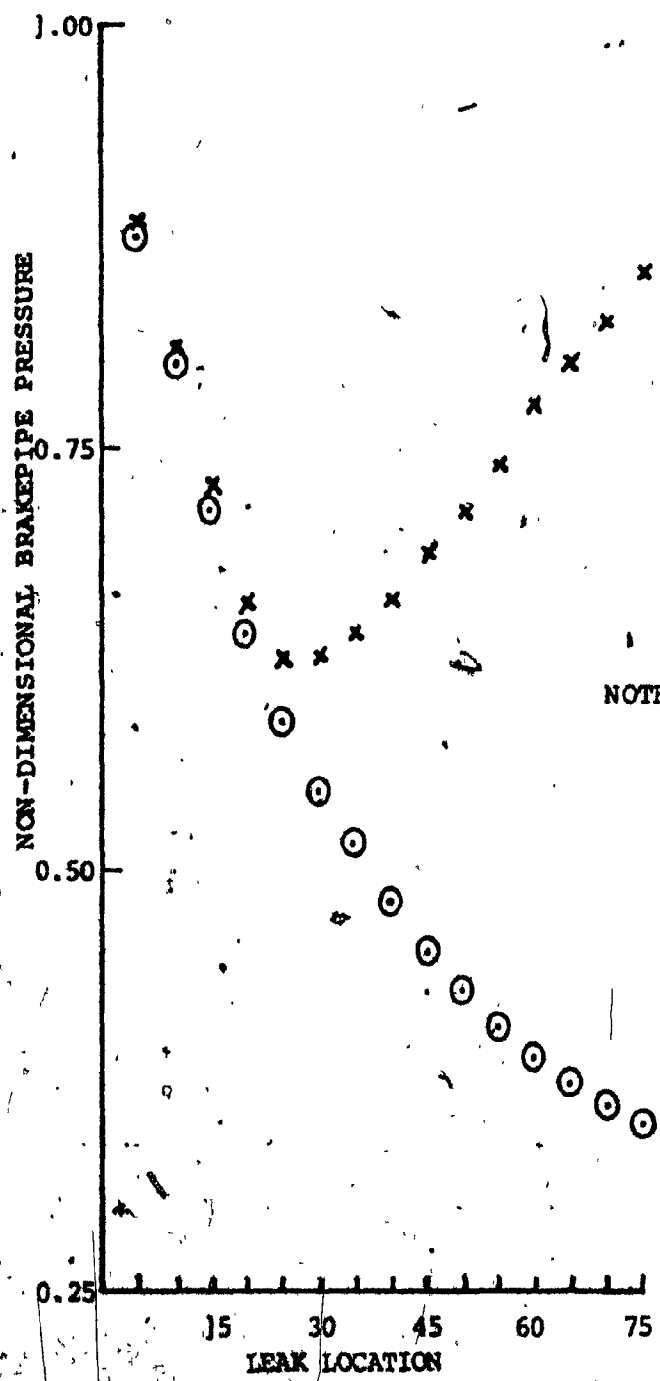
In order to show how the location of leaks would affect the pressure distribution, an experiment was demonstrated as follows: the head-end pressure was kept at 552kPag by the regulator; one leakage orifice of 1.854mm in diameter was located at the first cross-fitting

along with toggle valve while other toggle valves were switched off; pressure differential measurements were recorded at pipes no.25 and no.75 by pressure transducers. Then we relocated the leakage orifice to the second cross fitting until the fifteen cross fitting and repeated the above measurements. Hence, steady-state pipe pressure against leak position curves were plotted as shown in Fig. 4.10. As the location of leaks moved toward the rear end of the brakepipe model, the pressure of pipe 25th was increasing while the pressure of pipe 75th was decreasing. It implied that the concentration of leakage at rear-end was more serious in affecting the pressure distribution and gradient.

4.4.2.2 Pressure Reduction Test and Result

At first, all toggle valves were closed. All 75 brakepipes were charged to 552kPag from an air supply by the regulator while 3-way control valve allowed air flow only to the brakepipes. The control valve was switched to block the pressure supply and to direct air flow to pressure chamber through an orifice simultaneously. (three types of exhaust orifice between the chamber and the pipes were used, i.e. $d_e/d = 0.124, 0.22$ and 0.292)

Since it has been justified in Chapter 1 that the chamber (or air tank) could represent the relay valve, a



NOTE: \times MEASURED AT PIPE #25
○ MEASURED AT PIPE #75
FOR 552kPa AIR SUPPLY,
USE ONE 1.854mm DIA.
LEAKAGE ORIFICE.

FIG. 4.10 STEADY STATE PRESSURE VS. LEAK LOCATION CURVES

decrease of the brakepipe pressure at a rate and in an amount sufficient to cause a brake application can be achieved easily. Also, the amount of pressure reduction was related to the size of air tank and the brakepipe leakage.

In this experiment it was interesting to pay more attention to the pressure drop at the first pipe at the beginning of 10 seconds as illustrated in Figures 4.11 and 4.12. When exhaust orifice size (d_e) was increased (this is the same as reducing resistance or underdamping), brakepipe pressure fluctuated rapidly (as an undershoot). A sudden turbulent momentum occurred as toggle valve was suddenly opened, which made the pressure drop exceeding the amount of pressure reduction. Owing to higher pressure at the rear end, the backward flow from the rear end to the head end reinforced the pressure at the head end. Thus the head end pressure kept on increasing until the chamber pressure reached a maximum value (same as head end pressure). In Figure 4.11, time taken for pressure dropped from 552kPag to 449kPag at the first pipe was 10 seconds in the case of $d_e/d = 0.22$. It was found from Figure 4.12 that time taken for the last pipe pressure reduction from 529kPag to 426kPag was almost the same. Comparative study based on three results as shown in Figure 4.12 will be presented in Section 4.5.1.

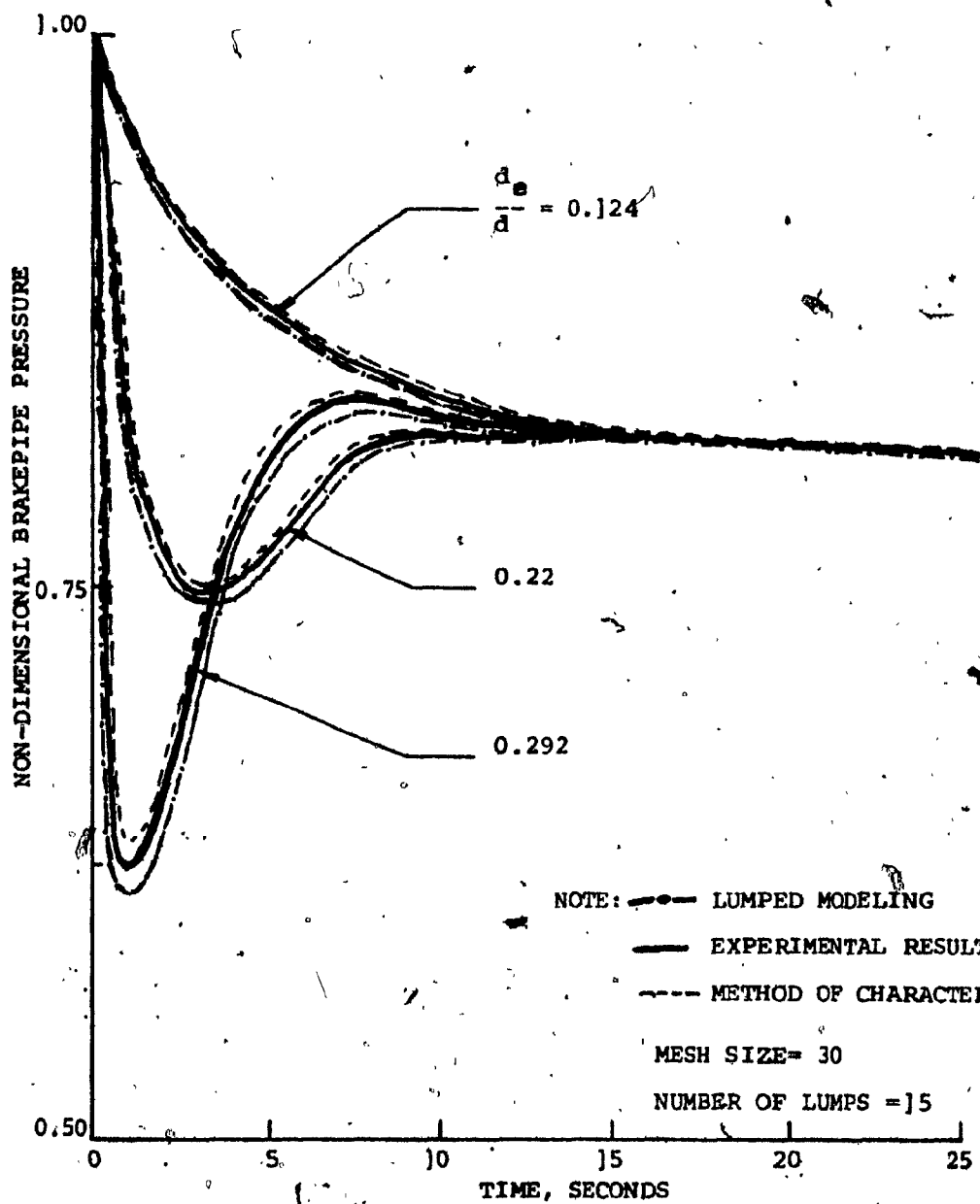


FIG. 4.11 PRESSURE REDUCTION ON FIRST PIPE WITH PLUMBING LEAKAGE AND DIFFERENT d_e/d

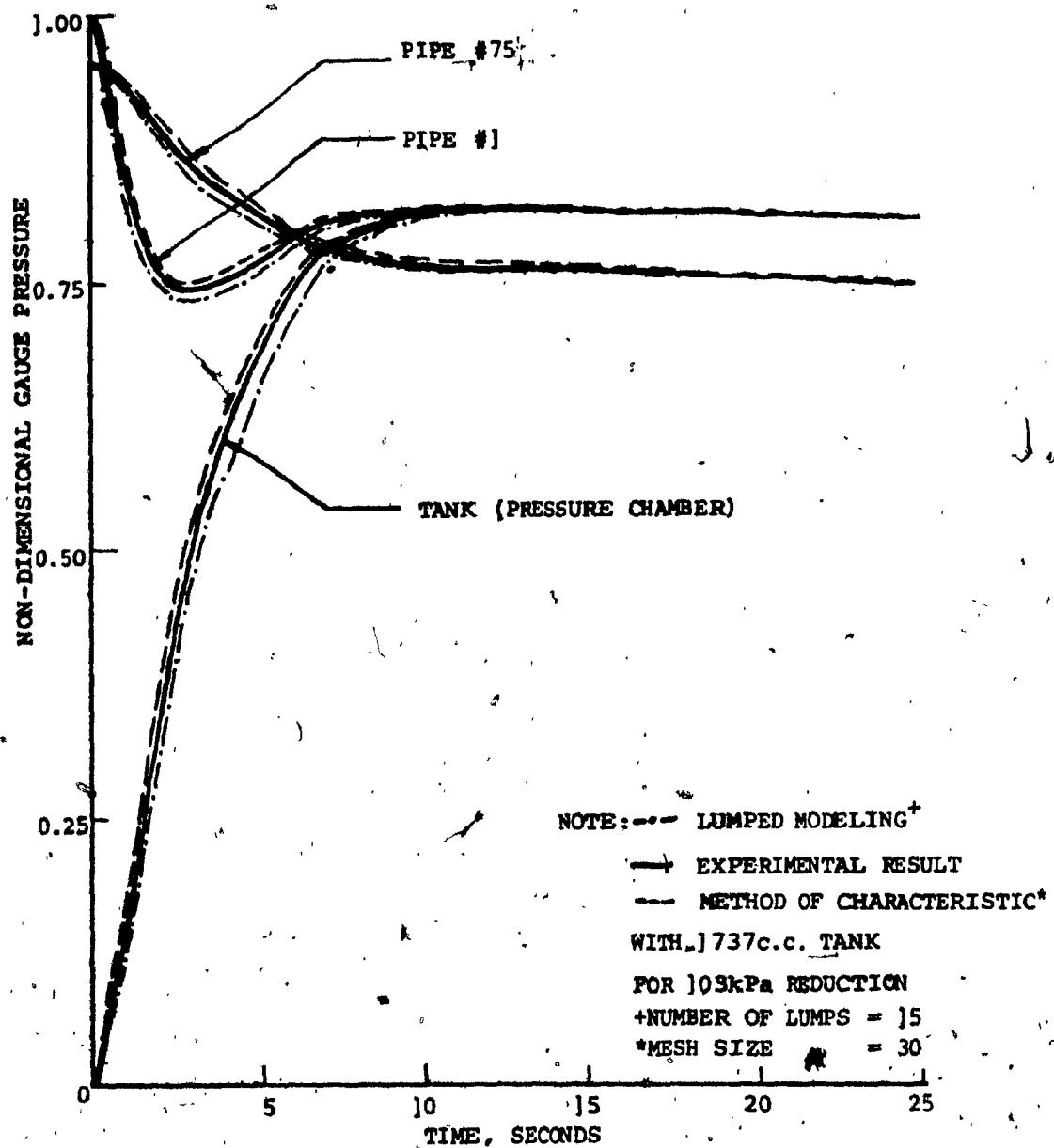


FIG. 4.12 PRESSURE REDUCTION FOR BRAKEPIPE MODEL
WITH PLUMBING LEAKAGE AND $d_o/d = 0.22$

In order to design and manage for good condition of train handling, it is very important to consider area ratio between exhaust area of the relay valve A_E (or in the model: exhaust orifice area A_e between tank and first pipe) and cross-sectional area of brakepipe A_1 . According to the above experimental results, area ratio (A_e/A_1) or (A_E/A_1) should be less than 1:25 so that undershoot fluctuation would not occur.

Note: $A_e = \pi d_e^2/4$ and A_E is given in equation(1-3).

4.4.2.3 Discharge Test and Result

There were 3 cases being examined for discharging air from the charged brakepipes. First, air was released through 15 leakage orifices of 0.33mm in diameter to the atmosphere only. Second, air was exhausted through an orifice to the tank and through 15 leakage orifices of 0.33mm in diameter to an ambient surrounding. Third, air was leaked out through one leakage orifice of 1.854mm in diameter to the atmosphere. For the above cases, transient pressures at the 1st, 25th and 75th pipes were measured by pressure transducers and were recorded by strip-chart recorder.

Referring to Figures 4.13 and 4.14, total time taken for the discharging process was 70 seconds and 80 seconds respectively. In Figure 4.14, six seconds

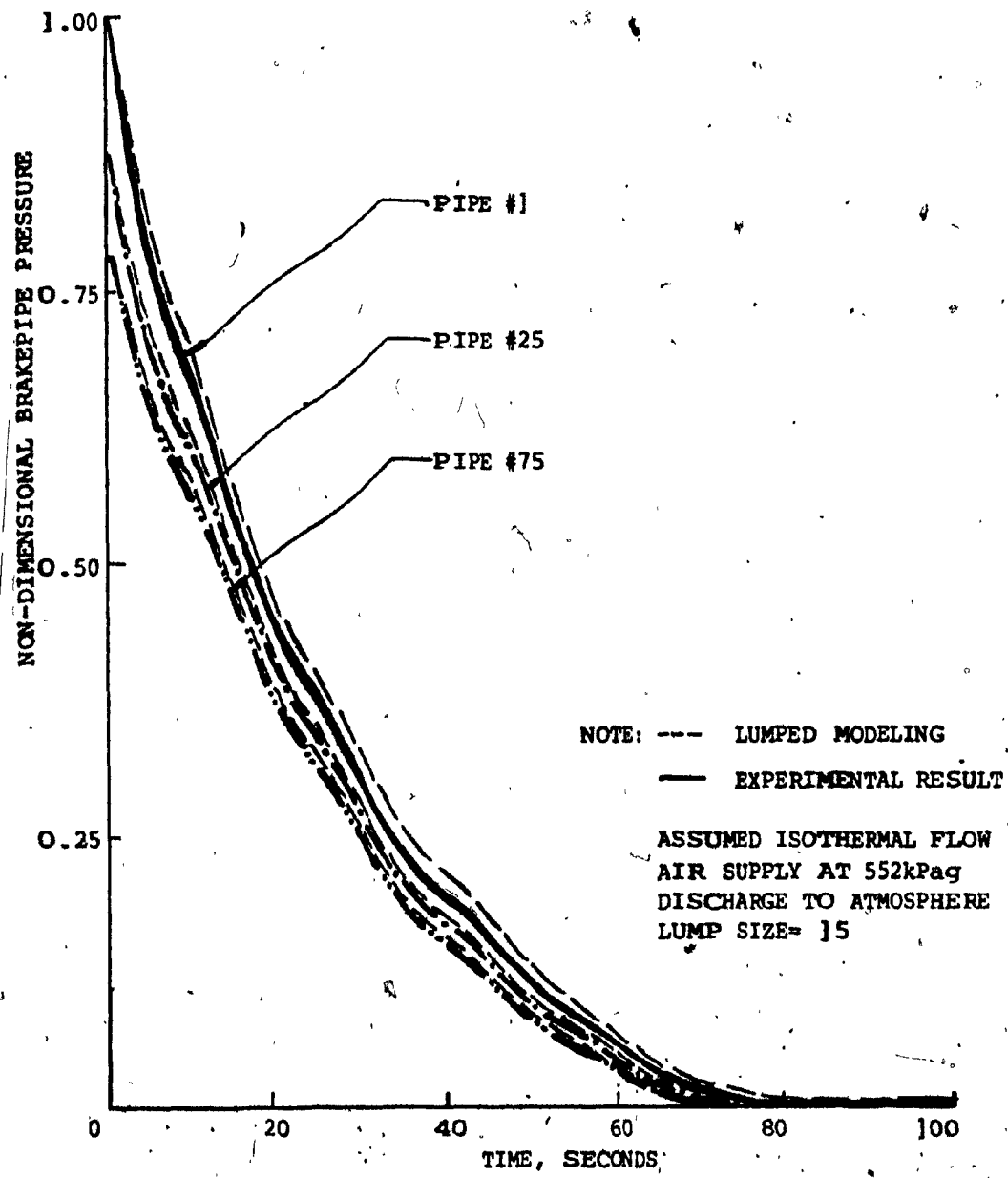


FIG. 4.13 DISCHARGE CURVES DUE TO 15 LEAKAGE ORIFICES
OF 0.33mm DIA.

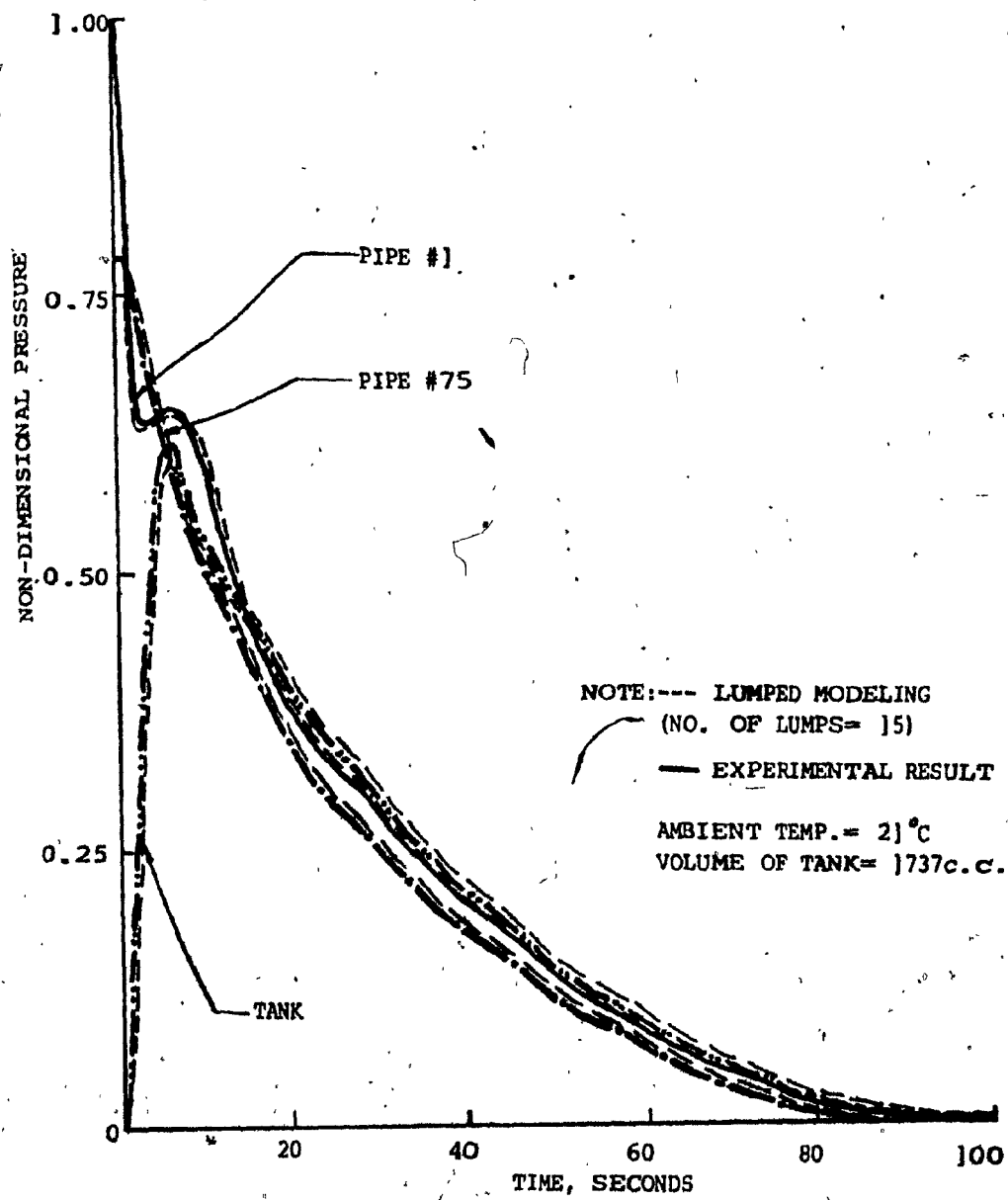


FIG. 4.14 DISCHARGE TO TANK WITH $d_o/d = 0.22$ FROM
75-PIPE-BEND-COMBINATION WITH 15 LEAKAGE
ORIFICES ALONG THE BRAKEPIPES

after discharging, the tank was charged and had 60% of initial pipe pressure. When compared with Figure 4.13, at the same time, the brakepipe pressure was 65% of initial pipe pressure. The discharge time at the head-end was slightly longer than the one at the rear-end under uniform leakage distribution. Superimposed on the experimental curves was the result obtained from the nonlinear brakepipe network model, that is, lumped modeling. The best-fitting theoretical curve was based on isothermal flow assumption rather than polytropical or adiabatical flow.

In Figure 4.15, where different exhaust orifices, d_e , were tested. A significant effect existed when d_e/d was greater than 1/5. If d_e/d is greater than 1/5, then brake application will be operated in an unsafe service since undershoot brakepipe pressure occurred.

In order to investigate the effect of leak location along the brakepipes to the discharge time, the results obtained in Figure 4.16 provide a valuable supplement to existing practical know-how. If concentration of leakage was placed at the middle of dead-ended pipes, that is, 38th pipe, the discharge time was minimum because there was higher propagation speed of air flow from the front to the middle of the brakepipes. However, the concentrat-

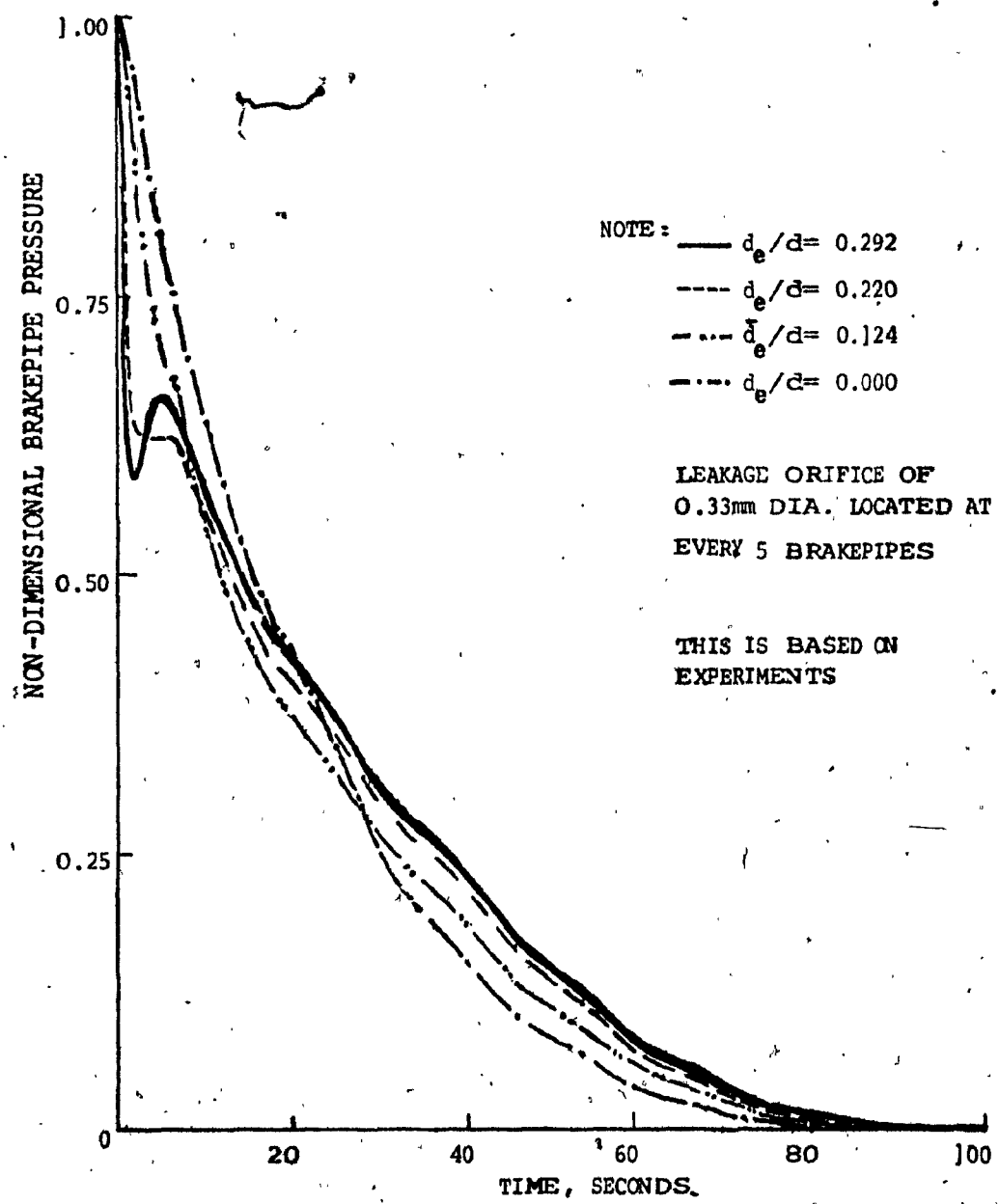


FIG.4.15 PRESSURE DROP AT FIRST PIPE WITH BRAKEPIPE LEAKAGE
AND DIFFERENT EXHAUST ORIFICE d_e

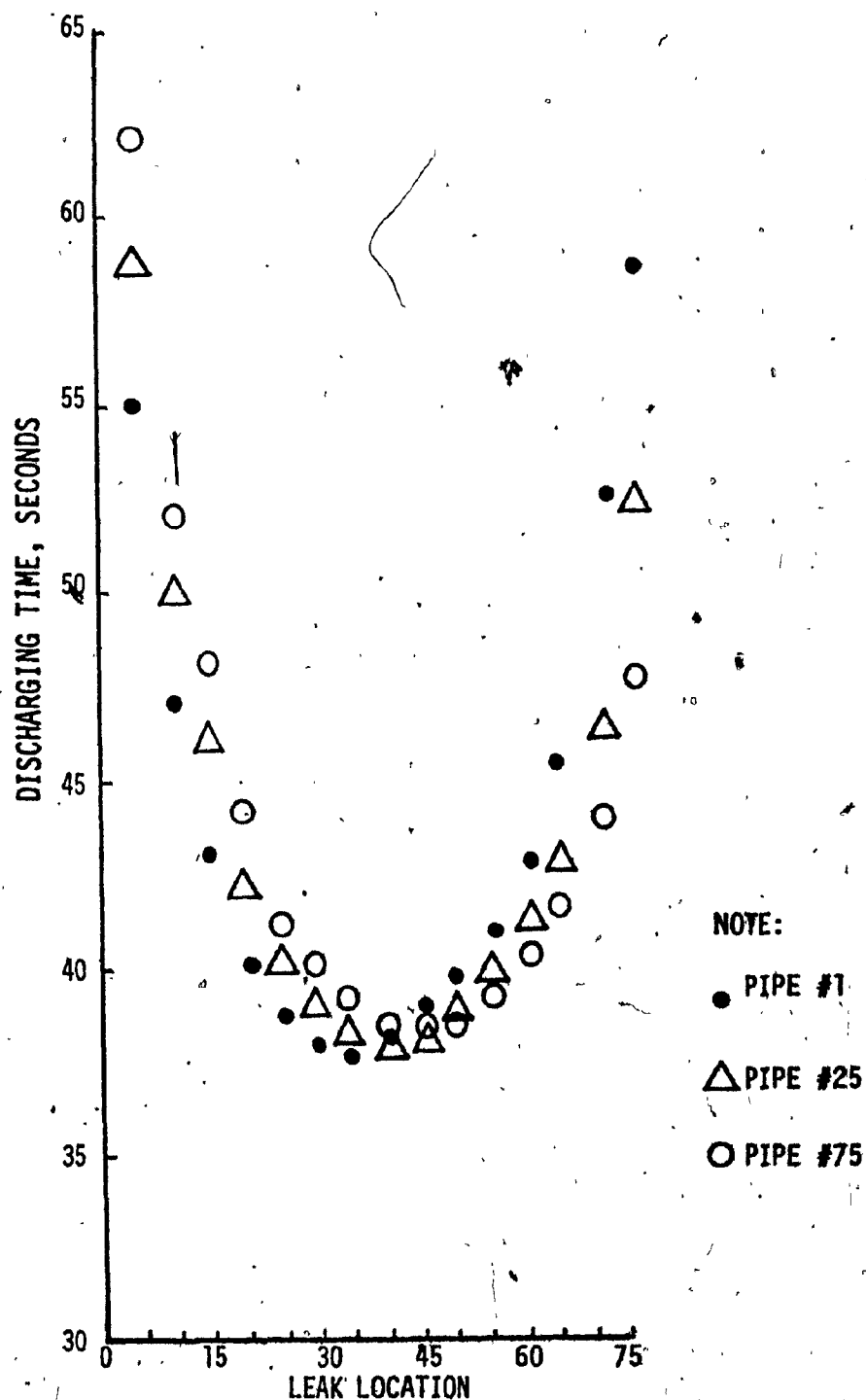


FIG. 4.16 DISCHARGING TIME VS. LEAK LOCATION CURVES
(Use one 1.854mm leakage orifice along the pipe model)

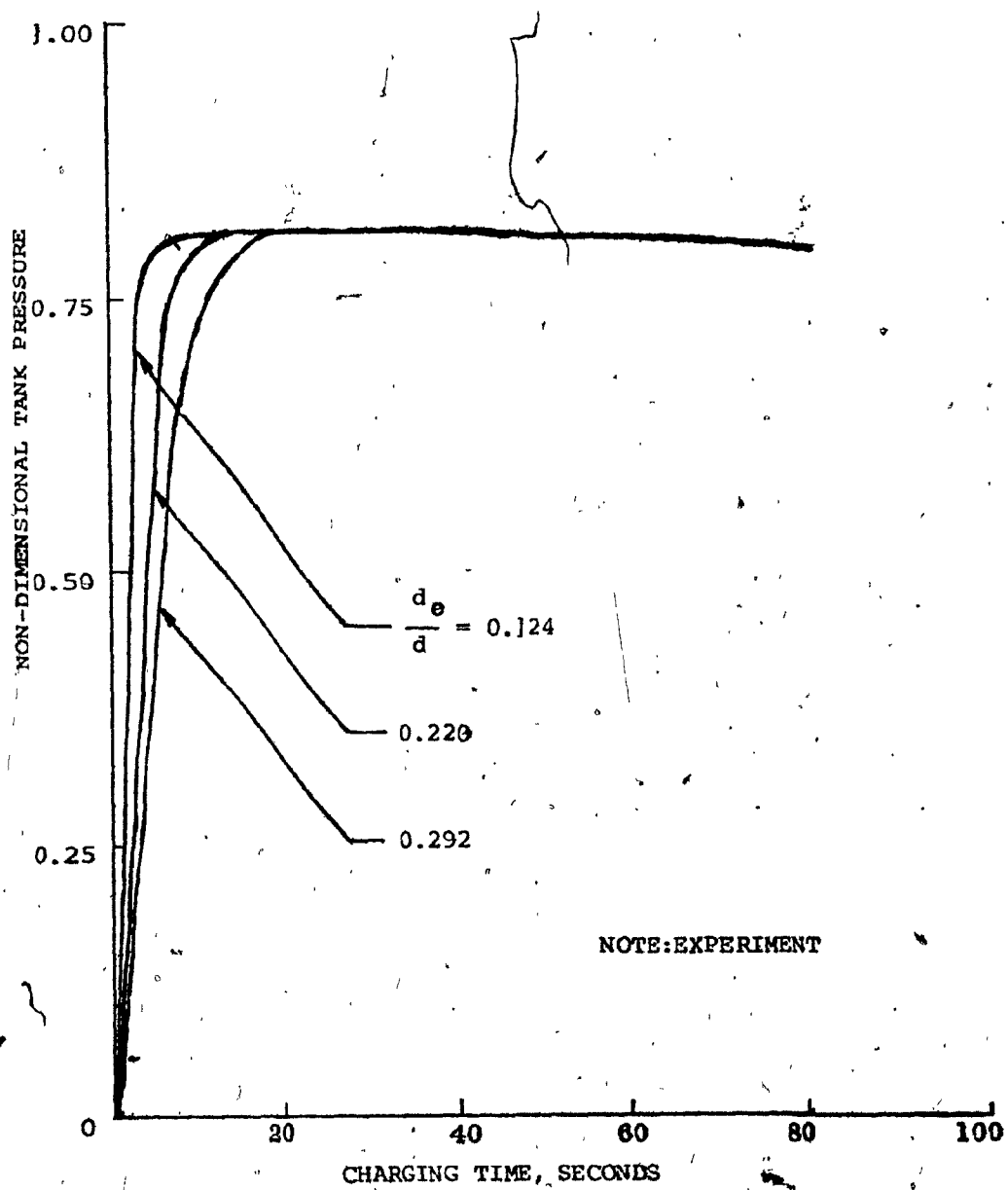


FIG. 4.17 AIR FLOW INTO AN 1737C TANK FROM THE PIPES
WITH PLUMBING LEAKAGE

ion of leakage either at head-end or at rear-end would take longer discharge time because propagation speed of air flow was reduced after passing through the plastic tubes and rough pipes. In this experiment, average discharge times for leakage at the ends and the middle were 55 seconds and 38 seconds respectively.

4.4.2.4 Charge Test and Result

As mentioned in Section 4.4.2.2, pressure of the tank could be measured by pressure transducer. Results of air flow into a fixed-volume tank from the brakepipes with plumbing leakage and/or resistance leakage orifices are shown in Figures 4.17 and 4.18 respectively. In former figure, the tank was acted as an auxiliary reservoir which was a storage volume to receive and store air for use in applying the brakepipe reduction. The latter figure was a typical feature whereby the emergency brakepipe reduction was passed rapidly from pipe to pipe throughout the brakepipe model since excessive leakage occurred along the brakepipes. For exhaust orifice size, $d_e/d = 0.292$, in both cases, rising time was the fastest one, that is, within 4 seconds in the former case. It was taken more than 16 seconds for $d_e/d = 0.124$ with plumbing leakage only. In Figure 4.18, it was obvious that longer time to rise up to peak tank pressure was required as

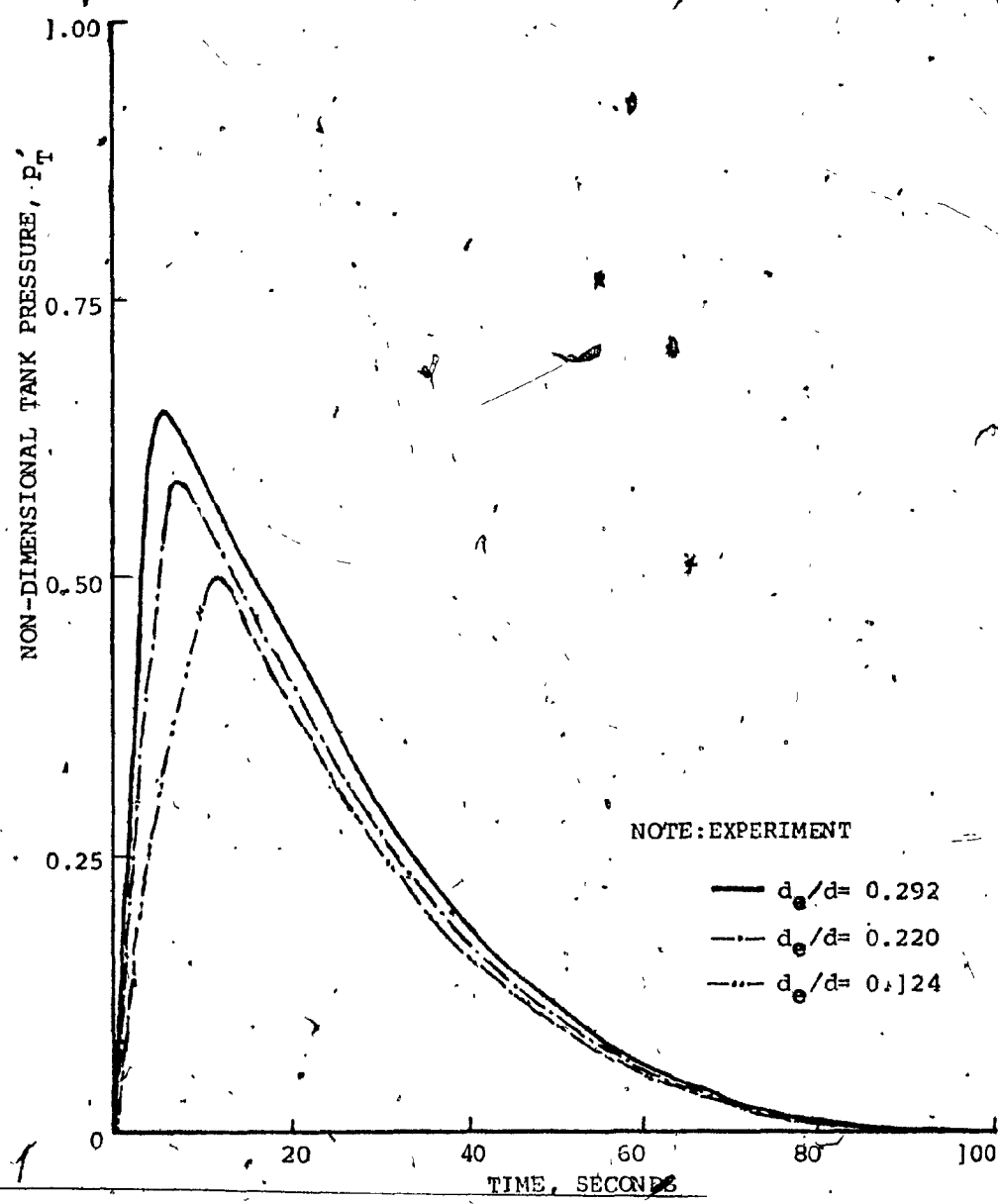


FIG. 4.18 AIR FLOW INTO AN 1737c c TANK FROM THE PIPES
WITH 15 LEAKAGE ORIFICES ALONG BRAKEPIPES.

smaller exhaust orifice size was used. Also, higher peak value was achieved as larger size orifice was put in. By using 15 leakage orifices in this experimental model, one found that the average ratio of charge time to discharge time was 1:5.

After discharging process, 3-way control valve was switched from exhaust port to supply port. Hence, the exhaust orifice was blocked and air supply was reopened. As air passed through the flowmeter to the brakepipes, the brakepipe pressure was built-up again. Figures 4.19 and 4.20 show the recharge time taken for the brakepipe pressure returning to 'service' position after fully discharge, under plumbing leakage and resistant leakage conditions respectively. It was worth to note that pipe No.1 curve was almost the same in both cases. The time taken for pipe No.1 was 35 to 40 seconds. Pipe pressure at 75th pipe, when only plumbing leakage existed, could take 30 seconds to gain 95% of 'service' pressure; when resistant leakage occurred, it needed twice the time to achieve steady state pipe pressure at 80% of 'service' pressure.

4.4.2.5 Evaluation of Time Delay

This section considers the evaluation of time delay t_d (t_{di} is designated as $(T_d - T_r)_i$) and is defined as the

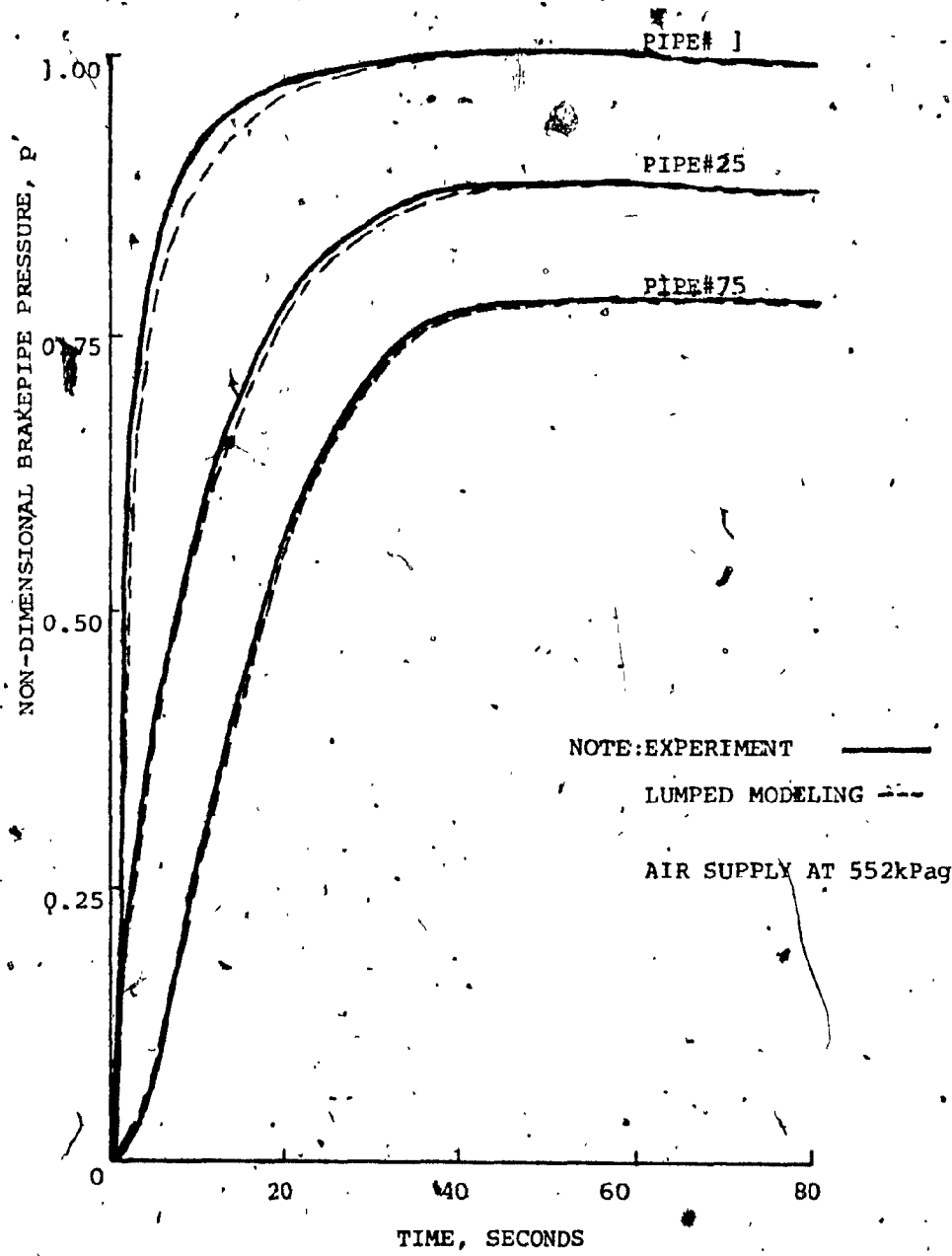


FIG. 4.19 BRAKEPIPES ARE RECHARGED WITH PLUMBING LEAKAGE

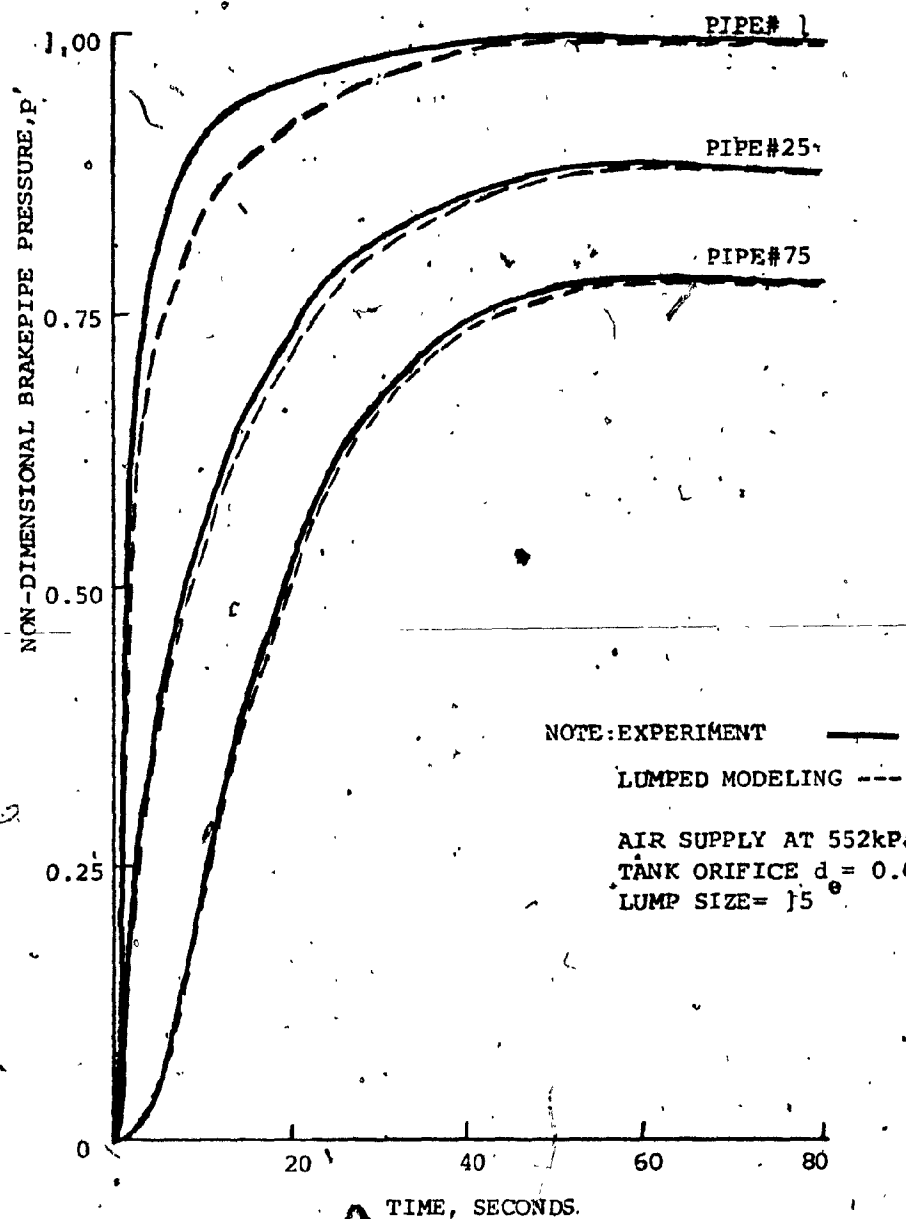


FIG. 4.20 BRAKEPIPE ARE RECHARGED WITH LEAKAGE ORIFICES

time taken for the brakepipe pressure at ith pipe to start reduction just after the air supply was shut off and the exhaust orifice was opened simultaneously.) according to different supply pressures, different leak sizes, & locations. Simple tests were achieved and given in Section 4.4.2.3. It was worth to point out that the percentage error in evaluating the time delay from the strip-charts was within $\pm 16\%$ due to 'flat' time-response as illustrated in Figure 4.21(a).

There was only one leakage orifice applied to the 40th brakepipe. As the air supply was regulated from 414kPag to 621kPag, five different leakage orifices (d_o) were tested. The brakepipe pressures at 1st, 25th & 75th pipes were recorded by a strip-chart recorder. Table 4.4 was then set up. Referring to Figure 4.21(b), at 552kPag air supply, time delay for 25th and 75th pipes to start reduction was 0.27 second and 0.78 second respectively while the smallest orifice of 0.33mm in diameter was used and controlled by the toggle valve. For leakage orifice of 1.854mm in diameter, the time delay for 25th and 75th pipes to start reduction was increased to 0.34 second and 1.25 seconds accordingly. When time delay curves were compared with different size orifices, it was found for larger diameter of orifice, the curve became more concave. It implied that larger leak would have longer time delay.

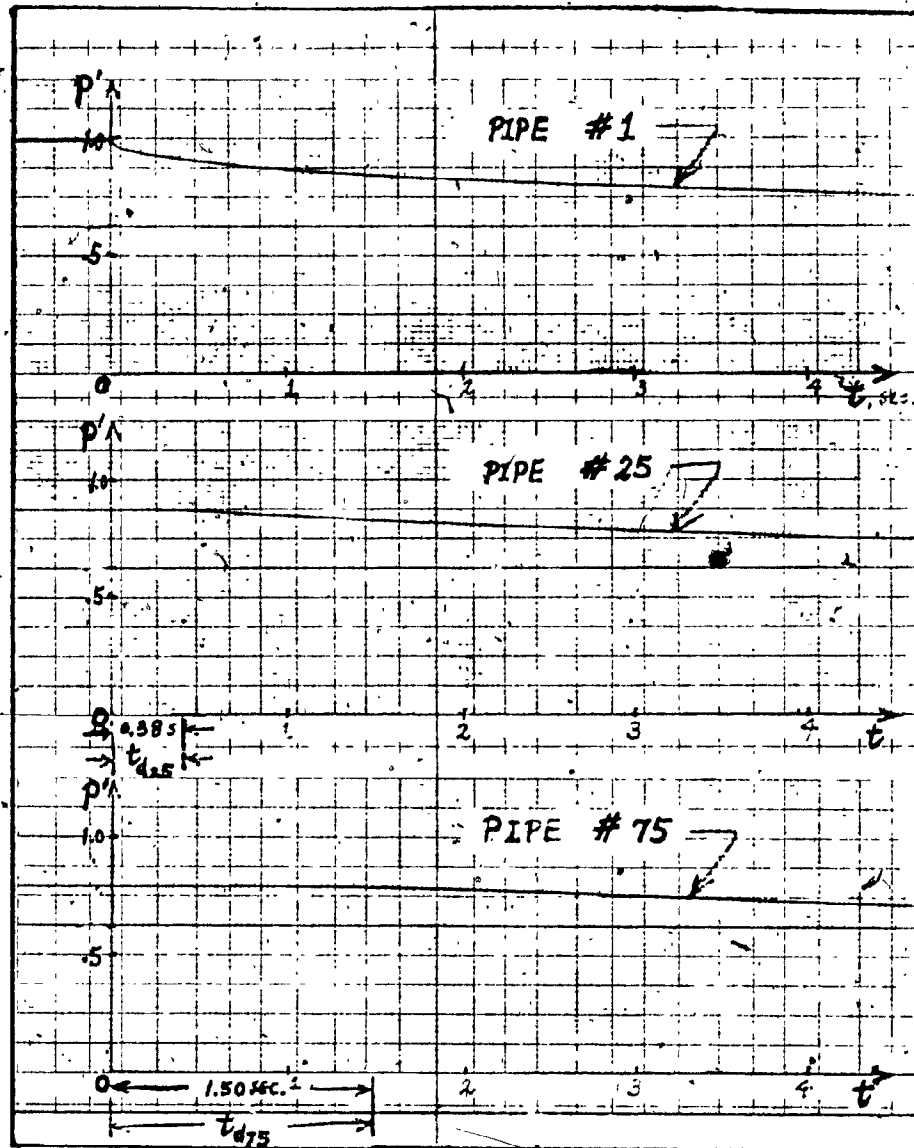


FIG. 1.21a TO SHOW TIME DELAY, t_{di}

(NOTE: PRESSURE REDUCTION
WITH LEAKAGE OR IF TORN)

TABLE 4.4 TIME DELAY VS. LEAKAGE ORIFICE SIZE

TIME DELAY, SEC.	SIZE	LEAKAGE ORIFICE DIAMETER, mm				
		0.330	0.584	0.787	1.397	1.854
AIR SUPPLY AT 414kPa	PIPE NO.25	0.29	0.30	0.32	0.36	0.42
	PIPE NO.75	0.82	0.88	1.05	1.24	1.45
AIR SUPPLY AT 483kPa	PIPE NO.25	0.28	0.29	0.31	0.33	0.37
	PIPE NO.75	0.80	0.88	1.00	1.15	1.38
AIR SUPPLY AT 552kPa	PIPE NO.25	0.27	0.28	0.30	0.31	0.34
	PIPE NO.75	0.78	0.88	0.94	1.07	1.25
AIR SUPPLY AT 621kPa	PIPE NO.25	0.26	0.27	0.29	0.30	0.32
	PIPE NO.75	0.76	0.81	0.89	1.00	1.18

NOTE:-

THIS IS BASED ON EXPERIMENTAL RESULTS:

ONLY 1 LEAKAGE ORIFICE WAS APPLIED AND LOCATED
AT BRAKEPIPE NO.40.

75 BRAKEPIPES WERE CONNECTED AS SHOWN IN FIG.4.8

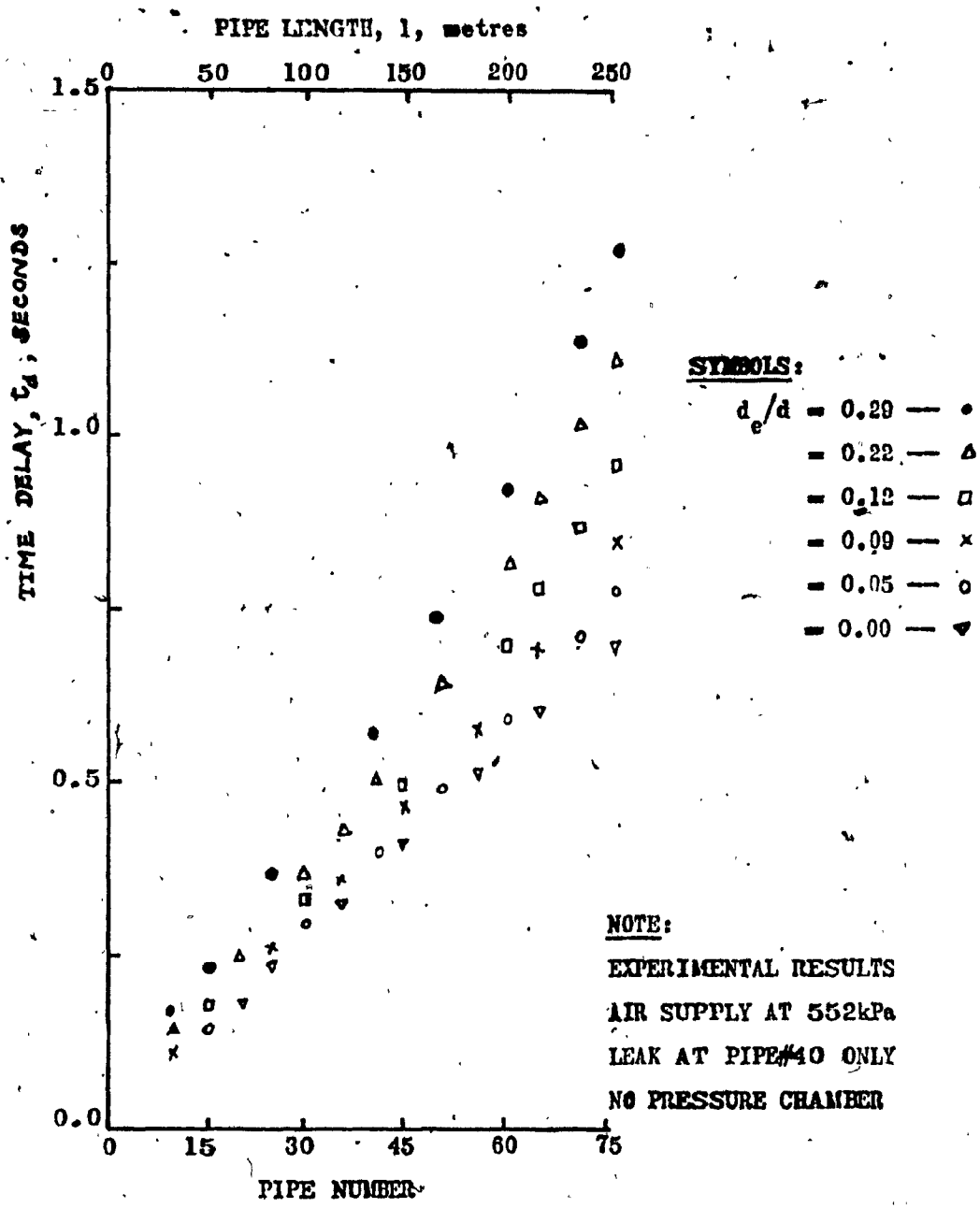


FIG.4.21b TIME DELAY CURVES

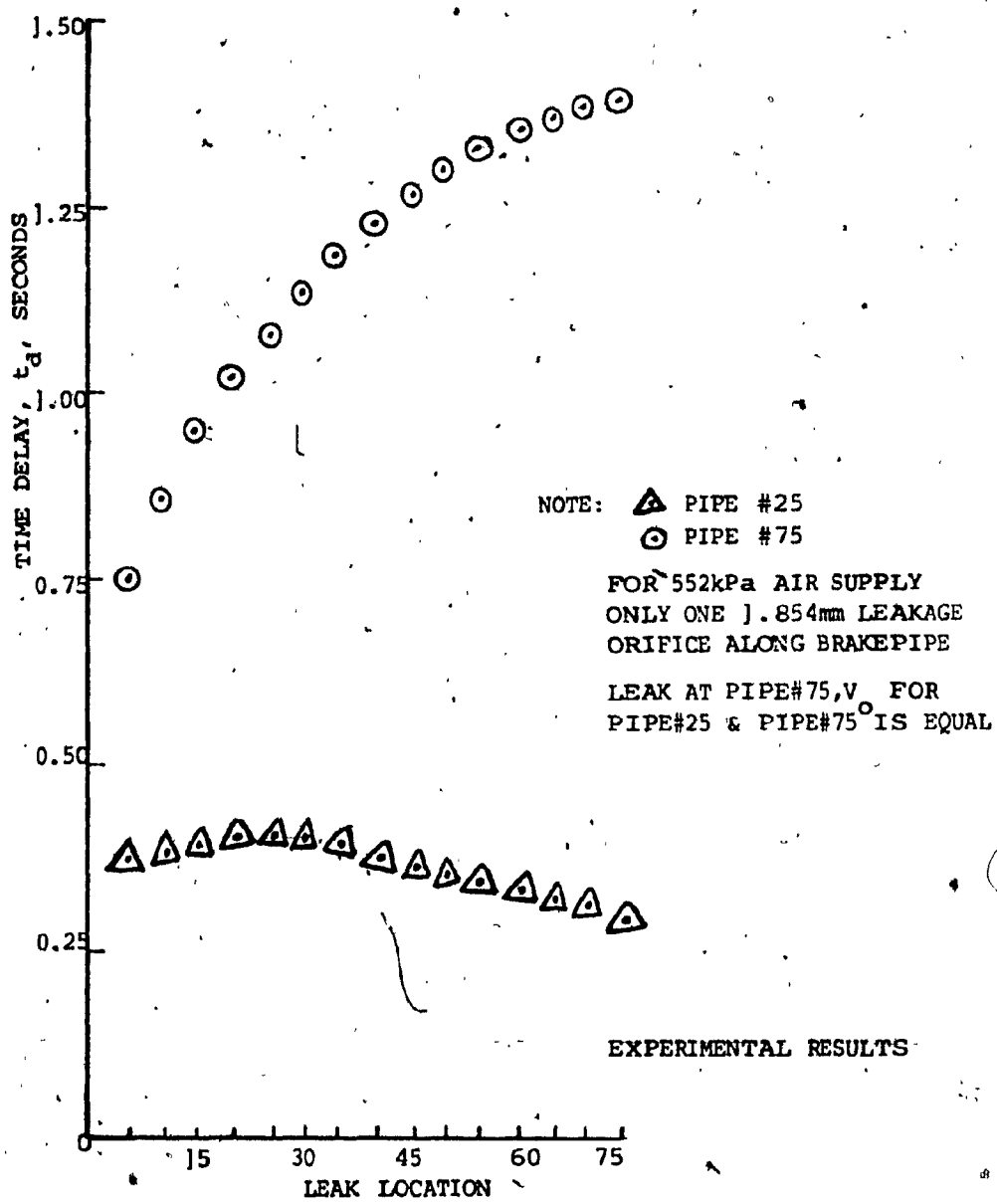


FIG.4.22 TIME DELAY VS. LEAK LOCATION CURVES

When air released through fifteen leakage orifices of 0.33mm diameter along the brakepipes to the atmosphere time delay for the 75th pipe to start pressure reduction was 1.50 seconds. If plumbing leakage existed only, then time delay for the last pipe to start the reduction was 0.80 second. It implied that brakepipe leakage could cause longer delay time to start pressure reduction.

At 552kPag air supply, only one leakage orifice of 1.854mm diameter was used at different locations, time delay, t_d , against leak location is shown in Fig.4.22. When leak occurred only at the 75th pipe, it caused the longest delay time for brakepipe pressure along the pipes to start pressure reduction.

4.5 DISCUSSION

4.5.1 COMPARATIVE STUDIES ON BRAKEPIPE MODEL

4.5.1.1 Pressure Reduction

Referring to Fig.4.12 again, 103kPa pressure reduction for brakepipe model was performed by theory and experiment. According to these results, it was found that rate of pressure drop at brakepipe No.1 was very fast at the beginning so that its pressure would drop below the final reduced pressure, p_d , if d_e/d was greater than 0.2. Brakepipe pressure along the model

would have 103kPa reduction under the condition of small plumbing leakage.

When compared two theoretical results with the experimental result, one found the method of characteristics for large-amplitude signal was more accurate than lumped modeling based on the same computation time. In Figure 4.12, mesh size was 30 and number of lumps was 15. Isothermal pipe flow was assumed for both methods. One looked at the pipe No.1, the curve obtained from the method of characteristics was always slightly above the experimental curve, while the lumped modeling curve was always below the experimental curve. The maximum discrepancy on brakepipe pressure at pipe No.1 between these two methods and experiment was +5% and -9.5% respectively. In order to improve the results, number of meshes or lumps should be increased and better numerical techniques on computing the differential equations should be applied.

The charging curve of tank depended on the exhaust orifice size d_e and brakepipe No.1's pressure. One looked at Figure 4.12 again, maximum discrepancy in tank pressure was $\pm 8\%$. The charging time of tank according to theory and experiment was 9.5 seconds and 10.5 seconds respectively.

4.5.1.2 DISCHARGE WITH LEAKAGE ORIFICES

In brakepipe model experiment, the initial static

pressure at pipe No.75 was about 435kPa when 15 leakage orifices of 0.33mm in diameter were located along the brakepipes. Percentage difference in initial brakepipe pressure between using the exact equation(3-19) and approximate equation(3-24) was about 5.5%. Formulation of equations by the method of characteristics was hard to develop for such leakage problem. Therefore, theoretical results were mainly obtained by lumped modeling technique.

In Figure 4.13, the discharge time for pipe No.1 was taken to be 80 seconds and 77 seconds with respect to theoretical and experimental results. The maximum error in brakepipe pressure was found to be about 14kPa when supply pressure of 552kPa was used. It was good enough to use 15 lumps in this case since the percentage error was within 6%.

In Fig.4.14, air discharge to tank through exhaust orifice of 1.397mm diameter ($d_e/d = 0.22$) from leaked brakepipes. The discharge time was found to be 10 seconds longer than the one without tank. The maximum discrepancy on brakepipe pressure was about 7kPa when a 1737cc tank was used. It was found that the discharge time for pipes No.1 and No.75 was 90 seconds and 80 seconds respectively. At the point where the tank pressure was maximum, the rate of brakepipe pressure drop for pipes No.1 and No.75 was

about 10.5kPa/sec (1.53psi/sec) and 12.5kPa/sec(1.8psi/s) respectively.

4.5.2 EFFICIENCY OF METHODS

4.5.2.1 MESH SIZE

Referring to Figure 4.23, it was found that time for the last pipe to have 103kPa reduction would be converged to a constant value while mesh size was more than 50. It meant that in order to show an accuracy of $\pm 5\%$ on our numerical calculation, mesh size should be at least 30.

The CPU(Central Processor Unit) for solution of the hyperbolic partial differential equations according to different mesh sizes was shown in Figure 4.24. It was approximated to be a parabolic curve. It was found that larger number of meshes would have higher accuracy but it was cumbersome and very time-consuming. Under the conditions of same length of brakepipes, same plumbing leakage and same pressure reduction, mesh size of 10 was used for 103kPa reduction, CPU time was about 50 sec.; if we enlarge the mesh size 5 times, the CPU time would be 8 times more.

4.5.2.2 EFFECT OF LUMPING

When lumping is based on length each lump is said

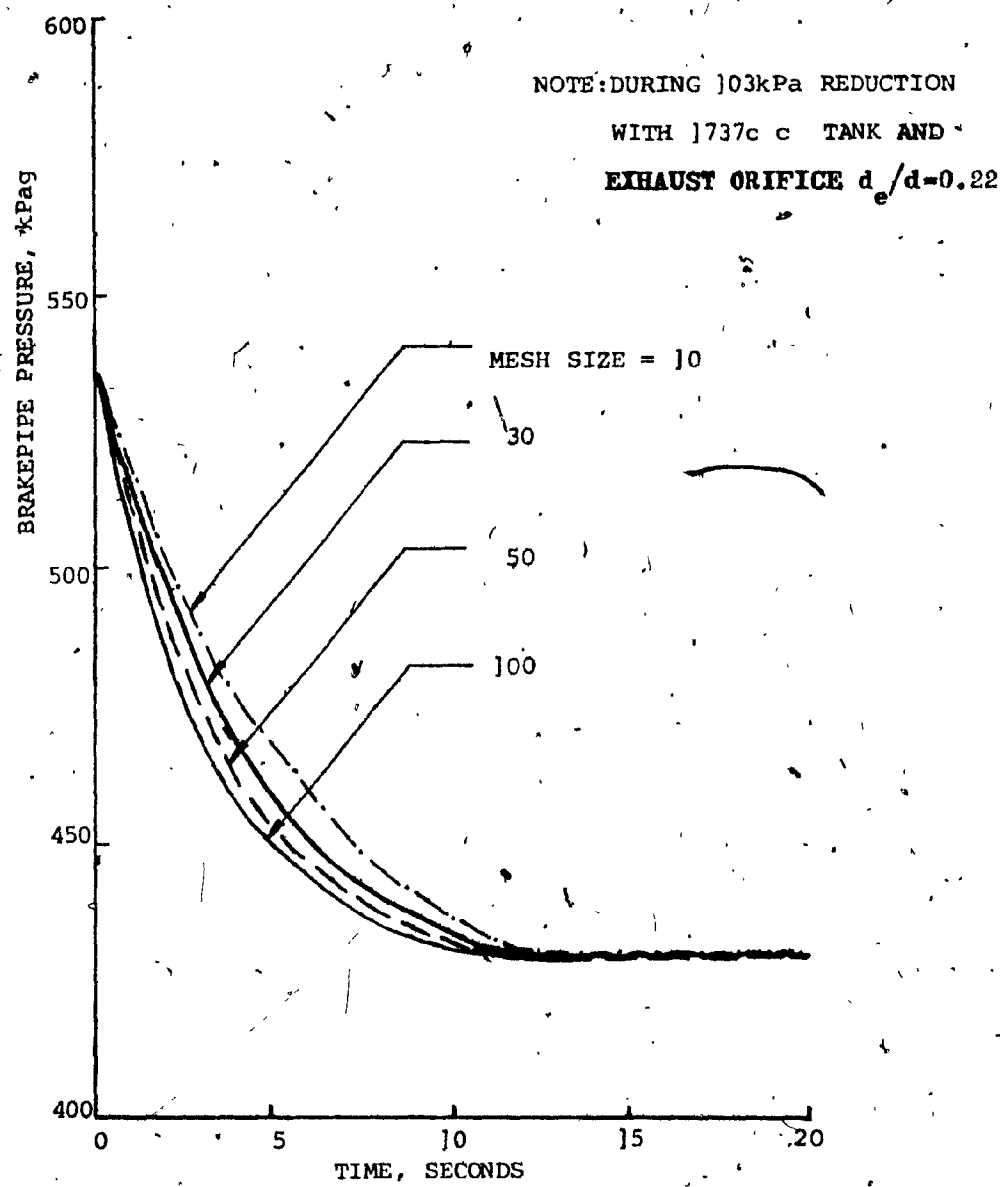


FIG.4.23 TOTAL TIME TAKEN FOR THE LAST PIPE AT STEADY STATE WITH DIFFERENT MESH SIZES

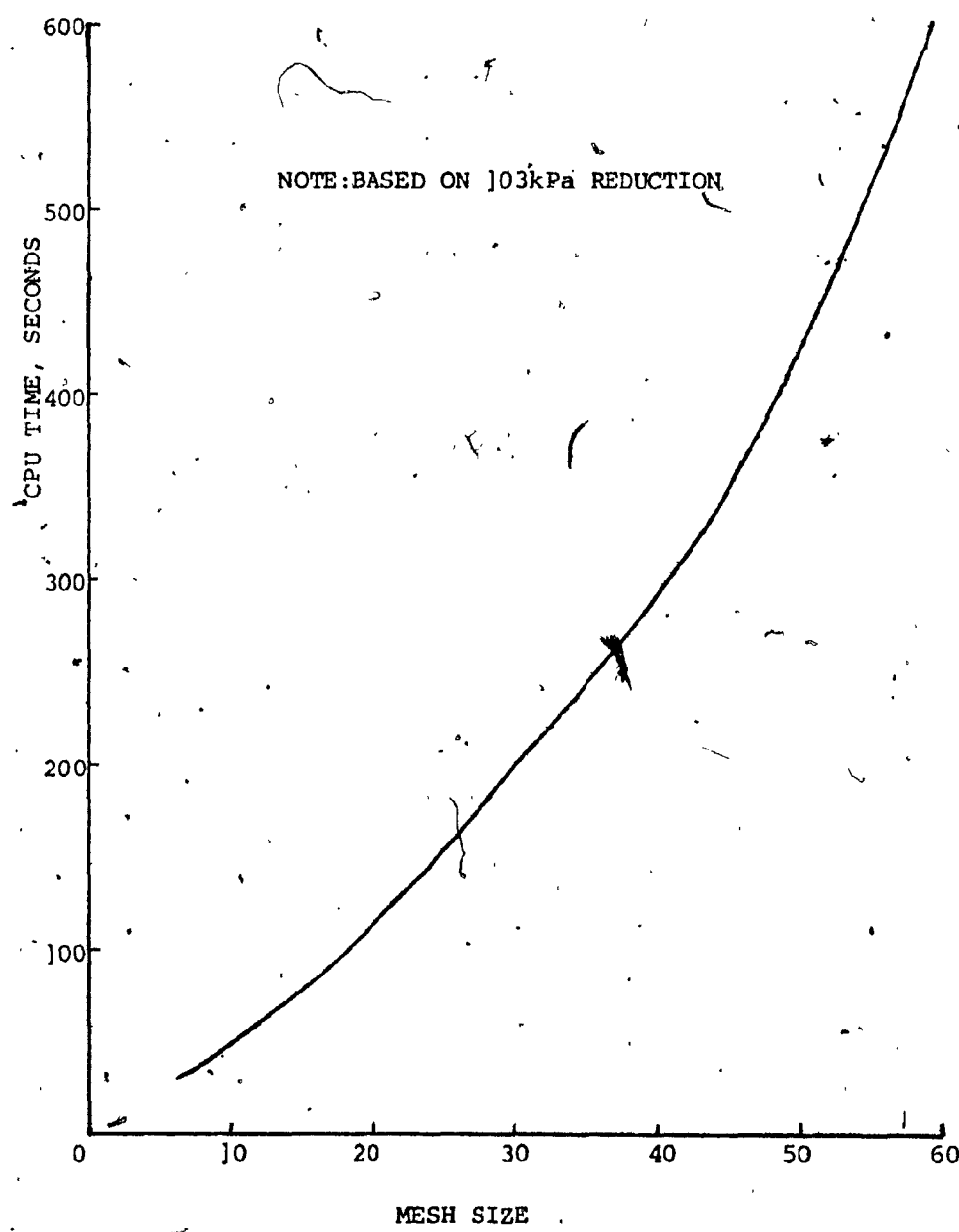


FIG.4.24 CPU TIMES FOR METHOD OF CHARACTERISTICS

to be identical. In order to observe the effect of lumping the lumped approximation in the case of 103kPa reduction with plumbing leakage only was used. Fig.4.25 shows the results with different lumps. Clearly accuracy of the approximate solution was improved as the number of lumps increased. However, a good approximation with a small number of lumps was desirable. The lumped modeling required a large number of lumps to obtain a dynamic simulation of the brakepipe model. For example, pressure reduction time was 12 seconds for 10 lumps and 10.5 sec. for 15 lumps while the experimental time was 9.5 sec..

The CPU time for solving the lumped network(pipe) equations is presented in Fig.4.26, the curve is in a parabolic form. For example, CPU time was about 40 sec. for 5 lumps; if the number of lumps was enlarged by 3 times, the CPU time was 5 times more under the same physical conditions. In order to compromise between the CPU time and accuracy of the model, minimum number of lumps should be fifteen.

4.6 SUMMARY

This chapter is confined to developing and verifying the two analytical methods only on a scaled-down brakepipe experimental model.

Method of characteristics for large-amplitude

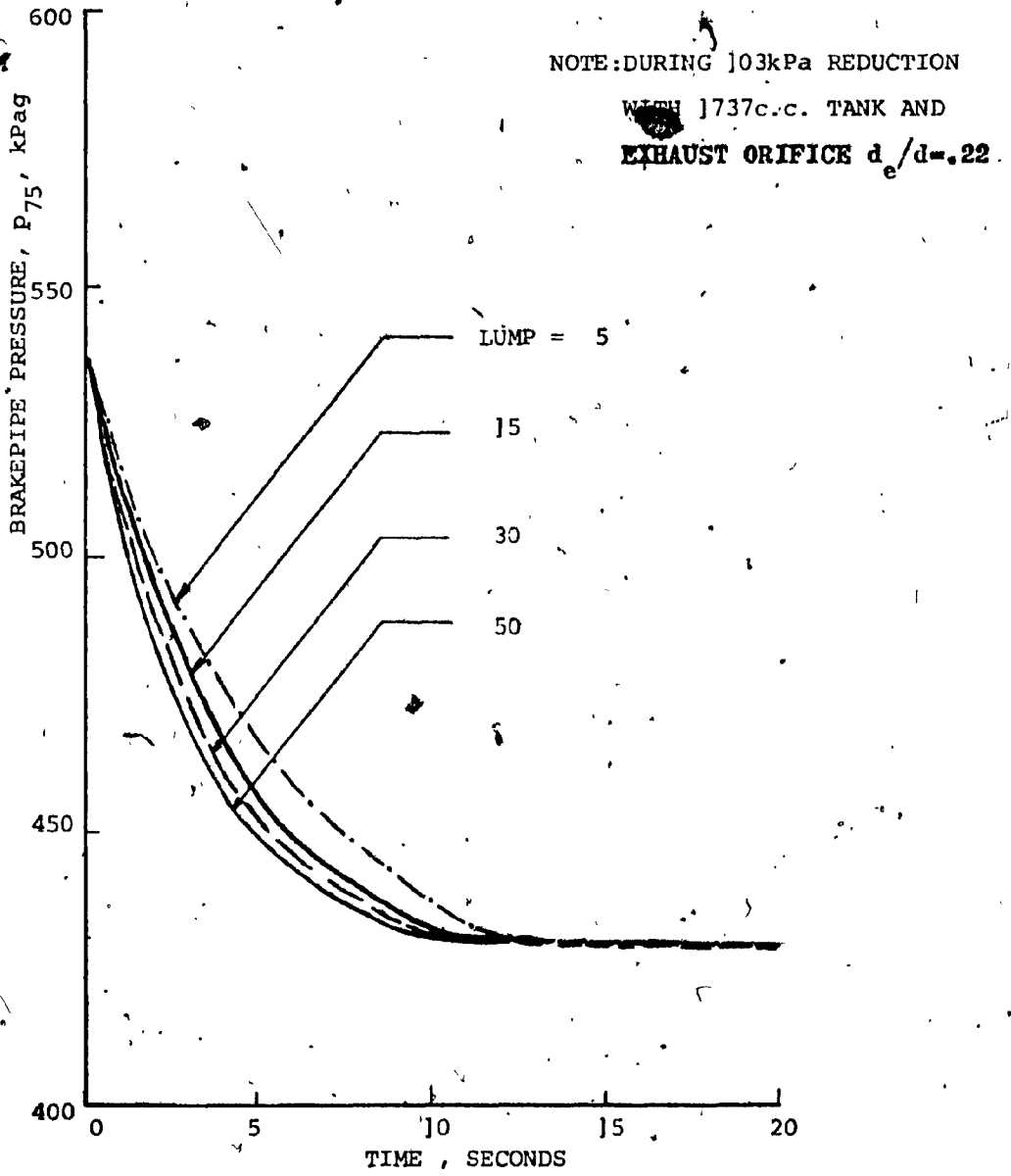


FIG. 4.25 TOTAL TIME TAKEN FOR THE LAST PIPE AT STEADY STATE WITH DIFFERENT NUMBER OF LUMPS

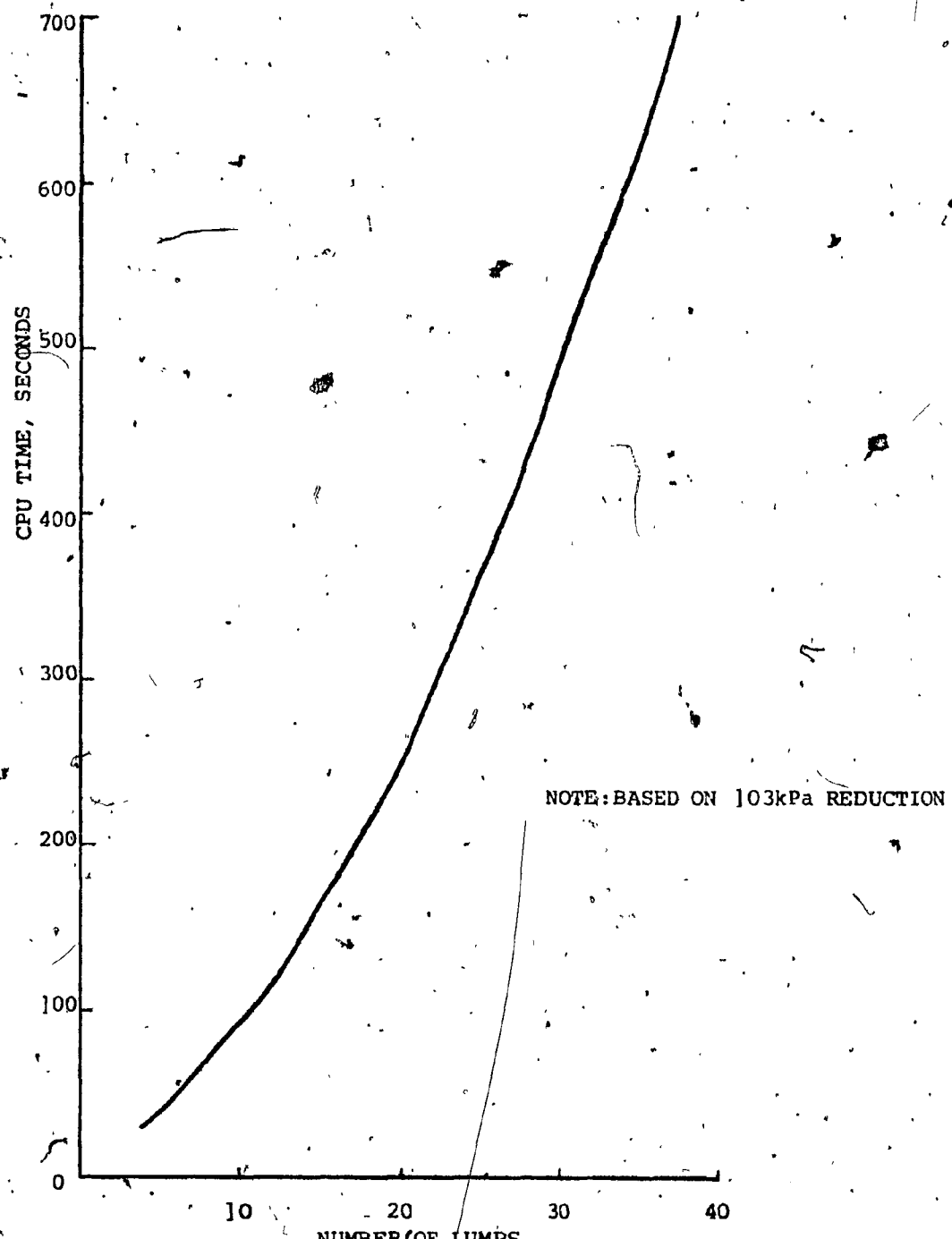


FIG. 4.26 CPU TIMES FOR LUMPED MODELING

signal is more accurate than lumped modeling when plumbing leakage occurs only. However, lumped modeling was preferred since it was much easier to apply & could investigate the effects of leakage. It was found that the percentage error in the solution between the experimental and analytical ways was within $\pm 10\%$. In order to minimize its computation time number of lumps should be compromised, & a better numerical technique of computing the differential equations should be applied. Also, in order to show an accuracy of $\pm 10\%$ on numerical calculation, mesh size and number of lumps were at least 30 and 15 respectively. In this chapter, all the best-fitting theoretical curve was based on isothermal flow assumption rather than polytropical or adiabatical flow. It was noted that fluid inertance was ignored in our simplified lumped network (therefore, time delay could not be predicted).

For the brakepipe model, resistance constant for turbulent-compressible flow in the brakepipe, K_2 had a mean value of $2.62 \times 10^{13} \text{ kPa}^2 \cdot \text{s}^2 / \text{kg}^2$ which was close to calculated K_2 . From the resistance leakage experiment, one obtained the discharge coefficient of the 'artificial' orifices to be about 0.82. After applying equation(3-19) with the individual values measured for the linear leakage resistance R_i and resistance constant K_2 on each brakepipe

and orifice one found that much closer agreement between experiment and theory in pressure gradient was achieved. To design and manage for good condition of train handling it is very important to consider area ratio between the exhaust area of the relay valve (or pressure chamber in our case) and cross-section area of brakepipe to be less than 1:25 so that undershoot fluctuation pressure will not occur.

The brakepipe leakage tended to accentuate the pressure gradient. The brakepipe leakage also made it longer to fully charge or recharge the braking system, thereby, shortening the brakepipe exhaust time. The sizes and locations of leakage affected the pressure gradient & distribution, and time delay. The larger leakage orifice size along the brakepipe would have longer time delay to start brakepipe reduction. The concentration of leakage at the rear end did produce the largest pressure gradient in the brakepipes, and the longest delay time to start pressure reduction. When excess leakage has developed within a certain section of the brakepipe, wrong signals were created thereby causing undesirable braking service or application.

CHAPTER 5

SIGNAL PROPAGATION VELOCITY

5.1 INTRODUCTION

The study of signal propagation in a fluid transmission line has been of continual interest since the early part of the nineteenth century. In 1808, Young(26) found the speed of propagation of an impulse in an elastic line. The signal propagation speed was defined as a speed relative to the observer at rest with respect to the line rather than the speed relative to the fluid flow. After the development of Navier-Stokes equations in fluid mechanics around 1850, significant advances were possible considering the fluid as compressible. In 1878, Korteweg (27) investigated that the radial deflection of a fluid-filled tube subject to sinusoidal pressure variations satisfied the one-dimensional wave equation. The speed of pressure wave propagation c (also known loosely as propagation velocity and phase velocity) with flexible line effect was found to be:-

$$c = \frac{c_0}{\left(1 + \frac{K_a d}{E e}\right)^{1/2}} \quad \dots \dots (5-1)$$

where c_0 and K_a are, respectively, the fluid sonic speed

(for the lossless line) and bulk modulus of air, and d , e , and E are, respectively, the diameter, wall thickness, and Young's modulus of the line. In 1898, Lamb(28) extended the work of Korteweg by considering the velocity of sound in a tube as affected by the elasticity of the walls.

Following the early work in fluid transients where frictional effects were mostly neglected, until the early part of the twentieth century, attention was tended toward investigating the nature of the fluid flow within fluid lines. Goodson and Leonard(12) discussed three distinct line propagation models such as the lossless line; the line with average friction and no heat transfer; and the circular line with distributed friction and heat transfer. Raizada(29) considered the special case of a fluid line with finite loss and leakage. He pointed out that the frequency response of a leakage line had a larger bandwidth than that of a normal leakproof system within certain limits (that is, the line would permit no phase fluctuations). Magnusson(31) derived an approximate expression for attenuation and phase velocity as functions of frequency in a uniform RLGC transmission line.

In the 1970's, Karam and Leonard(30) developed a simple, theoretically based time domain model for the propagation of small, arbitrary signals in a finite, circular, fluid transmission line which predicted three

dominant characteristics of the time domain behaviour of a line: (1) delay, (2) attenuation(decrease in amplitude of a propagating step), (3) dispersion(such as smoothing or distortion of the leading edge of a step input). In long fluid lines the delays were roughly of the order of the transit time for sound wave propagation through the medium, and in systems transmitting information or power at high frequencies such delays caused an instability or excessive pressure surges. Recently, Watters(25) modified the Equation(5-1) as follows:-

$$c = \frac{c_0}{\left(1 + \frac{K_a d}{E e}\right)^{1/2}} \quad \dots \dots (5-2)$$

where C' = arbitrary constant

$$c_0 = (K_a / \rho_a)^{1/2}$$

For the case of thick-walled pipes free to stress and strain both laterally and longitudinally, the value of C' will be equal to:

$$\frac{1}{1 + \frac{e}{d}} \left[\left(\frac{5}{4} - \mu\right) + \frac{2e}{d} (1 + \mu) \left(1 + \frac{e}{d}\right) \right], \text{ where } \mu = \text{Poisson's ratio,}$$

ρ_a = density of air, K_a = bulk modulus of air = absolute pressure in brakepipe(for isothermal process).

Equation(5-2) is used when air velocity changes suddenly and the brakepipe is relatively long, the elastic properties of thick-walled pipe ($d/e < 40$) and air enter

into the analysis. He pointed out that the effect of pipe elasticity in gaseous lines was negligible due to such a very large fluid compliance(that is, $E \gg K_a$).

In the remainder of this Chapter, the theoretical and experimental values of propagation speed in brakepipe model, transient response of brakepipe, and effect of leakage on propagation speed will be discussed.

5.2 EVALUATION OF PROPAGATION SPEED IN BRAKEPIPE MODEL

For the discussion that follows, a one-dimensional linearized brakepipe model will be used. A series of finite lumped parameter elements with finite loss and leakage was set up and shown in Fig.5.1. It was assumed that (1) the leakage of the air took place uniformly along the line, & was more or less the kind of leakage that would take place along a porous tube (plumbing leakage is neglected), (2) the pressure was uniform over the cross-section of pipe and that the radial velocity is zero, (3) the walls of the brakepipes were to be isothermal and there is no heat transfer between the air and walls of the pipes, (4) there was small viscous force from compressibility and average viscous effect, and (5) small amplitude signals were used(for example, density variation was small compared to the average density).

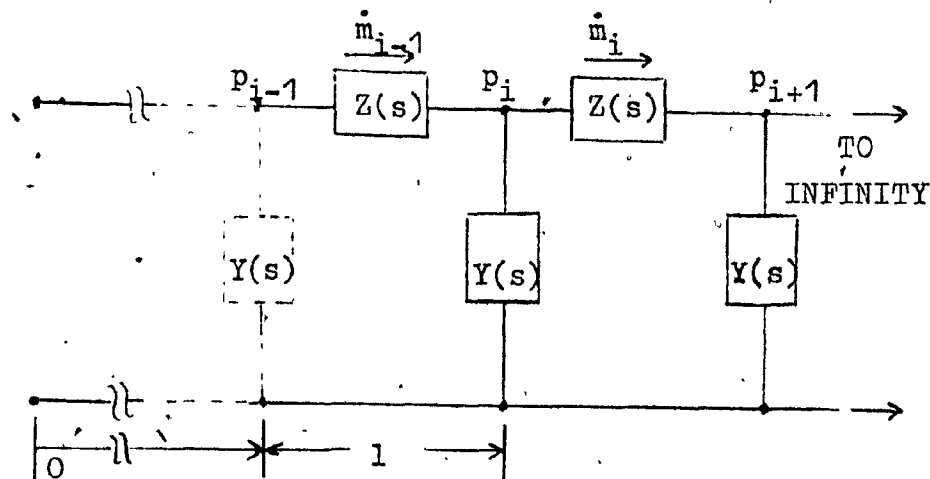


FIG. 5.1 ONE-DIMENSIONAL LINEARIZED BRAKEPIPE MODEL

For a linear uniform line, $Z(s)$ is the Laplace transform of the series impedance and $Y(s)$ is the Laplace transform of the shunt admittance. One can express $Z(s)$ and $Y(s)$ in terms of the line inertance, resistance, capacitance, and leakance, as follows:-

$$Z(s) = Ls + R \quad \dots \dots \quad (5-3a)$$

$$Y(s) = Cs + G \quad \dots \dots \quad (5-3b)$$

where $s = jw$ ($j = \sqrt{-1}$, w = circular frequency of the wave)

$$L = \text{line inertance per lump} = 4\rho_a/\pi d^2$$

$$R = \text{line resistance per lump}$$

$$C = \text{line capacitance per lump} \quad \} \quad (\text{Refer to Sect. 3.2.1})$$

$$G = \text{line leakance per lump} \quad }$$

From Ref. (21), in general, the propagation constant Γ and the characteristic impedance Z_c are given in the form:

$$\Gamma(s) = [Z(s)/Y(s)]^{1/2} \quad \dots \dots \quad (5-4)$$

$$Z_C(s) = [Z(s)/Y(s)]^{1/2} \quad \dots \dots \quad (5-5)$$

In the frequency domain ($s=j\omega$) the real and imaginary parts of the propagation constant ($\Gamma(j\omega)=\alpha+j\beta$) are:

$$\alpha = \frac{\omega}{c_0} \left[\frac{1}{2} \left\{ \left(\frac{GR}{w^2 LC} - 1 \right)^2 + \left(\frac{R}{wL} + \frac{G}{wC} \right)^2 \right\}^{1/2} + \frac{1}{2} \left(\frac{GR}{w^2 LC} - 1 \right) \right]^{1/2} \quad \dots \dots \quad (5-6a)$$

$$\beta = \frac{\omega}{c_0} \left[\frac{1}{2} \left\{ \left(\frac{GR}{w^2 LC} - 1 \right)^2 + \left(\frac{R}{wL} + \frac{G}{wC} \right)^2 \right\}^{1/2} - \frac{1}{2} \left(\frac{GR}{w^2 LC} - 1 \right) \right]^{1/2} \quad \dots \dots \quad (5-6b)$$

NOTE: The derivation of Equation(5-6) is presented in Appendix A.

The speed of wave propagation(signal propagation velocity) c is defined from Ref.(21,31) as:

$$c = \omega/\beta \quad \dots \dots \quad (5-7)$$

To substitute Equation(5-6b) into Equation(5-7), then, average theoretical propagation speed for this case is:

$$c = \frac{c_0}{\left[\frac{1}{2} \left\{ \left(\frac{GR}{w^2 LC} - 1 \right)^2 + \left(\frac{R}{wL} + \frac{G}{wC} \right)^2 \right\}^{1/2} - \frac{1}{2} \left(\frac{GR}{w^2 LC} - 1 \right) \right]^{1/2}} \quad \dots \dots \quad (5-8a)$$

From Ref.(31), an approximation for c is expressed as

$$c \approx \frac{c_0}{\left[1 + \frac{1}{8w^2} \left(\frac{R}{L} \frac{G}{C} \right)^2 \right]} , \quad (R \ll wL; G \ll wC) \quad \dots \dots \quad (5-8b)$$

$$\approx \sqrt{\frac{2w}{CR}} , \quad (R \gg wL; G \ll wC) \quad \dots \dots \quad (5-8c)$$

$$\approx \frac{2}{L\sqrt{\frac{G}{R}} + C\sqrt{\frac{R}{G}}} , \quad (R \gg wL; G \gg wC) \quad \dots \dots \quad (5-8d)$$

Let $w_v = \frac{R}{L}$ = viscous characteristic frequency..... (5-9)

$w_L = \frac{G}{C}$ = leakage characteristic frequency (5-10)

then the Equation(5-8a) will be written as:

$$c = \frac{c_0}{\left[\frac{1}{2} \left\{ \left(\frac{w_v}{w} \right)^2 \frac{w_L}{w_v} - 1 \right\}^2 + \left(\frac{w_v}{w} \right)^2 \left(1 + \frac{w_L}{w_v} \right)^2 \right]^{\frac{1}{2}} - \frac{1}{2} \left\{ \left(\frac{w_v}{w} \right)^2 \frac{w_L}{w_v} - 1 \right\}^{\frac{1}{2}}} \quad \dots \dots \quad (5-11a)$$

From Ref.(31), c is rewritten as:

$$c \approx \frac{c_0}{\left[1 + \frac{1}{8} \left(\frac{w_v}{w} \right)^2 \left(1 - \frac{w_L}{w_v} \right)^2 \right]} \quad , \quad (R \ll wL; G \ll wC) \quad \dots \dots \quad (5-11b)$$

$$\approx \frac{c_0}{\sqrt{\frac{w_v}{2w}}} \quad , \quad (R \gg wL; G \ll wC) \quad \dots \dots \quad (5-11c)$$

$$\approx \frac{c_0}{\frac{1}{2} \left[\sqrt{\frac{w_L}{w_v}} + \sqrt{\frac{w_v}{w_L}} \right]} \quad , \quad (R \gg wL; G \gg wC) \quad \dots \dots \quad (5-11d)$$

It is worth to note that pipe elasticity, friction and leakage are the major parameters which affect the propagation speed in the brakepipe.

To assist in calculating propagation speed in the brakepipes constructed of common materials, Table 5.1 shows the E-values and μ -values (Ref.(25)):-

PIPE MATERIAL	E, kPa	μ
Steel	210×10^6	0.30
Cast Iron	165×10^6	0.28
Copper	110×10^6	0.30
PVC	28×10^5	0.45

Due to the elastic effect only, we computed the average theoretical propagation speed in the brakepipe and plastic tube by using the following data:

<u>PARAMETERS</u>	<u>PIPE</u>	<u>TUBE</u>
Inside diameter, d	6.35mm	6.35mm
Wall thickness, e	1.5875mm	1.5875mm
Bulk modulus, K_a	653kPa(abs)	653kPa(abs)
Density of air, ρ_a	4.54kg/m ³	4.54kg/m ³
Constant factor, C	1.416	1.365
Young's modulus, E	165×10^6 kPa	28×10^5 kPa

The average theoretical propagation speeds in the brakepipe and plastic tube which were obtained from Equation(5-2) are 379.24m/sec and 378.77m/sec respectively. It is noted that the speed of wave propagation c is almost the same for different pipe materials in the medium of air.

For the brakepipe model, the typical viscous characteristic frequency (w_v) per lump was equal to 104Hz (16.6rad/sec) and the leakage characteristic frequency(w_L) per lump was about 2.5Hz(0.39rad/sec). Using Equation (5-11a) with different values of (w/w_v) and (w_L/w_v) , then in Figure 5.2a, the normalized signal propagation velocity (c/c_0) is plotted against the normalized frequency(w/w_v). For the lossless model (that is, $w_L = w_v = 0$), the velocity of propagation always equals the speed of sound in free space. For the distortionless model (that is, $w_L/w_v = 1$),

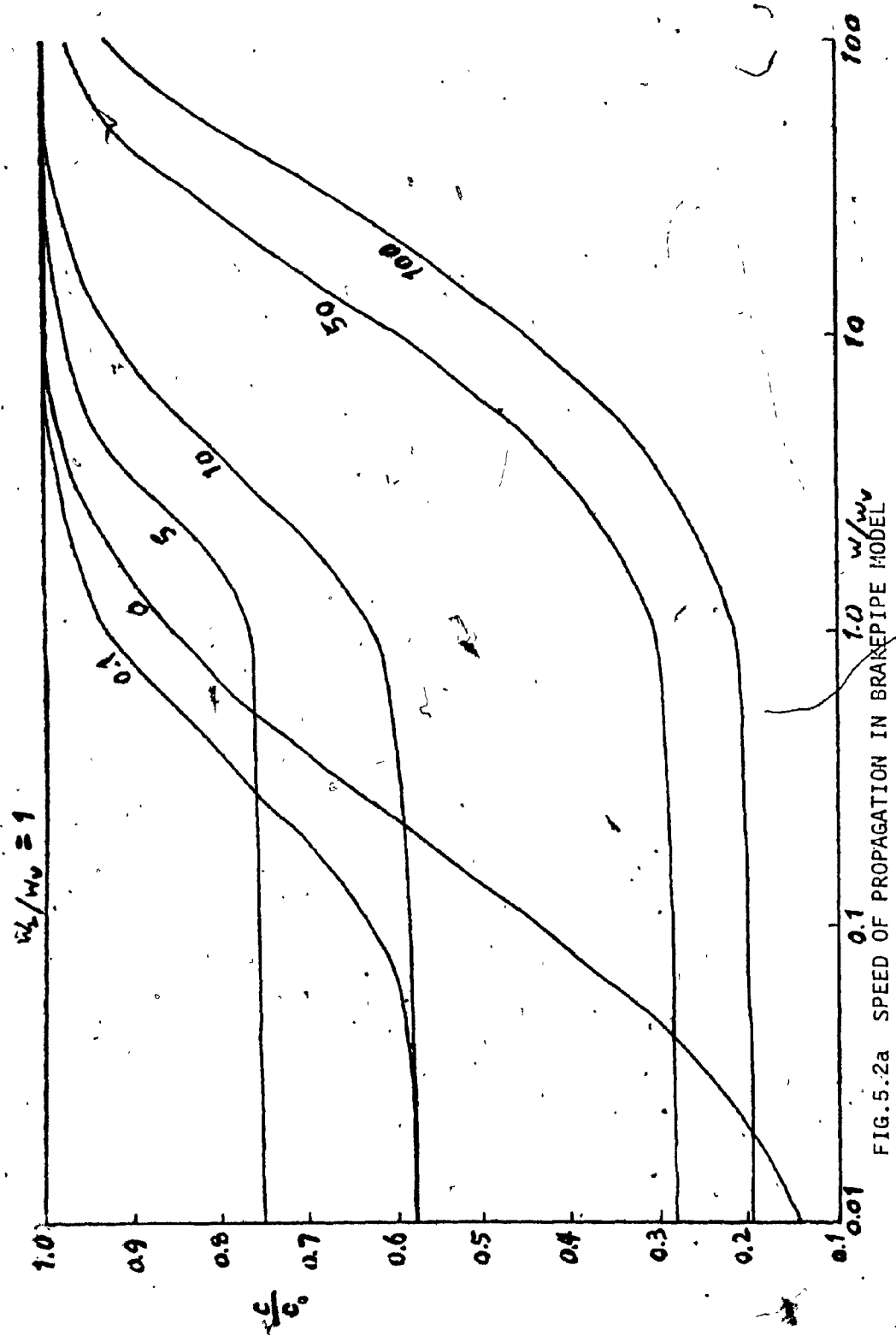


FIG. 5.2a SPEED OF PROPAGATION IN BRARPIPE MODEL

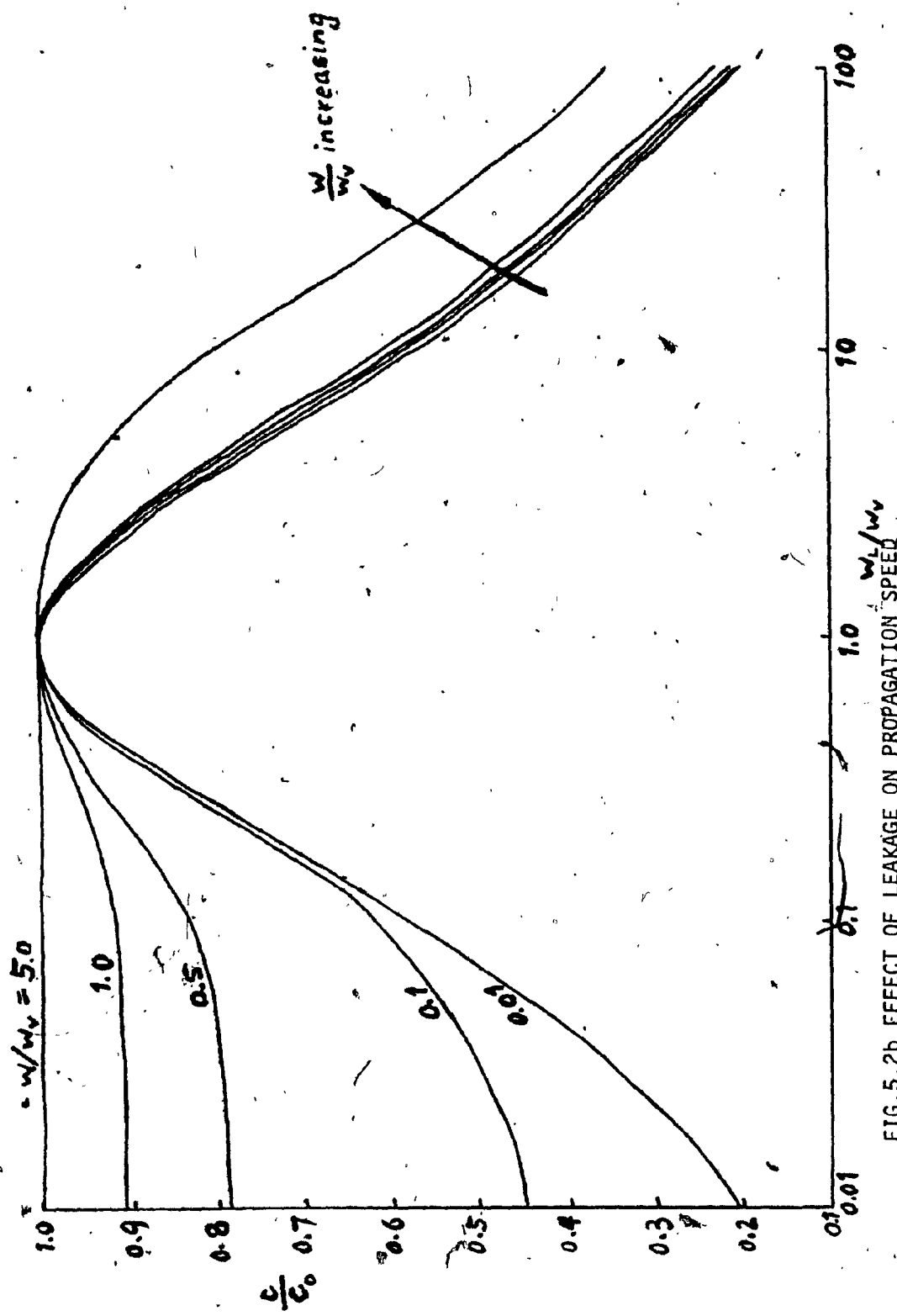


FIG. 5.2b EFFECT OF LEAKAGE ON PROPAGATION SPEED

the propagation speed always equals the acoustic speed of sound. The friction causes a significant reduction in propagation speed at low frequencies ($w/w_v < 5$). Effect of leakage on the propagation speed is shown in Figure 5.2b. Small leak (except $w_L/w_v = 1$) caused a significant decrease in propagation speed at low frequencies ($w/w_v \leq 1$). Also, large leak ($w_L/w_v \geq 20$) caused a large reduction in the propagation speed at any frequencies.

Figures 5.3a and 5.3b show how the model affects the propagation factor. In Figure 5.3a the ratio of the propagation attenuation factor to the propagation phase factor is plotted vs. frequency. Since the phase factor had a larger rate of increase, the ratio decreased and approached zero at high frequency. When leakage did not exist, at low frequencies the ratio approached unity. If leakage exists in the model, the attenuation factor will increase which is also shown in Figure 5.3b. It implies that for the transient response of an input signal in leaked brakepipe, the output magnitude is small enough not to be visualized (so as to show a longer time delay and lower propagation speed). It is necessary to verify such behaviour, by considering the theoretical analysis on the transient response of the brakepipe by a unit step function of pressure, on the following section.

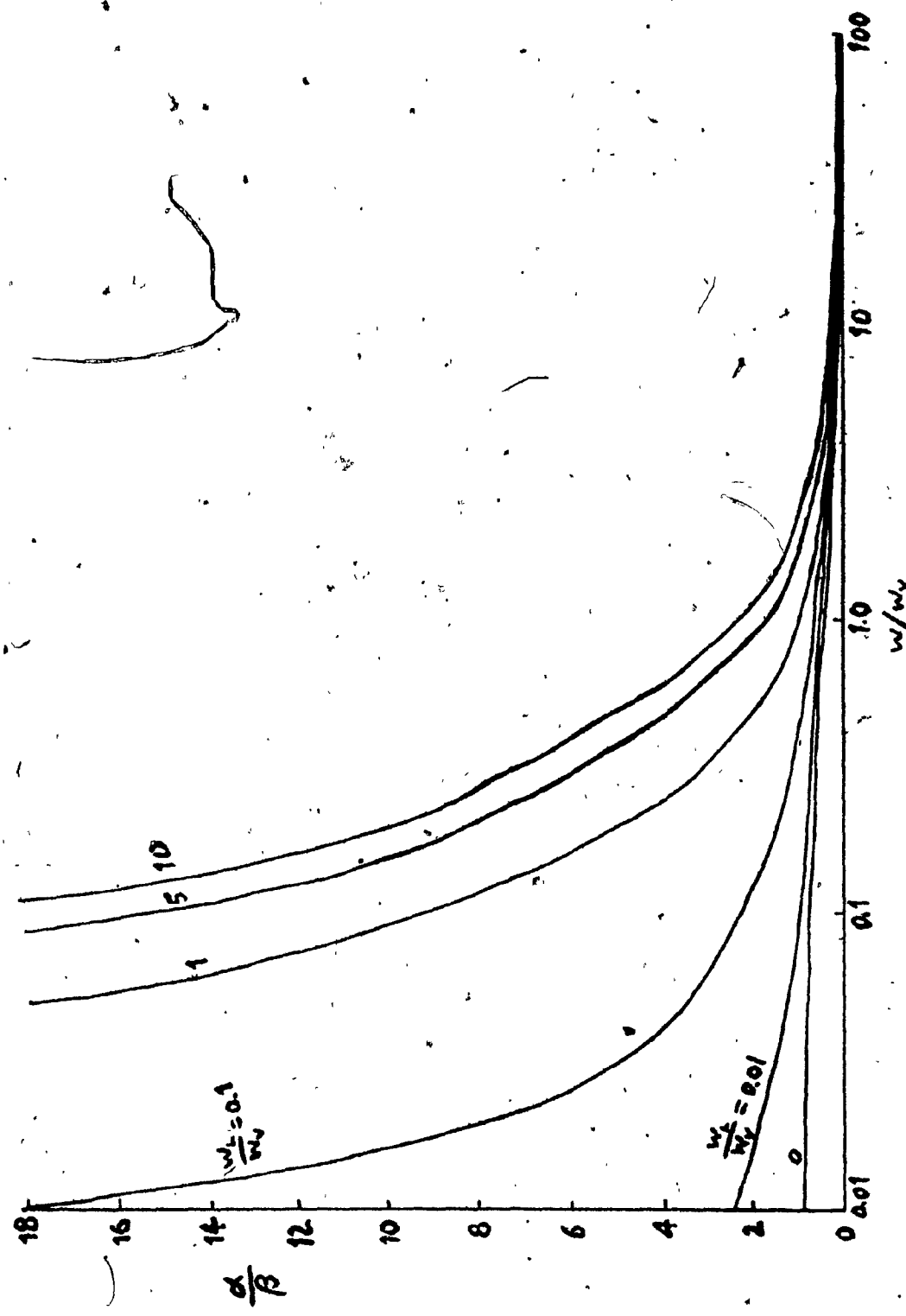


FIG. 5.3a ATTENUATION-PHASE RATIO IN BRAKEPIPE MODEL

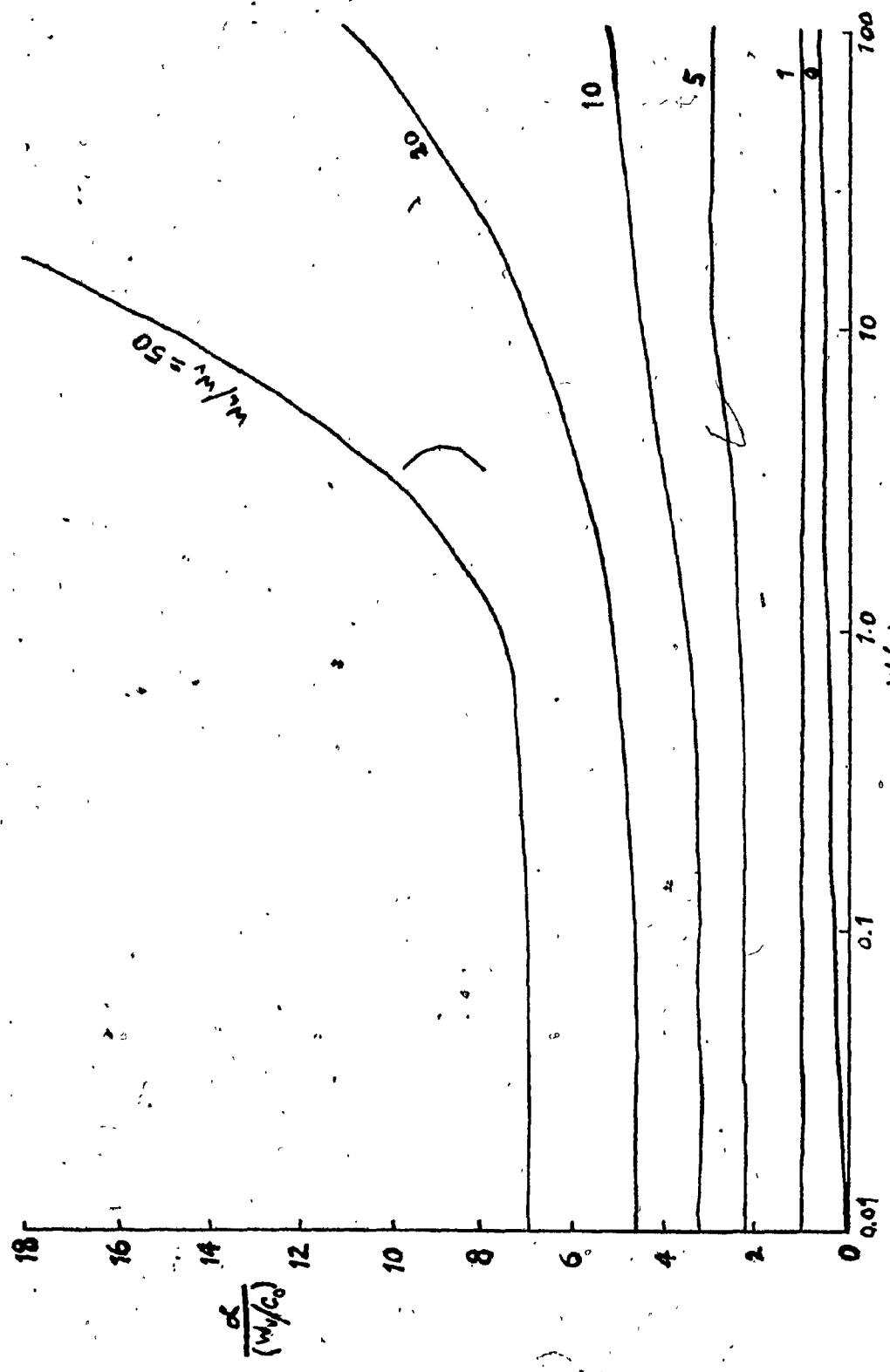


FIG. 5.3b NORMALIZED ATTENUATION VS. FREQUENCY WITH LEAKAGE AS A PARAMETER

5.3 TRANSIENT RESPONSE OF THE BRAKEPIPE MODEL

For a semi-infinite brakepipe, it was kept to use the same parameters in the equivalent circuit of an one-dimensional linearized brakepipe model which is shown in Figure 5.1. Then it was assumed that a semi-infinite brakepipe was supplied by a unit step-function pressure. An expression for the pressure was set up as a function of x and s , on a line with uniformly distributed and constant parameters, as follows:

$$P(x,s) = \frac{1}{s} e^{-x/\sqrt{LC}} \sqrt{(s+\gamma)^2 - \sigma^2} \quad \dots \dots \quad (5-12)$$

$$\text{where } \gamma = 0.5(\frac{R}{L} + \frac{G}{C}) = 0.5(w_v + w_L)$$

$$\sigma = 0.5(\frac{R}{L} - \frac{G}{C}) = 0.5(w_v - w_L)$$

x = location in the brakepipe

The inverse Laplace transform of $P(x,s)$ is derivable by contour integration(32), as follows(Note: $p(x,t)$ is the inverse transform of $P(x,s)$):

$$p(x,t) = \left[e^{-\gamma \bar{t}_d} + \sigma^2 \bar{t}_d \int_{\bar{t}_d}^t \frac{e^{-\gamma \tau} I_1(q)}{q} d\tau \right] u(t - \bar{t}_d) \quad \dots \dots \quad (5-13)$$

where \bar{t}_d = ideal time delay = $x/\sqrt{LC} = x/c_0$

$$q = \sigma \sqrt{\tau^2 - \bar{t}_d^2}, \quad u(t - \bar{t}_d) = \text{step function}$$

$I_1(q)$ = modified Bessel function of the first kind, first order = $\sum_{k=0}^{\infty} \frac{(q/2)^{2k+1}}{(k+1)!k!}$

The integral in Equation(5-13) can be obtained by using numerical means such as Simpson's Rule.

An alternate form for Equation(5-13) was given by Woodruff(33) as:

$$p(x,t) = e^{-\nu t} [J_0(q) + 2bhJ_1(q) + (4b^2 - 2)h^2J_2(q) + (8b^3 - 6b)h^3J_3(q) + (16b^4 - 16b^2 + 2)h^4J_4(q) + (32b^5 - 40b^3 + 10b)h^5J_5(q) + (64b^6 - 96b^4 + 36b^2 - 2)h^6J_6(q) + (128b^7 - 224b^5 + 112b^3 - 14b)h^7J_7(q) + (256b^8 - 512b^6 + 320b^4 - 64b^2 + 2)h^8J_8(q) + \dots] \quad (5-14)$$

where $J_n(q) = \frac{q^n}{2^n n!} \left[1 + \frac{q^2}{2^2 1!(n+1)} + \frac{q^4}{2^4 2!(n+1)(n+2)} + \dots \right]$

$$(n = 1, 2, 3, \dots, \infty)$$

$$h = \sqrt{(c_o t - x)/(c_o t + x)}$$

$$b = \nu/\sigma$$

c_o = acoustic speed of sound

The final value of the pressure can be obtained from the final value theorem as follows:-

$$p(x, \infty) = \lim_{s \rightarrow 0} e^{-x\sqrt{LC}} \frac{(s+\nu)^2 - \sigma^2}{s} = e^{-x\sqrt{RG}} \quad (5-15)$$

One can be able to plot the normalized, dynamic pressure, $p'(x,t)$, that is $p(x,t)/p(x,\infty)$, by dividing Equation(5-13) with Equation(5-15). Hence,

$$p'(x,t) = \left[e^{-t_c(1-r^{\frac{1}{2}})^2/2} + t_c^2(1-r)^2 e^{t_c r^{\frac{1}{2}}} \int_1^t f(y) dy \right] u(t-t_d) \quad (5-16a)$$

$$p'(x, \bar{t}_d+) = \left[e^{-t_c(1-r^2)/2} + t_c^2(1-r)^2 e^{t_c r} \int_1^{t'} f(y) dy \right] \dots \quad (5-16b)$$

$$\text{where } t_c = w_v \bar{t}_d$$

$$r = w_L / w_v$$

$$f(y) = \frac{e^{-t_c(1+r)y/2}}{I_1(q)} \quad , \quad (y = t/\bar{t}_d)$$

$$t' = t/\bar{t}_d$$

NOTE: The term " \bar{t}_d+ " is used as a value for t in expression for pressure at the wavefront to indicate that the value of the function immediately after the discontinuity is intended.

The unit function in Equation(5-16) states that no pressure is present at a given location x until \bar{t}_d seconds after the transient is initiated. A program which is used for computing $p'(x,t)$ is presented in Appendix B. Equation(5-16) consists of two parts. The first is $e^{-t_c(1-r^2)/2} u(t-\bar{t}_d)$. This represents distortionless transmission. It is just a square wave that will propagate with attenuation along the brakepipe. The second term represents the distortion component. Note that, in a distortionless case, $\sigma=0$ (or $r=1$) and the second term vanishes. Then, the ideal output is just a delayed unit step. The departure from the delayed unit step is the distortion term.

The behaviour of the pressure function immediately

after the wave-front arrival varies with the dimensionless quantity w_L/w_v . The results of the programme are plotted in Figure 5.4. For more leakage ($w_L/w_v \neq 1$), the greater the attenuation was found. Thus, it appeared that the leakage (and friction) affected the delay time of signal propagation in the brakepipe. Therefore, the propagation speed was found to be less than the acoustic speed of sound in free space.

It is worth to note that in the brakepipe model the typical ratio of frequencies, w_L/w_v , was about 0.02 according to the assumptions presented in Section 5.2. In general, larger ratio of the frequencies would give longer delay time due to the propagation attenuation factor α .

Notice in the RLGC circuit (distributed model) that there is a finite velocity of propagation of the signal. This is in contrast to the RCG line, where this type of propagation did not result. It was mentioned in Chapter 3, this paradox occurs because fluid inertance is ignored. Also, reflections which were omitted in this section can cause a different response but will not alter the time delay t_d .

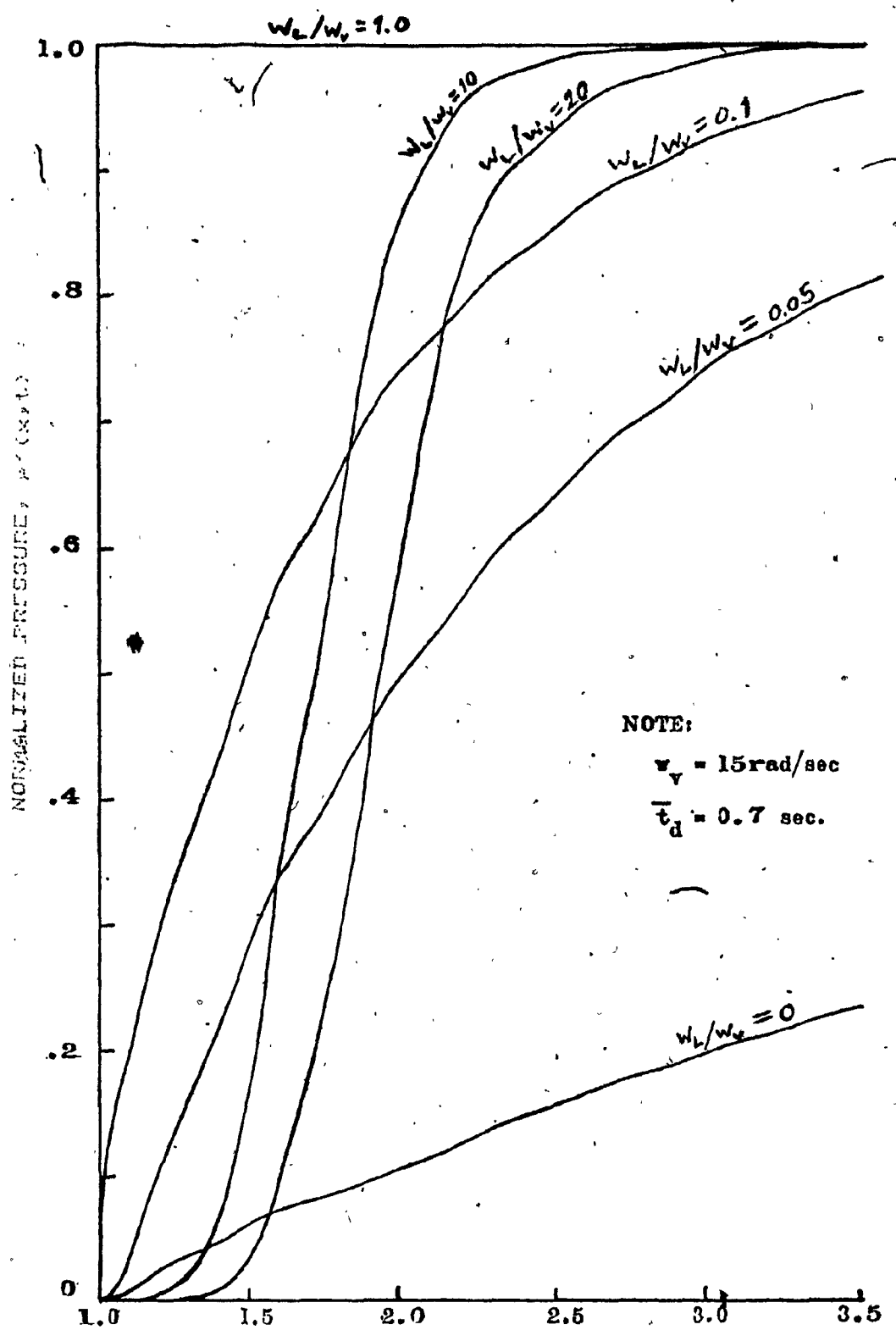


FIG. 5.4 TRANSIENT RESPONSE OF A SEMI-INFINITE BRAKEPIPE
WITH LEAKAGE AS A PARAMETER.

5.4 EFFECT OF LEAKAGE ON THE PROPAGATION SPEED

Referring to the evaluation of time delay described in Section 4.3.2.5 and Figure 4.21a, one can estimate the experimental value of propagation speed c_i for i^{th} pipe since the length of brakepipes between the i^{th} pipe and the front-end, ($l_i - l_0$) and propagation time t_{di} (similar to time delay for the brakepipe pressure at i^{th} pipe to start reduction) were measured. For example, only plumbing leakage existed in the experimental model, the propagation time for pressure wave transmitting from pipe No.1 to pipe No.75 was about 0.8 second. It implied that an approximate experimental propagation speed at pipe No.75 was 309m/sec (about 80% of sonic velocity of sound in pipe); while there were 15 leakage orifices (with 0.33mm diameter) along the brakepipes, similarly, propagation speed c was 165m/sec (46% of sonic velocity of sound in pipe).

One converts time delay t_{di} to propagation speed with such a relation of $c_i = (l_i - l_0)/t_{di}$, then Table 5.2 is transformed from Table 4.4, Figures 5.5 and 5.6 from Figure 4.21b and 4.22, respectively. It was obvious that transmission speed of air propagation c was less than acoustic speed of sound c_0 .

The effect of leakage size on the propagation speed is shown in Table 5.2 and Figure 5.5. When one

TABLE 5.2 PROPAGATION SPEED VS. LEAKAGE SIZE

SIZE		LEAKAGE ORIFICE DIAMETER (mm)				
SPEED (m/s)		0.330	0.584	0.787	1.397	1.854
AIR SUPPLY AT 414kPa	A'	284	274	259	229	196
	B'	301	277	235	199	170
AIR SUPPLY AT 483kPa	A'	294	284	266	249	222
	B'	309	287	247	215	186
AIR SUPPLY AT 552kPa	A'	305	294	274	266	242
	B'	317	298	263	231	198
AIR SUPPLY AT 621kPa	A'	317	305	284	274	257
	B'	325	308	277	247	209

NOTE: (i) ONLY ONE LEAKAGE ORIFICE WAS APPLIED AND LOCATED AT BRAKEPIPE NO.40 OF BRAKEPIPE MODEL.

(ii) INACCURACY ON READING THE EXPERIMENTAL RESULTS DUE TO 'FLAT' TIME-RESPONSE GIVEN IN STRIP-CHART. PERCENTAGE ERROR WOULD BE WITHIN $\pm 16\%$ IN MOST CASES.

(iii) A' -- WAVE TRAVELS FROM PIPE #1 TO #25
B' -- WAVE TRAVELS FROM PIPE #1 TO #75.

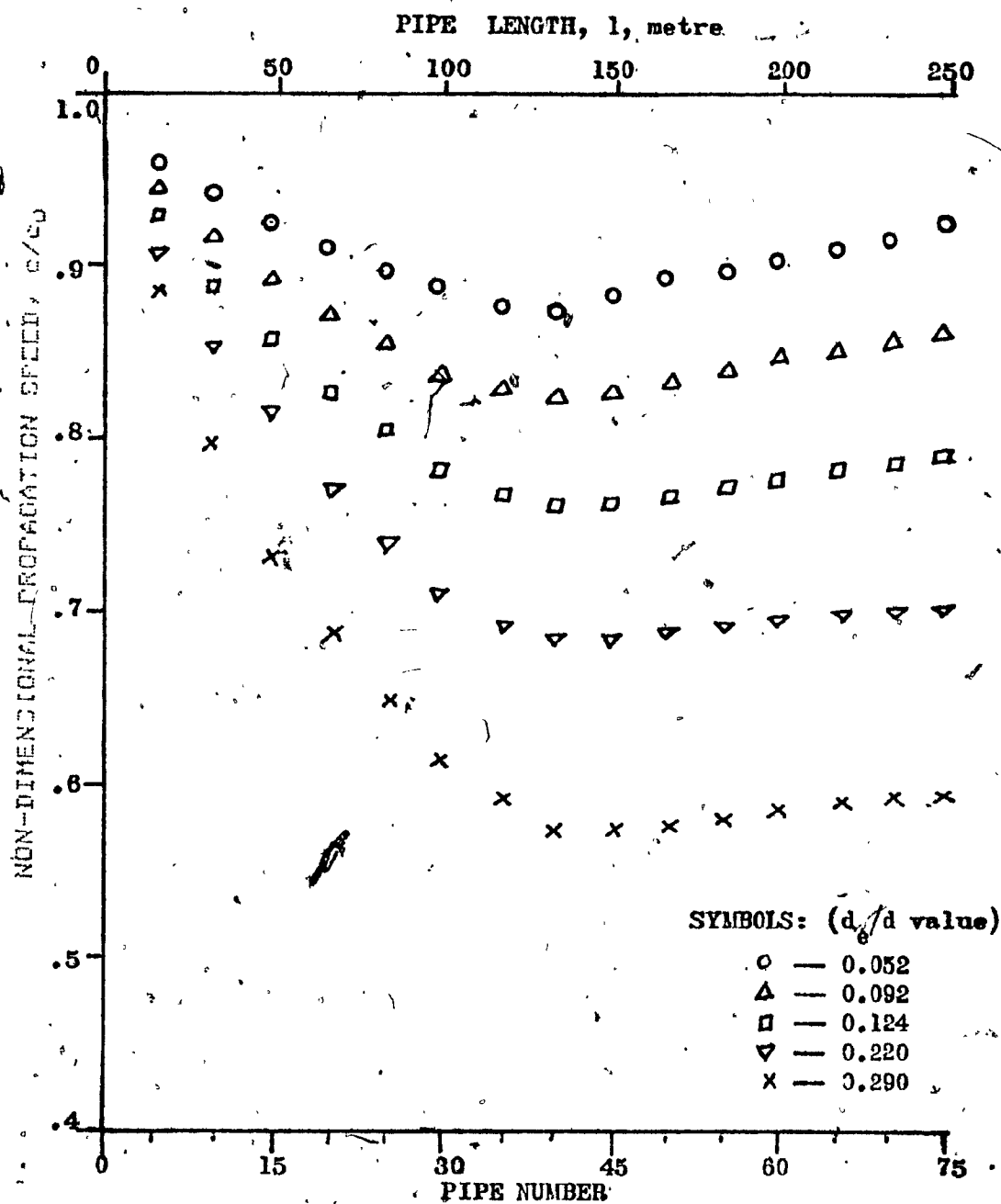


FIG.5.5 PROPAGATION SPEED CURVES

(NOTE: Experimental results — air supply at 552kPag,
leaks at pipe #40 only without pressure chamber.)

compared with the propagation speed in the case of smallest leakage orifice diameter and largest leakage orifice diameter being used one found that the propagation speed decreased by 10% and 43% for the last brakepipe respectively. Since only one leakage orifice was located at brakepipe No.40 of the brakepipe model, in general, the lowest propagation speed was existed near to pipe No.40. If leakage size is large, say $d_e/d > 0.1$, more serious reduction on propagation speed occurs at the rear end. For instance, when d_e/d equals to 0.29, the propagation speed for the last brakepipe was 60% of the acoustic speed of sound. Besides, when brakepipe pressure increased the propagation speed would increase slightly because of larger bulk modulus of elasticity of air.

In Figure 5.6, the effect of leak location on propagation speed is presented. When brakepipe leakage did occur at the head end of the brakepipes, the propagation speeds at the pipes No.25 and No.75 were 65% and 94% of the acoustic speed of air respectively; when leakage occurred at the rear end, the propagation speeds at the pipes No.25 and No.75 were 90% and 50% of the acoustic speed of air respectively. It implied that leak location at the rear end affected the transmission speed of air propagation seriously.

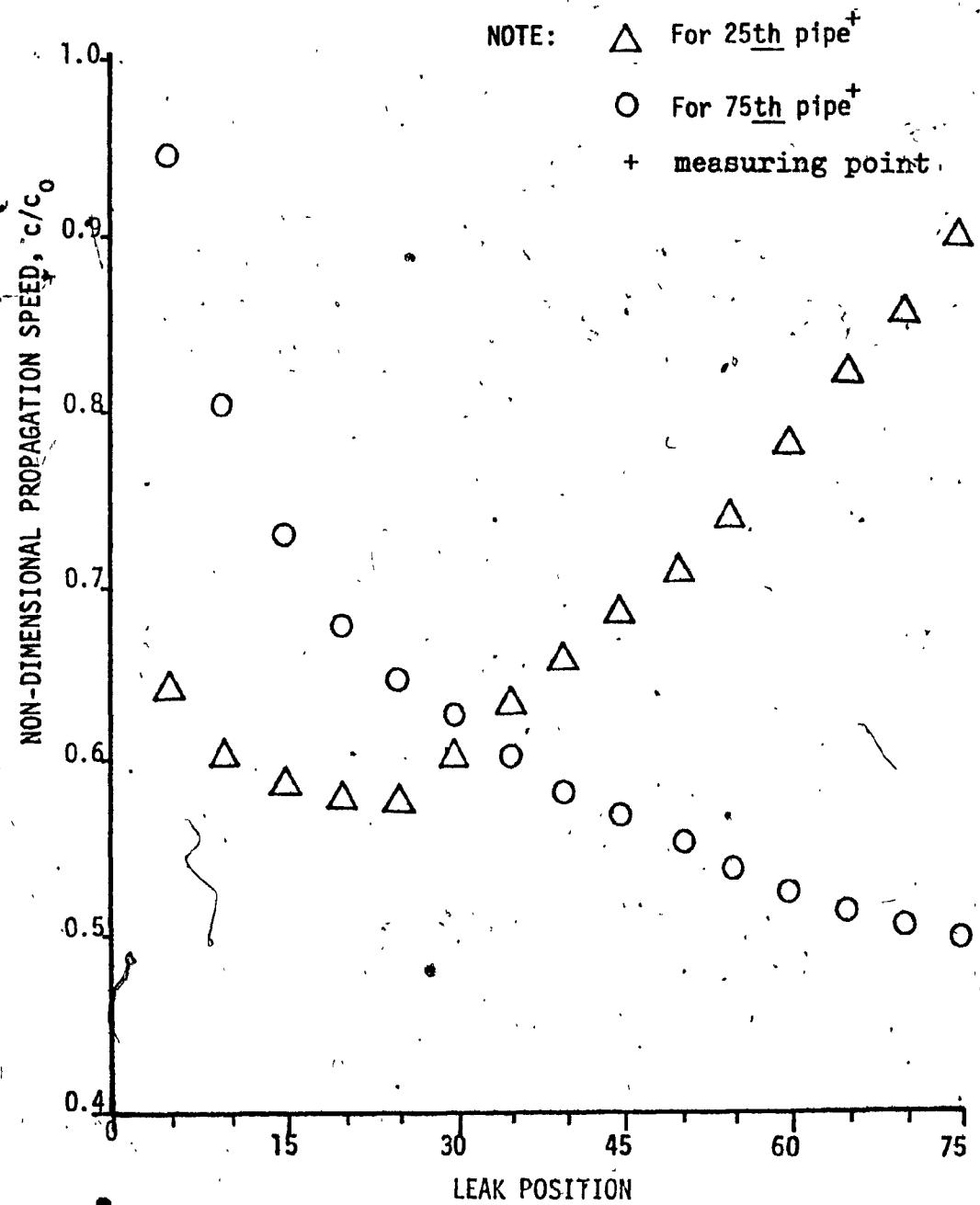


FIG.5.6 PROPAGATION SPEED VS. LEAK POSITION

(One leakage orifice was located at different pipe for each discharge process)

Summarizing this Chapter, it was found that leakage (and friction) would cause reduction in the propagation speed for the brakepipe model (although experimental results showed a difficulty in finding an accurate delay time). However, from the engineering point of view, the propagation speed c would increase if (1) the brakepipe leakage particularly for the leak concentrated in the rear end was eliminated; since it was known that the size and location of the leakage would affect not only the pressure gradient and distribution but also the propagation speed, it should be noted that when checking freight trains for leakage, correction of leakage at the rear of the train would produce greater improvement in the propagation speed than correction of comparable leakage at the head end of the train; (2) the fluid components should be modified such that w_L would be close to w .

CHAPTER 6

CONCLUSION

6.1 SUMMARY

The effects of leakage were demonstrated both by computer simulation and experiments on a scaled-down brakepipe model. It has to be pointed out that the fixed-volume pressure chamber could replace pneumatic pressure relay valve, which was located at the head end of the brakepipe, for an easier way of experimental testing procedures. The objective of this study was to provide a valuable supplement to existing practical know-how in the scaled model of the brakepipe.

A detailed mathematical model with computer simulation for generating pressure distribution for a scaled-down brakepipe model was well developed by utilization of lumped modeling. It was a good, simple approach on finding dynamic characteristics of the brakepipe. Another method : method of characteristics for large-amplitude signals was not greatly used in leakage problem because of difficulty in formulating complex equations. It was found that the percentage error in the pressure distribution between the experimental and theoretical results was within $\pm 10\%$. In

order to improve the theoretical results and to minimize its computation time, number of lumps should be wisely compromised, & a better numerical technique of computing the differential equations should be applied.

The location and size of leakages affected not only the pressure gradient and distribution, but also signal propagation velocity and time delay. The brakepipe leakage tended to accentuate the pressure gradient. The brakepipe leakage also made it longer to fully charge or recharge the braking system thereby reducing the brakepipe exhaust time. When excess leakage has developed within a certain section of the brakepipe, incorrect signals may be passed through therefore causing undesirable braking action. The larger leakage orifice size along the brakepipe and the concentration of leak at the rear end would have lower propagation speed. It was found that the transmission speed of air propagation was less than acoustic speed of sound while brakepipe leakage (and friction) existed. A possible reason why a significant reduction in propagation speed would occur in RLGC brakepipe model was that the output magnitude of an input signal in transient state was so small that it gave a longer time delay (or a lower propagation speed).

The ultimate goal of all this research is to find the dynamic characteristics of the brakepipe of a train.

Our brakepipe model provided simulation to charging and discharging processes in the brakepipe. It should be noted that, besides the physical configuration, there were some differences between the brakepipe of a train and our brakepipe model:- In the analytical and experimental models, brakepipe leakage was concentrated at one point while the leakage in an actual freight car is distributed at random; the flow through the connecting hose of a car has more restriction than the experimental pipe fitting; the brakepipe in a freight car has some degree of bend depending on location of other devices equipped on the car; and the use of relay valve in a real car has been replaced by pressure chamber and exhaust orifice in our model. This work was felt to be an important step forward in achieving the ultimate goal. When such goal is made it is expected that the difficulties of the railroad workers may considerably be eliminated.

6.2 SUGGESTION FOR FURTHER WORK

So far the transient brakepipe pressure was found satisfactorily with the lumped modeling and was verified by experiments. But the results for the nonlinear brakepipe model indicated that further work should be warranted therefore, the following suggestions may be considered:-

- (a) to include the fluid inertance into the nonlinear lumped parameter model (in Chapter 3) so as to show the nature of a delay time in the transient response of brakepipe pressure. (No time delay is predicted if the fluid inertance is ignored.)
- (b) to modify the method of characteristics for large amplitude signal by adding the leakage flow parameter into the characteristic equations such that any leakage distribution can be applicable.
- (c) to extend testing for a greater range of those physical parameters representing pipe resistance, plumbing leakage and brakepipe leakage.
- (d) finally, to apply simulation model to real brakepipe of a freight train. The test should be directed to the investigation of the pressure-flow characteristics of the brakepipe, hose and leakage. (The quantity of allowable brakepipe leakage can only be given through the optimization of the automatic brake system.)

REFERENCES

- 1) "Management Of Train Operation And Train Handling", The Air Brake Association Handbook, 1972.
- 2) V. AULA, "Single Fault Location Methods Applied To Brake Pipe Models", Master's Thesis, Concordia University, Montreal, March 1980.
- 3) C.T. KWAN, "Network Model For Brakepipe Leakage", Master's Thesis, Concordia University, Montreal, June 1977.
- 4) K. PORTER, "Freight Train Optimal Trajectory Calculation By Linear Programming", Master's Thesis, Concordia University, Montreal, 1974.
- 5) A.S. IBERALL, "Attenuation Of Oscillatory Pressure In Instrument Lines", Journal of Research, Research Paper RP2115, Vol.45, July 1950, pp.85-108.
- 6) J.C. MOISE, "Pneumatic Transmission Lines", ISA Journal, April 1954, pp.35-40.
- 7) C.P. ROHMANN and E.C. GROGAN, "On The Dynamics Of Pneumatic Transmission Lines", ASME Paper No.56-SA-1.
- 8) C.B. SCHUDER and R.C. BINDER, "The Response Of Pneumatic Transmission Lines To Step Inputs", ASME Paper No.58-A136.
- 9) N.B. NICHOLS, "The Linear Properties Of Pneumatic Transmission Lines", ISA Transactions, Vol.1, January 1962, pp.5-14.

- 10) J.T. KARAM, Jr. and M.E. FRANKE, "The Frequency Response Of Pneumatic Lines", ASME Transaction Journal Of Basic Engineering, June 1967, pp.371-378.
- 11) M.E. FRANKE, A.J. MALANOWSKI and P.S. MARTIN, "Effects Of Temperature, End-conditions, Flow, And Branching On The Frequency Response Of Pneumatic Lines", ASME Paper No.71-WA/Aut-5.
- 12) R.E. GOODSON and R.G. LEONARD, "A Survey Of Modeling Techniques For Fluid Lines Transients", ASME Paper No.71-WA/FE-9.
- 13) S. KATZ and R.M.H. CHENG, "A Network Approach To Brakepipe Leakage", ASME Paper No.77-WA/FLCS-12, December 1977.
- 14) K. AULA, R.M.H. CHENG and S. KATZ, "Single Fault Location Methods Applied To Brakepipe Models", ASME Paper No.79-WA/RT-11, 1979.
- 15) R.S. BENSON, R.D. GARG and D. WOOLLATT, "A Numerical Solution Of Unsteady Flow Problems", Int. J. Mech. Sci., Pergamon Press Ltd., 1964.
- 16) J.R. MANNING, "Computerized Method Of Characteristics Calculations For Unsteady Pneumatic Line Flows", ASME Paper No.68-FE-18.
- 17) A.K. TRIKHA, "Variable Time Steps For Simulating Transient Liquid Flow By Method Of Characteristics", Journal of Fluids Engineering, March 1977, pp.259-261.
- 18) W. ZIELKE, "Frequency-Dependent Friction In Transient Pipe Flow", ASME Paper No.67-WA/FE-15.
- 19) F.T. BROWN, "A Quasi Method Of Characteristics Application To Fluid Lines With Frequency

Dependent Wall Shear and Heat Transfer",
ASME Paper No.68-WA/Aut-7.

- 20) V.L. STREETER, "Unsteady Flow Calculations By Numerical Methods", Journal of Basic Engr., ASME Transaction, Series D, Vol.94, No2, June 1972, pp.457-466.
- 21) J.M. KIRSHNER and S. KATZ, Design Theory of Fluidic Components, Academic Press, 1975, Chapter 3.
- 22) K. OGATA, System Dynamics, Prentice-Hall, Inc., 1978.
- 23) B.W. ANDERSON, The Analysis and Design of Pneumatic System, John Wiley & Sons, Inc., New York, 1976.
- 24) Instruction Pamphlet, 26-Type Brake Equipment for Locomotive, Westinghouse Air Brake Division, WABCO, Wilmerding, Pennsylvania, October 1964.
- 25) G.Z. WATTERS, Modern Analysis and Control of Unsteady Flow in Pipelines. Ann Arbor Science Publishers Inc., Michigan, 1979.
- 26) T. YOUNG, "Propagation of Impulse Through an Elastic Tube," Trans. Royal Society of London, Vol. No.98, 1808, pp.164-186.
- 27) D.J. KORTEWEG, "Über die Fortpflanzungsgeschwindigkeit des Schalles in Elastisches Rohren," Annalen der Physik und Chemie, Vol.9 Folge, Band 5, 1878, pp.525-542.
- 28) H. LAMB, "On the Velocity of Sound in a Tube as Affected by the Elasticity of the Walls," Manchester Literary and Philosophical Soc., Memoirs and Proc., Vol.42, No.9, 1898.

- 29) R.S. RAIZADA, "Linear Dynamic Properties of Fluid Transmission Lines," Systems and Controls Laboratory Report, Pennsylvania State University, March 1967, pp.27-57.
- 30) J.T. KARAM,Jr. and R.G. LEONARD,"A Simple Yet Theoretically Based Time Domain Model for Fluid Transmission Line Systems," ASME Paper No.73-FE-27, December 1973,pp.498-504.
- 31) P.C. MAGNUSSON, Transmission Lines and Wave Propagation, Allynand Bacon, Inc., Boston, 2nd Edition, 1970.
- 32) P.M. CHIRLIAN, Signals, Systems and the Computer, INTEXT Educational Publisher, 1973.
- 33) L.F. WOODRUFF,"Transmission Line transients in Pictures", AIEE Transactions, Vol.57, 1938, pp.396-400.

APPENDIX A

DERIVATION OF EQUATIONS

(a) TO DETERMINE THE SIGNAL VARIABLES AT POINTS L & R

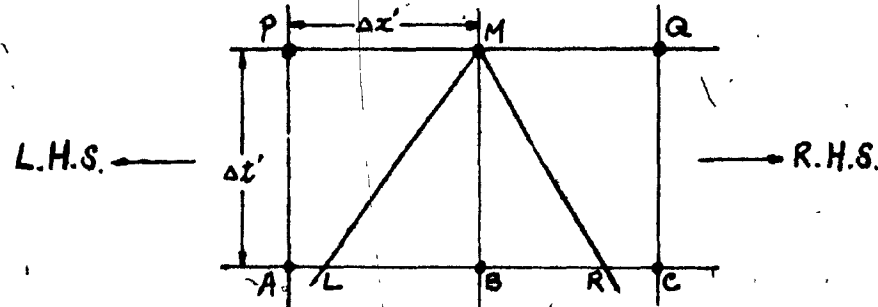


FIG.A.1 Show the characteristic lines & points

For right boundary(R.H.S.), we consider its similarity:

$$\frac{u'_L - u'_B}{u'_A - u'_B} = \frac{a'_L - a'_B}{a'_A - a'_B} \quad \dots \text{(A.1)}$$

$$\frac{u'_L - u'_B}{u'_A - u'_B} = \theta (u'_L + a'_L) \quad \dots \text{(A.2)}$$

From equations(A.1) & (A.2), we multiply (A.1) by θ and add into (A.2), then we get:

$$u'_L = \frac{u'_B + \theta (a'_B u'_A - u'_B a'_A)}{1 - \theta (u'_A - u'_B + a'_A - a'_B)} \quad \dots \text{(A.3)}$$

$$= \frac{u'_B + \theta Y'_L}{1 - \theta V'_L}$$

where $\theta = \frac{\Delta t'}{\Delta x'}$

$$Y'_L = u'_A a'_B - u'_B a'_A$$

$$V_L' = u_A' - u_B' + a_A' - s_B'$$

hence,

$$a_L' = \frac{a_B' - \theta Y_L'}{1 - \theta V_L'} \quad \dots \quad (A.4)$$

For left boundary(L.H.S.), we use its similarity:

$$\frac{u_R' - u_B'}{u_C' - u_B'} = \frac{a_R' - a_B'}{a_C' - a_B'} \quad \dots \quad (A.5)$$

$$\frac{u_R' - u_B'}{u_C' - u_B'} = \theta (a_R' - u_R') \quad \dots \quad (A.6)$$

From equations (A.5) and (A.6), we multiply (A.5) by θ

and add into (A.6), then we obtain

$$u_R' = \frac{u_B' + (a_B' u_C' - a_C' u_B')}{1 + \theta(u_C' - a_C' + a_B' - u_B')} \quad \dots \quad (A.7)$$
$$= \frac{u_B' + \theta Y_R'}{1 + \theta V_R'}$$

where $Y_R' = u_C' a_B' - u_B' a_C'$

$$V_R' = u_C' - a_C' + a_B' - u_B'$$

$$\text{hence, } a_R' = \frac{a_B' + \theta Y_R'}{1 + \theta V_R'} \quad \dots \quad (A.8)$$

(b) DERIVATION OF EQUATION(3-12)

When air flow through an orifice to atmosphere, p_f , and the upstream pressure is p_i , the pressure ratio (p_f/p_i) is less than 0.5283, thus, the flow is a choked flow.

The mass through the orifice will be proportional to the

upstream pressure (from Ref.(23)):

$$\dot{m}_i = \frac{K p_i A_{oi} N}{\sqrt{T}} \quad \dots \text{(A.9)}$$

The factors K & N are given by:

$$K = \left[\frac{\gamma g_c}{R} \left(\frac{2}{\gamma+1} \right)^{(\gamma+1)/(\gamma-1)} \right]^{1/2}$$

$$N = 1.0$$

If A_{oi} is the effective exhaust area at i th pipe, equation (A.9) may be written as:

$$p_i = R_i \dot{m}_i \quad \dots \text{(A.10)}$$

$$\text{where resistance } R_i = \frac{\sqrt{T}}{K N A_{oi}}$$

(c) TO ESTIMATE VOLUME OF PRESSURE CHAMBER

Assuming isothermal process, the initial mass of air in the brakepipe is:

$$M_{lI} = \frac{p_{lI} V_l}{n RT} \quad \dots \text{(A.11)}$$

and the initial mass of air in the chamber is

$$M_{cI} = \frac{p_{cI} V_c}{n RT} \quad \dots \text{(A.12)}$$

where subscripts, l: brakepipe & c: chamber

For steady state, the final mass of air in the brakepipe and the chamber is:

$$M_{cF} + M_{lF} = \frac{p_F (V_c + V_l)}{n RT} \quad \dots \text{(A.13)}$$

where p_F is final brakepipe pressure and chamber

From the law of conservation of mass, we get

$$|M_{cF} - M_{cI}| = |M_{lF} - M_{lI}| \quad \dots \dots \text{ (A.14)}$$

where subscript F is meant the final or steady state during discharging process

By substitution, the equation (A.14) becomes

$$\frac{\Delta p_1}{\Delta p_c} = \frac{V_c}{V_l} \quad \dots \dots \text{ (A.15)}$$

where $\Delta p_1 = p_{lI} - p_{lF}$ & $\Delta p_c = p_{cF} - p_{cI}$

Thus, we get V_c , since V_l was shown.

(d) DERIVE DARCY FORMULA: $h_L = f l u^2 / 2 d g_c$

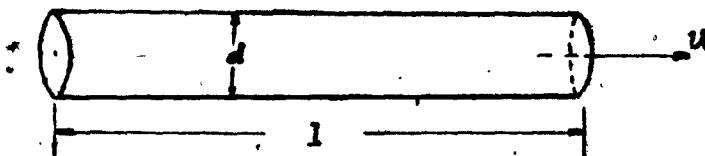


FIG.A.2 Pipe flow

Consider a cylinder of fluid (air) of length l completely filling the pipe of cross-sectional area A and moving with a mean velocity u .

The forces acting on the cylinder are the force due to pressure difference and the force due to frictional resistance. Since the velocity is constant and there is no acceleration, the resultant of these two forces in the direction of motion must be zero.

Force due to pressure difference = $(p_1 - p_2) A$.

If, q = frictional resistance per unit area at unit velocity

and the frictional resistance varies as u^2 .

Frictional resistance/unit area at $u = qu^2$

Force due to friction on surface of pipe

$$= qu^2 Pl \dots \dots \text{(A.16)}$$

where P = perimeter of the cross-section

Force due to pressure difference = force due to friction

$$(p_1 - p_2) A = qu^2 Pl \dots \dots \text{(A.17)}$$

If h_f = head lost in friction in length l

$$= (p_1 - p_2)/\rho$$

$$= qu^2 Pl / \rho A \dots \dots \text{(A.18)}$$

Multiply top and bottom by $2g_c$

$$h_f = \frac{2qg_c Pl}{\rho A} \frac{u^2}{2g_c}$$

For $A/P = \text{hydraulic radius of pipe} = r_h$

$$= \frac{\pi d^2/4}{\pi d} = d/4 \dots \dots \text{(A.19)}$$

and $2qg_c/\rho$ is a constant called the dimensionless coefficient and denoted by λ

$$\begin{aligned} h_f &= \frac{\lambda}{r_h} \frac{u^2}{2g_c} \\ &= \frac{f l}{d} \frac{u^2}{2g_c} \dots \dots \text{(A.20)} \end{aligned}$$

Note: For steady turbulent compressible flow in pipes

$$= f/4$$

where f is called frictional resistance

For mass flow rate $\dot{m} = \rho A u$

$$\text{density } \rho = (p_1 + p_2)/2RT \dots \dots \text{(A.21)}$$

where

R = gas constant

T = ambient temperature

g_c = gravitational acceleration

Substituting equations (A.20) & (A.21) in $(p_1-p_2)=\rho h_1$,

then we get:

$$p_1-p_2 = \frac{f l \bar{R} T}{d(p_1+p_2) A^2 g_c} \quad \dots \dots \text{(A.22)}$$

$$\text{hence, } p_1^2 - p_2^2 = K_2 \frac{m^2}{g_c} \quad \dots \dots \text{(A.23)}$$

where K_2 = frictional constant

$$= \frac{16 f l \bar{R} T}{\pi^2 d^5 g_c} \quad \dots \dots \text{(A.24)}$$

Note: Equation (A.24) is derived which is same as eqn.(3-2).

Using Darcy formula, its defect for estimation of the loss of head in a pipeline under turbulent flow condition is:-

It is assumed that the frictional resistance varied as the square of the mean velocity(flow) for such flow and thus $h_1 = f l u^2 / 2 d g_c$, since h_1 & $u^2 / 2 g_c$ are heads, and l/d is a ratio, & f will be a pure number.

In practice the loss of head with turbulent flow does not vary as the square of the velocity, but as some power varying from 1.7 to 2.3. Thus f must vary as some power of the velocity and will not be a constant for a given pipe for all rates of flow. Also, the value of f is dependent on the roughness of the pipe surface and may vary for steep slopes compared with flat slopes.

(e) DERIVATION OF EQUATION(5-6):

The propagation constant $\Gamma(jw)$ is

$$\Gamma(jw) = \sqrt{(R+jwL)(G+jwC)} \text{ to be transformed into}$$

$$\Gamma(jw) = \alpha + j\beta$$

where α = attenuation function

β = phase function

$$j = \sqrt{-1}$$

w = circular frequency of the wave

$$\sqrt{(R+jwL)(G+jwC)} = w\sqrt{LC}\sqrt{(RG/w^2LC-1)+j(G/wC+R/wL)}$$

Let $c_0 = 1/\sqrt{LC}$ = sonic velocity of sound

$$p = RG/w^2LC - 1 \text{ and } q = (G/wC + R/wL)$$

$$\text{then } \alpha + j\beta = w/c_0(p+jq)^{\frac{1}{2}} \quad \dots \quad (\text{A.25a})$$

$$= w/c_0(p^2+q^2)^{\frac{1}{2}}(\cos \frac{\theta}{2} + j \sin \frac{\theta}{2}) \quad \dots \quad (\text{A.25b})$$

$$\text{where } \sin \frac{\theta}{2} = [(1 - \cos \theta)/2]^{\frac{1}{2}}$$

$$\cos \frac{\theta}{2} = [(1 + \cos \theta)/2]^{\frac{1}{2}}$$

$$\text{hence } \alpha + j\beta = w/c_0 \left\{ \left[\frac{1}{2}(p^2+q^2)^{\frac{1}{2}} + \frac{p}{2} \right]^{\frac{1}{2}} + j \left[\frac{1}{2}(p^2+q^2)^{\frac{1}{2}} - \frac{p}{2} \right]^{\frac{1}{2}} \right\} \quad \dots \quad (\text{A.26})$$

$$\alpha = w/c_0 \left[\frac{1}{2} \left\{ \left(\frac{GR}{w^2LC} - 1 \right)^2 + \left(\frac{R}{wL} + \frac{G}{wC} \right)^2 \right\}^{\frac{1}{2}} + \right. \\ \left. \frac{1}{2} \left\{ \frac{GR}{w^2LC} - 1 \right\} \right]^{\frac{1}{2}} \quad \dots \quad (\text{A.27a})$$

$$\beta = w/c_0 \left[\frac{1}{2} \left\{ \left(\frac{GR}{w^2LC} - 1 \right)^2 + \left(\frac{R}{wL} + \frac{G}{wC} \right)^2 \right\}^{\frac{1}{2}} - \right. \\ \left. \frac{1}{2} \left\{ \frac{GR}{w^2LC} - 1 \right\} \right]^{\frac{1}{2}} \quad \dots \quad (\text{A.27b})$$

APPENDIX B

COMPUTER PROGRAMS

INDEX	PAGE
B.1 BRAKEPIPE MODELED BY METHOD OF CHARACTERISTICS -- A Study on pressure reduction ...	141
B.2 BRAKEPIPE MODEL BY LUMPED MODELING -- Studies on pressure reduction, discharging process with plumbing leakage and brakepipe leakage, and charging process with plumbing leakage and/or brakepipe leakage etc. ...	148
B.3 TRANSIENT RESPONSE OF A RLGC SEMI-INFINITE BRAKEPIPE WITH A UNIT STEP OF PRESSURE SUPPLY -- To show the time delay due to leakage and friction ...	157
B.4 ACTUAL BRAKEPIPE ANALYSIS BY THE METHOD OF LUMPED MODELING -- Studies on discharging air to the tank or through relay valve ...	159
B.5 ACTUAL BRAKEPIPE ANALYSIS BY THE METHOD OF CHARACTERISTICS -- Studies on discharging air from the brakepipe to the tank or through relay valve ...	164
B.6 RELAY VALVE DETAILED MODEL -- Fully nonlinear system analysis ...	173

```

C ****
C *
C * THIS PROGRAM IS TO SIMULATE THE DYNAMIC CHARACTERISTICS OF *
C * A BRAKEPIPE MODEL BY USING METHOD OF CHARACTERISTICS FOR *
C * LARGE-AMPLITUDE SIGNALS -- A STUDY ON PRESSURE REDUCTION. *
C *
C ****
C
C DOUBLE PRECISION UA(2,101),AA(2,101),P(101),PA(101)
C DOUBLE PRECISION YRL,VRL,URL,ARL,FN,C1,FTL,FC,DT,EP,DM,FM1
C DOUBLE PRECISION YLI,YRI,VRI,VLI,URI,ARI,ULI,ALI,F1,F2,PRI
C DOUBLE PRECISION YLR,VLR,ULR,ALR,FTR,C3,BI,BPL,BPC,AOP,R,E
C DOUBLE PRECISION RTIME,C,DPC,RSPRI,FP,C2,Q,B1,B4,AREA,B3
C DOUBLE PRECISION B5,BPL1,BPL2,FNLC,AAA,PR,C5,THETA,DEN1,C7
C DIMENSION ARX(101),ARY(3,101),KP(3)
C COMMON /BLK1/CD,AREA,BPL,BPC,TH,DM
C COMMON /BLK2/ARX,ARY
C COMMON /BLK3/AMX,AMN
C COMMON /BLK4/UA,AA
C COMMON /BLK5/T,M,MESH
C COMMON /BLK8/KP
C COMMON /BLK9/NC
C COMMON /BLK10/XP,NP
C COMMON /BLK11/PR,Q
C COMMON /BLK12/C
C COMMON /BLK13/FNLC
C COMMON /BLK15/PPC
C COMMON /BLK16/PA
C DATA KP(1)/1HL/,KP(2)/1HM/,KP(3)/1HR/
C DATA AMX/100./,AMN/50./
C DATA ARX(1)/0./,ARY(1,1)/80./,ARY(2,1)/80./,ARY(3,1)/80./
C
C N- NUMBER OF MESHES
C NI- NUMBER OF ITERATIONS
C DIA- TANK ORIFICE SIZE
C THETA- SLOPE OF GRID LINE
C FC- FRICTION CONSTANT
C CD- DISCHARGE COEFFICIENT
C P(I)- INITIAL BRAKEPIPE PRESSURE
C FM(I)- INITIAL FLOW RATE
C BPC- CHAMBER PRESSURE
C PR- PRESSURE RATIO
C TH- AMBIENT TEMPERATURE
C UA- VELOCITY OF AIR FLOW
C
C ACCEPT THE FOLLOWING DATA
C FOR EXAMPLE: MESH=31,NI=1500,DIA=0.055
C
C ACCEPT 101,MESH,NI,DIA
101 FORMAT(I3,I4,F5.3)
N=MESH-1
M=(1+MESH)/3
ML=2*M
NP=75
THETA=0.6790123457D00
PL=FLOAT(NP)*10.8

```

```

D=0.25
XL=PL/FLOAT(N)
PRI=0.3141592654D01
G=386.
B3=PRI*D**2/4.
AREA=PRI*DIA**2/4.
VC=106.
VL=B3*12.*PL
P0=80.
FF=0.06
FN=FF*PL*6./D
DX=1./FLOAT(N)
DT=THETA*DX
FC=FN*DT
GC=640.104
Q=0.5282817877D00
C=0.531797514D00
EN=1.0
EP=1./7.
TH=530.
RTN=EN*GC*TH
BPL=9.47D01
BPC=1.47D01
RTIME=DT*PL/1100.
XP=P0*(VC/(VC+VL))
C4=BPL-XP
C1=0.578703704D00
CD=0.82
C5=(C4/14.7)**EP
B1=CD*AREA*C/DSQRT(TH)
B4=2.56924384D01
B5=B1*B4/B3
RSPRI=16.*FF*XL*12.*GC*TH/(D**5*PRI*PRI*G)
FP=0.2154171/FLOAT(N)**3.
AOP=DSQRT(FP*TH/(RSPRI*C*C*CD*CD))
R=DSQRT(TH)/(C*CD*AOP)
E=2.*R**2.

```

INITIAL CONDITIONS

```

TT=0.0
PA(1)=0.0D00
P(1)=9.47D01
DO 1 I=2,MESH
II=I-1
IF(I .LE. ML) GO TO 297
BI=(1.-(1.-FLOAT(II)/FLOAT(N))**3.)/3.
GO TO 296
297 BI=(1.-(1.-FLOAT(II)/FLOAT(N))**3.)/4.
296 P(I)=P(1)*(1.-(RSPRI/E)*FLOAT(N)**3.*BI)
PA(I)=P(1)-P(I)
UA(1,I)=0.0D00
AA(1,I)=(P(1)/14.7)**EP
CONTINUE
DEN1=0.0749*(P(1)/14.7)**(5./7.)
FM1=-CD*C*AREA*P(1)/DSQRT(TH)

```

```

UA(1,1)=FM1*B3*1100.)
AA(1,1)=(P(1)/14.7)**EP
UUL=UA(1,1)*1100.
UUM=UA(1,M)*1100.
PPC=BPC-14.7
PPL=P(1)-14.7-PA(1)
PPM=P(1)-14.7-PA(M)
PPR=P(1)-14.7-PA(MESH)
C7=((P(1)-XP)/14.7)**EP

C PRINT THE HEADING
C TYPE 48
C TYPE 47
47 FORMAT(15X,'METHOD OF CHARACTERISTICS FOR LARGE-AMPLITUDE')
TYPE 48
48 FORMAT(15X,'*****')
TYPE 49,PL
49 FORMAT(15X,'DURING PRESSURE REDUCTION,',F4.0,' FT. PIPE')
TYPE 50,R
50 FORMAT(15X,'MESH SIZE=',I3,' ',1X,'L:FIRST PIPE',',
1'M:PIPE NO. 25, ','R:LAST PIPE, ')
TYPE 51
51 FORMAT(15X,'U:VELOCITY OF AIR FLOW, P: PRESSURE')
TYPE 52,DIA
52 FORMAT(15X,'WITH TANK ORIFICE DIAMETER= ',F5.3,'INCH')
TYPE 53
53 FORMAT(15X,'UNIT CONVERSION:1PSI=6896N/SQ.M., 1FT/SEC=.3M')
TYPE 57
TYPE 55
55 FORMAT(6X,'TIME',7X,'P(L)',7X,'P(M)',7X,'P(R)',7X,
1' PPC',7X,'U(L)',7X,'U(M)')
TYPE 56
56 FORMAT(6X,'(SEC)',18X,'P IN (PSIG)',22X,'U IN (FT/SEC)').)
TYPE 57
57 FORMAT(4X,'-----')
1-----')
TYPE 76,TT,PPL,PPM,PPR,PPC,UUL,UUM
76 FORMAT(4X,F6.2,5X,3(F6.2,5X),3(F6.2,5X))

C NC=1
C TRANSIENT RESPONSE
C TIME TAKEN FOR FLOW OF AIR
DO 3 JT=1,NI
T=DT*PL*FLOAT(JT)/1100.
C LEFT BOUNDARY NODAL POINTS
YRL=UA(1,2)*AA(1,1)-UA(1,1)*AA(1,2)
VRL=AA(1,1)-UA(1,1)+UA(1,2)-AA(1,2)
URL=(UA(1,1)+THETA*XRL)/(1.+THETA*XRL)
ARL=(AA(1,1)+THETA*XRL)/(1.+THETA*XRL)
FTL=FC*URL*DABS(URL)
C2=URL-5.*ARL-FTL
FNLC=1.0D00
CALL FLOW
DPC=RTN*DM*RTIME/VC
BPC=BPC+DPC
PPC=BPC-14.7
IF(PPC .GT. (80.-XP)) BPC=C4
PR=BPC/BPL

```

```

IF((1.-PR) .LT. 0.) PR=BPL/BPC
IF(PR .EQ. 1.0D00) GO TO 999
IF(PR .GT. 0) CALL FUN
AAA=(-5.+DSQRT(25.-4.*B5*C2*FNLC))/(2.*B5*FNLC)
BPL1=(AAA**7)*14.7
BPL=BPL1
PR=BPC/BPL
IF((1.-PR) .LT. 0.) PR=BPL/BPC
IF(PR .LE. 0) GO TO 111
CALL FUN
AAA=(-5.+DSQRT(25.-4.*B5*C2*FNLC))/(2.*B5*FNLC)
BPL2=(AAA**7)*14.7
BPL=DSQRT(BPL1*BPL2)
111 IF(T .GT. 8. .AND. BPL .LE. C4) BPL=C4
AA(2,1)=(BPL/14.7)**EP
UA(2,1)=5.*AA(2,1)+C2
C INTERIOR POINTS
DO 4 MX=2,N
YLI=UA(1,MX-1)*AA(1,MX)-UA(1,MX)*AA(1,MX-1)
YRI=UA(1,MX+1)*AA(1,MX)-UA(1,MX)*AA(1,MX+1)
VLI=UA(1,MX)+AA(1,MX)-UA(1,MX-1)-AA(1,MX-1)
VRI=AA(1,MX)-UA(1,MX)+UA(1,MX+1)-AA(1,MX+1)
ULI=(UA(1,MX)+THETA*XLI)/(1.+THETA*XLI)
ALI=(AA(1,MX)-THETA*XLI)/(1.+THETA*XLI)
URI=(UA(1,MX)+THETA*YRI)/(1.+THETA*YRI)
ARI=(AA(1,MX)+THETA*YRI)/(1.+THETA*YRI)
F1=FC*ULI*DABS(ULI)
F2=FC*URI*DABS(URI)
AA(2,MX)=.1*(ULI-URI+5.*(ALI+ARI)+F2-F1)
IF(MX .GE. 3 .AND. AA(2,MX) .LE. C7) AA(2,MX)=C7
UA(2,MX)=.5*(ULI+URI+5.*(ALI-ARI)-F2-F1)
4 CONTINUE
C RIGHT BOUNDARY NODAL POINTS
UA(2,MESH)=0.0
YLR=UA(1,N)*AA(1,MESH)-UA(1,MESH)*AA(1,N)
VLR=UA(1,MESH)+AA(1,MESH)-UA(1,N)-AA(1,N)
ULR=(UA(1,MESH)+THETA*YLR)/(1.+THETA*VLR)
ALR=(AA(1,MESH)-THETA*YLR)/(1.+THETA*VLR)
FTR=FC*ULR*DABS(ULR)
C3=ULR+5.*ALR-FTR
AA(2,MESH)=C3/5.
IF(AA(2,MESH) .LT. C7) AA(2,MESH)=C7
C PRINT THE RESULTS
KT=JT/(NI/100)
IF((NI/100)*KT-JT) 80,81,80
81 NC=NC+1
C PRINT THE RESULTS
CALL OUTP
C
C TRANSFER OF GRID FROM THE PREVIOUS RESULTS
80 DO 5 K=1,MESH
AA(1,K)=AA(2,K)
UA(1,K)=UA(2,K)
AA(2,K)=0.0
UA(2,K)=0.0
5 CONTINUE
3 CONTINUE
999 DO 22 JJ=NC,NI
T=DT*PL*FLOAT(JJ)/1100.
DO 33 I=1,MESH

```

```

AA(2,I)=AA(1,I)
UA(2,I)=0.0
33    CONTINUE
      CALL OUTP
22    CONTINUE
      TYPE 57
      CALL PLOTXY
      STOP
      END

      SUBROUTINE FLOW
      DOUBLE PRECISION AREA,BPL,BPC,D,DM,Q,C,PR
      COMMON /BLK1/CD,AREA,BPL,BPC,TH,DM
      COMMON /BLK11/PR,Q
      COMMON /BLK12/C
      COMMON /BLK13/FNLC

C
      P=BPL
      PR=BPC/BPL
      D=C
      IF(1.-PR) 1,2,2
1     P=BPC
      PR=BPL/BPC
      D=-C
2     D=D*P*AREA*CD/DSQRT( TH)
      IF(PR .LE. Q) GO TO 22
      IF(PR .GT. Q) CALL FUN
      D=D*FNLC
22   DM=D
      RETURN
      END

      SUBROUTINE FUN
      DOUBLE PRECISION CF1,CF2,F,FNLC,A,B
      COMMON /BLK11/PR,Q
      COMMON /BLK13/FNLC

C
      DATA CF1/0.285714286D00/,CF2/3.863925465D00/
C
      F=0.0
      A=PR**CF1
      B=A*A
      A=A-B
      IF(A .GT. 0.0D00) F=CF2*B*DSQRT(A)
      FNLC=F
      RETURN
      END

      SUBROUTINE PLOTXY
      DIMENSION ARX(101),ARY(3,101),KP(3),KPT(101)
      COMMON /BLK2/ARX,ARY
      COMMON /BLK3/AMX,AMN
      COMMON /BLK6/KPT
      COMMON /BLK7/I,IFLAG
      COMMON /BLK8/KP
      COMMON /BLK9/NC
      COMMON /BLK10/XP,NP

C
      XSCALE=(ARX( NC)-ARX( 1))/100.
C
      PLOT THE RESULTS
      TYPE 93
93    FORMAT(1H1,37X,'BRAKE PIPE PRESSURES VS. TIME')

```

```

94   TYPE 94
      FORMAT(37X,'-----')
      TYPE 92,NP
      FORMAT(1H ,37X,'DURING PRESSURE REDUCTION, /,I3,
      1'-PIPE SCALED DOWN MODEL')
      TYPE 95
      FORMAT(1H ,37X,'L: P(L), M: P(M), R: P(R)')
      YMIN=AMN
      YSCALE=(AMX-AMN)/100.
      DO 10 I=1,3
      TYPE 100,AMN,(AMN+YSCALE*L*10.),L=1,9),AMX,KP(I)
100   FORMAT(4X,F7.2,10(3X,F7.2),2X,A1)
      CONTINUE
      MNP=1
      DO 20 II=1,101
      I=II-1
      IFLAG=I/10*10
      CALL COOPRT
      MXSC=INT((ARX(MNP)-ARX(1))/XSCALE+.5)
      IF(I .NE. MXSC) GO TO 21
      DO 22 L=1,3
      IYPT=INT((ARY(L,MNP)-YMIN)/YSCALE+.5)
      KPT(IYPT)=KP(L)
22    CONTINUE
      MNP=MNP+1
21    CONTINUE
      IF(IFLAG .EQ. I) GO TO 23
      TYPE 101,(KPT(I),I=1,101)
101   FORMAT(8X,101A1)
      GO TO 24
23    CONTINUE
      XX=ARX(1)+XSCALE*I
      TYPE 102,XX,(KPT(I),I=1,101)
102   FORMAT(F8.2,101A1)
24    CONTINUE
20    CONTINUE
      RETURN
      END
      SUBROUTINE COOPRT
      DIMENSION KPT(101)
      COMMON /BLK6/KPT
      COMMON /BLK7/I,IFLAG
      DATA K1/1H/,K2/1H./,K3/1H./,K4/1H./,K5/1H./
      LFLAG=0
      KK=K1
      KPT(1)=K2
      KPT(101)=K2
      IF(IFLAG .NE. I) GO TO 10
      KK=K4
      IF(I .EQ. 0 .OR. I .EQ. 100) KK=K3
      KPT(1)=K5
      KPT(101)=K5
      LFLAG=1
10    CONTINUE
      DO 20 J=2,100
      KPT(J)=KK
      IF((J-1)/10*10 .EQ. (J-1)) KPT(J)=K4
      IF(LFLAG .EQ. 1 .AND. (J-1)/10*10 .EQ. (J-1)) KPT(J)=K5
20    CONTINUE

```

```
RETURN  
END  
SUBROUTINE OUTP  
DOUBLE PRECISION UA(2,101),AA(2,101),PA(101)  
DIMENSION ARX(101),ARY(3,101)  
COMMON /BLK15/PPC  
COMMON /BLK2/ARX,ARY  
COMMON /BLK4/UA,AA  
COMMON /BLK5/T,M,MESH  
COMMON /BLK9/NC  
COMMON /BLK16/PA
```

C

```
PPL=(AA(2,1)**7-1.)*14.7-PA(1)  
PPM=(AA(2,M)**7-1.)*14.7-PA(M)  
PPR=(AA(2,MESH)**7-1.)*14.7-PA(MESH)
```

UUL=UA(2,1)*1100.
UUM=UA(2,M)*1100.

TYPE 66,T,PPL,PPM,PPR,PPC,UUL,UUM

66 FORMAT(4X,F6.2,5X,3(F6.2,5X),3(F6.2,5X))

```
ARX(NC)=T  
ARY(1,NC)=PPL  
ARY(2,NC)=PPM  
ARY(3,NC)=PPR  
RETURN  
END
```

*

C JOB BY MR. ANDREW HO, CONCORDIA GRADUATE 1981

C USE PDP-11 MINICOMPUTER AT FLUID CONTROL CENTRE.
C
C

THIS PROGRAM IS TO COMPUTE PRESSURE DISTRIBUTION
ALONG A SCALED DOWN BRAKEPIPE MODEL BY MEANS OF
LUMPED MODELING. THIS MAIN PROGRAM CAN BE USED
FOR ANY NUMBER OF LUMPS. IT CAN ALSO BE APPLIED
TO DISCHARGING OR CHARGING PROCESS, WITHOUT OR
WITH LEAKAGE AND TANK COMBINATION, SINCE IT IS
CONTROLLED BY INPUT DATA. THIS SIMULATION MODEL
WILL THEN BE APPLIED TO ANALYSE SOME DYNAMIC
CHARACTERISTICS OF ACTUAL BRAKEPIPE OF A FREIGHT
TRAIN BY SLIGHTLY MODIFYING THE BOUNDARY LAYER
CONDITIONS AND CHANGING THE VALUES OF DIMENSION.

C
C

C LUMPED PARAMETERS

C A0-LEAKAGE ORIFICE AREA
C BPL-BRAKEPIPE PRESSURE
C BPT-TANK PRESSURE
C CD-DISCHARGE CONSTANT
C CAP-CAPACITANCE OF PIPE COMPONENT
C D-INTERNAL DIAMETER OF PIPE
C DIA-DIAMETER OF TANK ORIFICE
C DT-TIME INCREMENT
C FF-FRICTION FACTOR OF THE BRAKEPIPE MODEL
C G-GRAVITATIONAL CONSTANT
C GC-GAS CONSTANT
C L-LAST LUMP/PIPE
C NL-NUMBER OF LUMPS
C PR-PRESSURE RATIO
C Q-CRITICAL PRESSURE RATIO
C R-LEAKAGE LINEAR RESISTANCE
C RP-PRESSURE RATIO
C RSL-BRAKEPIPE LINEARIZED RESISTANCE
C RSPRI-BRAKEPIPE NONLINEAR RESISTANCE
C TL-TOTAL LENGTH OF PIPES+TUBES
C TO-AMBIENT TEMPERATURE
C VC-VOLUME OF TANK AS PRESSURE CHAMBER
C VL-TOTAL VOLUME OF PIPES+TUBES
C XP-PRESSURE REDUCTION
C

DOUBLE PRECISION P(2,76),R(76),RS(75),DF(76)

DOUBLE PRECISION FM(75),RP,X,PI(76),PA(76)

DOUBLE PRECISION PRI,A,V,CAP,RSPRI,C,B,FN,DP1,DPI

DOUBLE PRECISION BPL,BPT,D,DM,Q,PR,RSL

DOUBLE PRECISION CF1,CF2,F,FNPT,A1,B1

DIMENSION PP(76),ARX(51),ARY(3,51),KP(3)

COMMON /MAY1/AA,BPL,BPT,TO,IM

COMMON /MAY2/FR,Q

COMMON /MAY3/C
COMMON /MAY4/FNPT
COMMON /MAY5/ARX,ARY
COMMON /MAY6/AMX,AMN
COMMON /MAY7/KP,NP
DATA KP(1)/1HL/,KP(2)/1HM/,KP(3)/1HR/
C
ACCEPT 101,A0,NL,DT,DIA,VC
101 FORMAT(F11.10,I2,F5.3,F5.3,F4.0)
IF(A0 .EQ. 0. ,OR. VC .EQ. 0.) GO TO 555
C ACCEPT THE FOLLOWING DATA
ARX(1)=0.
AMX=100.
AMN=0.
G=386.
DC=640.
T0=530.
FF=0.06
TL=750.*1.08
Q=0.5282817877D00
C=0.531797514D00
C CONSIDER ISOTHERMAL PROCESS N=1.0
XN=1.0
C
RTN=XN*GC*T0
EL=TL/FLOAT(NL)
D=0.25
PRI=3.141592654D00
A=(PRI*D**2)/4.
AA=(PRI*DIA**2)/4.
V=A*EL*12.
VL=NL*V
P0=80.
XP=P0*VC/(VC+VL)
CAP=V/RTN
C
L=NL+1
M=L/3
ML=2*M
C
RSPRI=16.*FF*EL*12.*GC*T0/(D**5*PRI*PRI*G)
FP=6.382729E-05
C
C CONSIDER SQUARE-EDGED ORIFICE
CD=0.82
C
C CONSIDER PLUMBING LEAKAGE, PUT AO=AOP
AOP=SQRT(FP*T0/(RSPRI*C*C*CD*CD))
C
IF(A0 .LE. AOP) AMX=85.
IF(A0 .LE. AOP) AMN=60.
DO 30 I=1,2
DO 40 J=1,L
P(I,J)=0.0
40 CONTINUE
30 CONTINUE
C
C INITIAL CONDITION

```

T=0.0
P(1,1)=9.47D01
BPL=P(1,1)
IF(BPL .LE. 1.4705D01) TYPE 209
IF(BPL .LE. 1.4705D01) GO TO 777
BPT=1.47D01
C
PA(1)=0.0
C INITIAL PIPE PRESSURE
PI(1)=9.47D01
DO 10 I=2,L
R(I)=DSQRT(T0)/(C*CD*AOP)
E=2.*R(I)**2.
II=I-1
IF(I .LE. ML) GO TO 297
B=(1.-(1.-FLOAT(II)/FLOAT(NL))**3.)/3.
GO TO 296
297 B=(1.-(1.-FLOAT(II)/FLOAT(NL))**3.)/4.
296 PI(I)=PI(1)*(1.-(RSPRI/E)*B*FLOAT(NL)**3.)
10 CONTINUE
C
DO 4 I=2,L
PA(I)=PI(1)-PI(I)
CONTINUE
C
DO 3 I=2,L
R(I)=DSQRT(T0)/(C*CD*A0)
E=2.*R(I)**2.
II=I-1
IF(I .LE. ML) GO TO 299
B=(1.-(1.-FLOAT(II)/FLOAT(NL))**3.)/3.
GO TO 298
299 B=(1.-(1.-FLOAT(II)/FLOAT(NL))**2.3)/4.
298 P(1,I)=P(1,1)*(1.-(RSPRI/E)*B*FLOAT(NL)**3.)
3 CONTINUE
C
PPT=BPT-14.7
PP1=P(1,1)-14.7-PA(1)
PPM=P(1,M+1)-14.7-PA(M+1)
PPL=P(1,L)-14.7-PA(L)
ARY(1,1)=PP1
ARY(2,1)=PPM
ARY(3,1)=PPNL
C PRINT THE HEADING
TYPE 150
TYPE 205
TYPE 151
TYPE 205
TYPE 210
IF(AO .GT. AOP .AND. DIA .EQ. 0.) GO TO 310
IF(AO .LE. AOP .AND. DIA .GT. 0.) GO TO 311
IF(AO .LE. AOP .AND. DIA .EQ. 0.) GO TO 666
TYPE 199
TYPE 196,VC
TYPE 195,DIA
TYPE 200,A0,TL
TYPE 206

```

```

TYPE 210
TYPE 203
TYPE 198,M,NL
TYPE 197
TYPE 203
GO TO 401
310   TYPE 199
      TYPE 200,A0,TL
      TYPE 206
      TYPE 210
      TYPE 204
      TYPE 170,M,NL
      TYPE 171
      TYPE 204
      GO TO 401
311   TYPE 160
      TYPE 207
      TYPE 161,TL
      TYPE 196,VC
      TYPE 195,DIA
      TYPE 210
      TYPE 203
      TYPE 198,M,NL
      TYPE 197
      TYPE 203
401   IF(DIA .EQ. 0.) GO TO 300
      IF(A0 .GT. AOP) A0=0.00013
C
      TYPE 201,T,PP1,PPM,PPL,PPT
      GO TO 301
300   TYPE 172,T,PP1,PPM,PPL
C
C TRANSIENT RESPONSE
301   NI=INT(50/DT)
      NP=1
      DO 12 JT=1,NI
      T=DT*FLOAT(JT)
C CONSIDER R(I) AS LEAKAGE RESISTANCE I
      DO 14 I=2,L
      IF(P(1,I) .LE. 1.4702D01) P(1,I)=1.4701D01
      RP=14.7/P(1,I)
      IF(RP .LE. Q) GO TO 7
      FN=DSQRT((RP**(2./1.4)-RP***(2.4/1.4))/6.697959953D-02)
      GO TO 8
7     FN=1.0D00
8     R(I)=DSQRT(T0)/(C*CD*A0*X)
14    CONTINUE
C
C CONSIDER RS(K) AS FRICTION RESISTANCE CONSTANT
      DO 11 K=1,NL
      RS(K)=RSPRI/(P(1,K)+P(1,K+1))
      CONTINUE
C
C LEFT BOUNDARY
      DP1=P(1,2)-P(1,1)

```

```

IF(DP1 .GT. 0.0) FM(1)=DSQRT(DP1/RS(1))
IF(DP1 .EQ. 0.0) FM(1)=0.0
IF(DP1 .LT. 0.0) FM(1)=-DSQRT(-DP1/RS(1))
IF(DIA .EQ. 0.0) GO TO 500
FNPT=1.0D00
CALL FLOW
C PRESSURE CHANGE IN TANK, DPT
DPT=RTN*DM*DT/VC
BPT=BPT+DPT
IF(BPT .LE. 1.4702D01) BPT=1.4701D01
PFT=BPT-14.7
PR=BPT/BPL
IF((1.-PR) .LT. 0.) PR=BPL/BPT
IF(PR .GT. Q) CALL FUN
C PRESSURE CHANGE IN BRAKEPIPE, DP
DP(1)=(-FM(1)+DM)/CAP
P(2,1)=P(1,1)-DP(1)*DT
BPL1=P(2,1)
BPL=BPL1
PR=BPT/BPL
IF((1.-PR) .LT. 0.) PR=BPL/BPT
IF(PR .LE. Q) GO TO 700
CALL FLOW
500 IF(DIA .EQ. 0.0) DM=0.0
DP(1)=(-FM(1)+DM)/CAP
P(2,1)=P(1,1)-DP(1)*DT
IF(DIA .EQ. 0.0) GO TO 501
BPL2=P(2,1)
BPL=DSQRT(BPL1*BPL2)
700 P(2,1)=BPL
IF(T .LE. 18) GO TO 501
IF(A0 .LE. AOP .AND. DIA .GT. 0.) GO TO 140
GO TO 501
140 IF(P(2,1) .GT. (PP1-XP+14.7)) P(2,1)=PP1-XP+14.7
501 IF(P(2,1) .LE. 1.4702D01) P(2,1)=1.4701D01
C
C INTERIOR BOUNDARIES
DO 13 I=2,NL
DPI=P(1,I+1)-P(1,I)
IF(DPI .GT. 0.0) FM(I)=DSQRT(DPI/RS(I))
IF(DPI .EQ. 0.0) FM(I)=0.0
IF(DPI .LT. 0.0) FM(I)=-DSQRT(-DPI/RS(I))
DP(I)=(-FM(I)+FM(I-1)+P(1,I)/R(I))/CAP
P(2,I)=P(1,I)-DP(I)*DT
IF(P(2,I) .LE. PA(I)+1.4702D01) P(2,I)=1.4701D01+PA(I)
13 CONTINUE
C
C RIGHT BOUNDARY
RSL=2.*DSQRT(RS(NL)*DABS(P(1,NL)-P(1,L)))
DP(L)=DP(NL)*R(L)/(RSL+R(L))
P(2,L)=P(1,L)-DP(L)*DT
IF(P(2,L) .LE. PA(L)+1.4702D01) P(2,L)=1.4701D01+PA(L)
IF(A0 .LE. AOP .AND. DIA .GT. 0.0) GO TO 141

```

```

GO TO 502
141 IF(P(2,L) .LE. (PPL-XP+14.7)) P(2,L)=PPL-XP+14.7
C
C PRINT THE RESULTS
502 PP(1)=P(2,1)-14.7-PA(1)
PP(M+1)=P(2,M+1)-14.7-PA(M+1)
PP(L)=P(2,L)-14.7-PA(L)
KT=JT/(NI/50)
IF(T .GT. 1.5) GO TO 600
TT=DT*FLOAT(JT)*10.
IF(TT .EQ. INT(TT)) GO TO 999
600 IF((NI/50)*KT-JT) 80,81,80
81 NP=NP+1
ARY(NP)=T
ARY(1,NP)=PP(1)
ARY(2,NP)=PP(M+1)
ARY(3,NP)=PP(L)
999 IF(DIA .EQ. 0.0) GO TO 400
TYPE 201,T,PP(1),PP(M+1),PP(L),PPT
GO TO 80
400 TYPE 172,T,PP(1),PP(M+1),PP(L)
C
C TRANSFER AND UPDATE THE RESULTS
80 DO 20 I=1,L
P(1,I)=P(2,I)
P(2,I)=0.0
20 CONTINUE
12 CONTINUE
150 FORMAT(1H0)
151 FORMAT(15X,'METHOD OF LUMPED MODELING')
160 FORMAT(15X,'RESULT ON BRAKEPIPE MODEL')
161 FORMAT(15X,'WITHOUT LEAKAGE, FOR 'F4.0,'FT. PIPES')
171 FORMAT(15X,'SEC',6X,'PSI',6X,'PSI',6X,'PSI')
170 FORMAT(17X,'T',7X,'P1',6X,'P',I2,6X,'P',I2)
172 FORMAT(13X,F6.2,3X,F5.2,4X,F5.2,4X,F5.2)
204 FORMAT(15X,'-----')
205 FORMAT(15X,'-----')
196 FORMAT(15X,'DISCHARGE TO ',F4.0,'CU. IN. OF TANK')
195 FORMAT(15X,'WITH ORIFICE SEAT DIAMETER =',F5.3,'INCH')
197 FORMAT(15X,'SEC',6X,'PSI',6X,'PSI',6X,'PSI',6X,'PSI')
198 FORMAT(17X,'T',7X,'P1',6X,'P',I2,6X,'P',I2,7X,'PT')
199 FORMAT(15X,'RESULT ON UNIFORM LEAKAGE DISTRIBUTION')
200 FORMAT(4X,'WITH LEAKAGE AREA OF ',F8.6,'SQ.IN.',1X,
1'DN EACH LUMP OF ',F4.0,'FEET PIPES')
201 FORMAT(13X,F5.2,4X,F5.2,4X,F5.2,4X,F5.2)
202 FORMAT(15X,'WRONG DATA, ***TRY AGAIN***')
203 FORMAT(13X,'-----')
206 FORMAT(15X,'DURING DISCHARGING PROCESS')
207 FORMAT(15X,'DURING PRESSURE REDUCTION')
208 FORMAT(15X,'NO CHANGE IN PRESSURE, MODIFICATION IS NEEDED')
209 FORMAT(15X,'THIS IS A CHARGING PROCESS,ADJUST PROGRAM')
210 FORMAT(1H )
C
CALL PLOTXY
GO TO 777
555 TYPE 202

```

```

GO TO 777
666 TYPE 208
777 STOP
END
SUBROUTINE FLOW
C
C AA-ORIFICE AREA
C BPL-BRAKEPIPE PRESSURE
C BPT=TANK PRESSURE
C TO-AMBIENT TEMPERATURE
C
    DOUBLE PRECISION A,BPL,BPT,D,DM,Q,C,PR,P,FNPT
    COMMON /MAY1/AA,BPL,BPT,TO,DM
    COMMON /MAY2/PR,Q
    COMMON /MAY3/C
    COMMON /MAY4/FNPT
C
CD=0.95
P=BPL
PR=BPT/BPL
D=C
IF(1.-PR) 1,2,2
1 P=BPT
PR=BPL/BPT
D=-C
2 D=D*P*AA*CD/DSQRT(TO)
IF(PR .LE. Q) GO TO 22
IF(PR .GT. Q) CALL FUN
D=D*FNPT
22 DM=D
RETURN
END
SUBROUTINE FUN
C
C PR-PRESSURE RATIO
    DOUBLE PRECISION CF1,CF2,F,FNPT,A1,PR,B1
    COMMON /MAY2/PR,Q
    COMMON /MAY4/FNPT
    DATA CF1/0.285714286D00/,CF2/3.8639135465D00X
C
F=0.0
A1=PR**CF1
B1=A1*A1
A1=A1-B1
IF(A1 .GT. 0.0) F=CF2*B1*DSQRT(A1)
FNPT=F
RETURN
END
SUBROUTINE PLOTXY
C
C ARX-INDEPENDENT VARIABLE
C ARY-DEPENDENT VARIABLE
C AMN-MINIMUM DEPENDENT VARIABLE
C AMX-MAXIMUM DEPENDENT VARIABLE
C
DIMENSION ARX(51),ARY(3,51),KP(3),KPT(51)

```

```
COMMON /MAY5/ARX,ARY
COMMON /MAY6/AMX,AMN
COMMON /MAY7/KP,NP
COMMON /MAY8/KPT
COMMON /MAY9/I,IFLAG
C
      XSCALE=(ARX(NP)-ARX(1))/50.
C      PLOT THE RESULTS
      TYPE 93
93    FORMAT(///,15X,'BRAKE PIPE PRESSURE VS. TIME')
      TYPE 94
94    FORMAT(15X,'-----')
      TYPE 95
95    FORMAT(1H ,15X,'L: P(L), M: P(M), R: P(R)',/)
      YMIN=AMN
      YSCALE=(AMX-AMN)/50.
      DO 10 I=1,3
10     TYPE 100,AMN,((AMN+YSCALE*L*10.),L=1,4),AMX,KP(I)
      FORMAT(4X,F7.2,5(3X,F7.2),2X,A1)
      CONTINUE
      MNP=1
      DO 20 II=1,51
      I=II-1
      IFLAG=I/10*10
      CALL COOPRT
      MXSC=INT((ARX(MNP)-ARX(1))/XSCALE+.5)
      IF(I .NE. MXSC) GO TO 21
      DO 22 L=1,3
      IYPT=INT((ARY(L,MNP)-YMIN)/YSCALE+.5)
      KPT(IYPT)=KP(L)
22    CONTINUE
      MNP=MNP+1
21    CONTINUE
      IF(IFLAG .EQ. I) GO TO 23
      TYPE 101,(KPT(I),I=1,51)
101   FORMAT(8X,51A1)
      GO TO 24
23    CONTINUE
      XX=ARX(1)+XSCALE*I
      TYPE 102,XX,(KPT(I),I=1,51)
102   FORMAT(F8.2,51A1)
24    CONTINUE
20    CONTINUE
      RETURN
      END
      SUBROUTINE COOPRT
C
      DIMENSION KPT(51)
      COMMON /MAY8/KPT
      COMMON /MAY9/I,IFLAG
C
      >C
```

C DATA K1/1H ./,K2/1H./,K3/1H./,K4/1H./,K5/1H./

LFLAG=0
KK=K1 *
KPT(1)=K2
KPT(51)=K2
IF(IFLAG .NE. I) GO TO 10
KK=K4
IF(I .EQ. 0 .OR. I .EQ. 50) KK=K3
KPT(1)=K5
KPT(51)=K5
LFLAG=1
10 CONTINUE
DO 20 J=2,50
KPT(J)=KK
IF((J-1)/10*10 .EQ. (J-1)) KPT(J)=K4
IF(LFLAG .EQ. 1 .AND. (J-1)/10*10 .EQ. (J-1)) KPT(J)=K5
20 CONTINUE
RETURN
END
C PROGRAM COMPLETED *****
*

74/835 JPT=1

PROGRAM ILT (INPJ,OUTPUT)

```
*****  

C THIS PROGRAM IS TO COMPUTE THE TRANSIENT RESPONSE  

C OF A GENERAL RLGC SEMI-INFINITE TRANSMISSION LINE  

C WITH A UNIT STEP OF PRESSURE SUPPLY. THE EQUATION  

C OF NORMALIZED PRESSURE (PN) IS SOLVED BY INVERSE  

C LAPLACE TRANSFORM AND THE INTEGRAL CAN BE RELATED  

C TO SOME INTEGRALS WHOSE SOLUTIONS CAN BE EXPRESSED  

C IN TERMS OF MODIFIED BESSSEL FUNCTIONS. REFLECTIONS  

C WHICH WERE OMITTED HERE CAN CAUSE A DIFFERENT KIND  

C OF RESPONSE BUT IT WILL NOT CHANGE THE TIME DELAY.  

C HENCE, THE EFFECT OF LEAKAGE ON PROPAGATION SPEED  

C CAN BE INDIRECTLY FOJND.
```

```
*****  

C DOUBLE PRECISION F(401),SEV,SOD,SUM,PN,BESFU  

COMMON /SMAY/TC,B,C,Z  

COMMON /ANDREW/BESFU
```

```
C READ THE GIVEN DATA
```

```
DO 1 I=1,5
```

```
C R IS RATIO OF FREQUENCIES
```

```
101 FORMAT(F5.1)
```

```
B=1.-R
```

```
C=1.+R
```

```
R5=SQR(TC)
```

```
PRINT 200
```

```
200 FORMAT(1H1,///)
```

```
C COMPRESSED TIME TC
```

```
DO 2 J=1,2
```

```
TC=10.*FLOAT(J)
```

```
X1=EXP(-TC*C/2.)
```

```
X2=(TC*B/2.)**2
```

```
X3=EXPT-TC*R5)
```

```
C FIRST TERM OF MODIFIED BESSSEL FUNCTION IS
```

```
F(1)=X1/2.
```

```
C COMPUTE THE BESSSEL FUNCTION OF THE FIRST KIND,F(K)
```

```
DO 3 K=2,401
```

```
Z=1.+0.01*FLOAT(K-1)
```

```
CALL BESSEL
```

```
F(K)=BESFU
```

```
3 CONTINUE
```

```
C INITIAL CONDITION
```

```
C IDEAL TIME DELAY TD AND NORMALIZED PRESSURE PN
```

```
TD=1.0
```

```
PN=X1/X3
```

```
C PRINT THE INITIAL CONDITION
```

```
PRINT 201,TD,R,TD,PN
```

```
201 FORMAT(5X,2F10.1,F10.2,D15.4)
```

```
C COMPUTE TRANSENT RESPONSE
```

```
DO 4 N=10,400,10
```

```
C TN IS NORMALIZED TIME
```

```
TN=TD+0.01*FLOAT(N)
```

74/835 OPT=1

```

C USE SIMPST RULE TO COMPUTE INTEGRATION
 1=N+1
 MA=N-1
 C SOD IS SUM OF ALL ODD TERMS
 SOD=0.0
 DO 5 L=2,N,2
 SOD=SOD+F(L)
 5 CONTINUE
 C SEV IS SUM OF ALL EVEN TERMS
 SEV=0.0
 DO 6 LL=3,MA,2
 SEV=SEV+F(LL)
 6 CONTINUE
 C SUM IS ADDITION OF ALL TERMS
 SUM=0.01*(4.*SOD+2.*SEV+F(1)+F(M))/3.
 PN=(X1+X2*SUM)/X3
 PRINT 201,TC,R,T4,PN
 4 CONTINUE
 2 CONTINUE
 1 CONTINUE
 STOP
 END

```

74/835 OPT=1

```

SUBROUTINE BESSEL
DOUBLE PRECISION A1,A2,A3,A4,A5,A6
DOUBLE PRECISION D1,D2,D3,D4,D5
DOUBLE PRECISION D6,D7,D8,D9
DOUBLE PRECISION G1,G2,G,BESFU
COMMON /SMAY/TC,B,C,Z
COMMON /ANDREN/BESFU

```

```

C
Z=TC*B*SQRT(Z*Z-1.J/2.
X=ABS(Z)
N=X/3.75
Y=TC*C*Z/2.
E=EXP(-Y)
IF(X=3.75) 80,81,81
A1=0.87890594*H**2
A2=0.51498869*H**4
A3=0.15084934*H**6
A4=0.02658733*H**8
A5=0.00301532*H**10
A6=0.00032411*H**12
G1=0.5+A1+A2+A3+A4+A5+A6
3 BESFU=E*G1
GO TO 82
80 D1=0.39894228
D2=-0.03988024/H
D3=-0.00362018/H**2
D4=0.00163801/H**3
D5=-0.01031555/H**4
D6=0.02282967/H**5
D7=-0.02895312/H**5
D8=0.01787654/H**7
D9=-0.00420059/H**8
S=D1+D2+D3+D4+D5+D6+D7+D8+D9
G2=G/(EXP(-X)*X*SQRT(X))
BESFU=E*G2
82 RETURN
END

```

C *****
C JOB BY MR. ANDREW HO, CONCORDIA GRADUATE 1981
C -----
C USE PDP-11 MINICOMPUTER AT FLUID CONTROL CENTRE.
C -----

C THIS PROGRAM IS TO COMPUTE PRESSURE DISTRIBUTION
C ALONG THE ACTUAL BRAKEPIPE OF A FREIGHT TRAIN BY
C MEANS OF LUMPED MODELING. IT CAN BE APPLIED TO
C DISCHARGING THE AIR TO THE TANK OR THROUGH RELAY
C VALVE.

C *****
C
C DOUBLE PRECISION P(2,51),RS(50),DP(51)
C DOUBLE PRECISION FM(50),RP,RE,FNPT
C DOUBLE PRECISION PRI,A,V,CAP,RSPRI,C,FN,DP1,DPI
C DOUBLE PRECISION BPL,BPT,D,DM,Q,PR
C DOUBLE PRECISION BPL1,BPL2,TO
C DIMENSION PP(51)
C COMMON /SMAY1/AA,BPL,BPT,TO,DM
C COMMON /SMAY2/FR,Q
C COMMON /SMAY3/C
C COMMON /SMAY4/FNPT

C
C LET AO BE LEAKAGE AREA AND ASSUME ALL AO ARE EQUAL
C SET DT AS INCREMENT OF TIME
C CONSIDER NL AS NUMBER OF LUMPS
C VC IS VOLUME OF TANK AS PRESSURE CHAMBER
C DIA IS DIAMETER OF TANK ORIFICE
C ACCEPT 101,NL,DT,DIA,VC
101 FORMAT(I3,F6.4,F4.2,F6.0)
C ACCEPT THE FOLLOWING DATA

G=386.
GC=640.
TO=530.
FF=0.802
TL=7500.
Q=0.5282817877D00
C=0.531797514D00

C CONSIDER POLYTROPIC PROCESS N=1.3

XN=1.3
RTN=XN*GC*TO
EL=TL/FLOAT(NL)
D=1.25
PRI=3.141592654D00
A=(PRI*D**2)/4.
AA=(PRI*DIA**2)/4.
V=A*EL*12.
VL=NL*V
PO=80.
XP=PO*VC/(VC+VL)
C4=94.7-XP
CAP=V/RTN
L=NL+1
M=L/3

```
RSPRI=16.*FF*EL*12.*GC*T0/(D**5*PRI*PRI*G)
C INITIAL CONDITION
C AT TIME ZERO
T=0.0
DO 10 I=1,L
P(1,I)=9.47D01
10    CONTINUE
BPL=P(1,1)
IF(BPL .LE. 1.4705D01) TYPE 209
IF(BPL .LE. 1.4705D01) GO TO 777
BPT=1.47D01
PPT=BPT-14.7
PP1=P(1,1)-14.7
PPM=P(1,M+1)-14.7
PPL=P(1,L)-14.7
TYPE 205
TYPE 151
TYPE 205
TYPE 210
TYPE 160
TYPE 207,XP
TYPE 161,TL
IF(DIA .GT. 0.) GO TO 4
TYPE 162
TYPE 163
TYPE 210
TYPE 204
TYPE 170
TYPE 171
TYPE 204
GO TO 300
311    TYPE 196,VC
TYPE 195,DIA
TYPE 163
TYPE 210
TYPE 203
TYPE 198
TYPE 197
TYPE 203
TYPE 201,T,PP1,PPM,PPL,PPT
GO TO 301
300    TYPE 172,T,PP1,PPM,PPL
C TRANSIENT RESPONSE
301    NI=INT(70/DT)
IF(XP .LE. 10.) NI=INT(40/DT)
DO 12 JT=1,NI
T=DT*FLOAT(JT)
IF(T .LT. 3.1) GO TO 82
C CONSIDER RE AS EXHAUST VALVE RESISTANCE
IF(DIA .NE. 0.) GO TO 124
PD=P(1,1)-C4
IF(PD .GT. 1.2) A0=0.03984
IF((PD .LE. 1.2) .AND. (PD .GT. 0.50)) GO TO 120
IF((PD .LE. 0.50) .AND. (PD .GT. 0.40)) GO TO 121
```

```

IF((PD .LE. 0.40) .AND. (PD .GT. 0.30)) GO TO 122
IF((PD .LE. 0.30) .AND. (PD .GT. 0.0)) GO TO 123
IF(PD .LE. 0.0) A0=1./10.**8
    ) GO TO 112
120 A0=0.0008*PD+0.03885
    ) GO TO 112
121 A0=0.005*PD+0.03675
    ) GO TO 112
122 A0=0.0175*PD+0.03175
    ) GO TO 112
123 A0=0.1233*PD
112 RP=14.7/P(1,1)
    IF(A0 .EQ. 0. .OR. VC .EQ. 0.) GO TO 555
    IF(RP .LE. 0) GO TO 7
    FN=DSQRT((RP**2./1.4)-RP**2.4/1.4)/6.697959953D-02
    GO TO 8
7 FN=1.0D00
8 RE=DSQRT(T0)/(C*A0*FN)
    GO TO 125
124 RE=10.**10.
C CONSIDER RS(K) AS FRICTION RESISTANCE CONSTANT
125 DO 11 K=1,NL
    RS(K)=RSPRI/(P(1,K)+P(1,K+1))
11 CONTINUE
C LEFT BOUNDARY
    DP1=P(1,2)-P(1,1)
    IF(DP1 .GT. 0.0) FM(1)=DSQRT(DP1/RS(1))
    IF(DP1 .EQ. 0.0) FM(1)=0.0
    IF(DP1 .LT. 0.0) FM(1)=-DSQRT(-DP1/RS(1))
    IF(DIA .EQ. 0.0) GO TO 500
    FNPT=1.0D00
    CALL FLOW
    DPT=RTN*DM*DT/VC
    BPT=BPT+DPT
    IF(BPT .LE. 1.4702D01) BPT=1.4701D01
    PPT=BPT-14.7
    PR=BPT/BPL
    IF((1.-PR) .LT. 0.) PR=BPL/BPT
    IF(PR .GT. 0) CALL FUN
    DP(1)=(P(1,1)/RE-FM(1)+DM)/CAP
    P(2,1)=P(1,1)-DP(1)*DT
    BPL1=P(2,1)
    BPL=BPL1
    PR=BPT/BPL
    IF((1.-PR) .LT. 0.) PR=BPL/BPT
    IF(PR .LE. 0) GO TO 700
    CALL FLOW
500 IF(DIA .EQ. 0.0) DM=0.0
    DP(1)=(P(1,1)/RE-FM(1)+DM)/CAP
    P(2,1)=P(1,1)-DP(1)*DT
    IF(DIA .EQ. 0.0) GO TO 501
    BPL2=P(2,1)
    BPL=DSQRT(BPL1*BPL2)
700 P(2,1)=BPL
501 IF(P(2,1) .GT. (PP1-XP+14.7)) P(2,1)=PP1-XP+14.7
C INTERIOR BOUNDARIES
DO 14 I=2,NL

```

```

DPI=P(1,I+1)-P(1,I)
IF(DPI .GT. 0.0) FM(I)=DSQRT(DPI/RS(I))
IF(DPI .EQ. 0.0) FM(I)=0.0
IF(DPI .LT. 0.0) FM(I)=-DSQRT(-DPI/RS(I))
DP(I)=(-FM(I)+FM(I-1))/CAP
P(2,I)=P(1,I)-DP(I)*DT
IF(P(2,I) .LE. (PPM-XP+14.7)) P(2,L)=PPL-XP+14.7
14 CONTINUE
C RIGHT BOUNDARY
P(2,L)=P(2,NL)
IF(P(2,L) .LE. (PPL-XP+14.7)) P(2,L)=PPL-XP+14.7
GO TO 502
82 IF(T .NE. INT(T)) GO TO 12
IF(DIA .GT. 0.) GO TO 83
TYPE 172,T,PP1,PPM,PPL
GO TO 12
83 TYPE 201,T,PP1,PPM,PPL,PPT
GO TO 12
C PRINT THE RESULTS
502 PP(1)=P(2,1)-14.7
PP(M+1)=P(2,M+1)-14.7
PP(L)=P(2,L)-14.7
IF(T .NE. INT(T)) GO TO 99
IF(DIA .EQ. 0.0) GO TO 400
TYPE 201,T,PP(1),PP(M+1),PP(L),PPT
GO TO 99
400 TYPE 172,T,PP(1),PP(M+1),PP(L)
C TRANSFER AND UPDATE THE RESULTS
99 DO 20 I=1,L
      P(1,I)=P(2,I)
      P(2,I)=0.0
20 CONTINUE
12 CONTINUE
150 FORMAT(1HO)
151 FORMAT(15X,'METHOD OF LUMPED MODELING')
160 FORMAT(15X,'RESULT ON ACTUAL BRAKEPIPE')
161 FORMAT(15X,'WITHOUT LEAKAGE, FOR ',F5.0,'FT. 150-CAR TRAIN')
162 FORMAT(15X,'WITH CONTROL VALVE AT THE FRONT END')
163 FORMAT(15X,'UNIT CONVERSION-- 1 PSI=6895N/SQ.M., 1 FT.=0.3M')
170 FORMAT(17X,'T',7X,'P1',6X,'P50',5X,'P150')
171 FORMAT(15X,'SEC',6X,'PSI',6X,'PSI',6X,'PSI')
172 FORMAT(13X,F6.1,3X,F5.2,4X,F5.2,4X,F5.2)
204 FORMAT(15X,'-----')
205 FORMAT(15X,'-----')
196 FORMAT(15X,'DISCHARGE TO ',F6.0,'CU.IN. OF TANK')
195 FORMAT(15X,'WITH TANK ORIFICE DIAMETER = ',F5.3,'INCH')
197 FORMAT(15X,'SEC',6X,'PSI',6X,'PSI',6X,'PSI')
198 FORMAT(17X,'T',7X,'P1',6X,'P50',6X,'P150',7X,'FT')
201 FORMAT(13X,F5.1,4X,F5.2,4X,F5.2,4X,F5.2,4X,F5.2)
202 FORMAT(15X,'WRONG DATA, ***TRY AGAIN***')
203 FORMAT(13X,'-----')
206 FORMAT(15X,'DURING DISCHARGING PROCESS')
207 FORMAT(15X,'DURING ',F3.0,'-PSI PRESSURE REDUCTION')
208 FORMAT(15X,'NO CHANGE IN PRESSURE, MODIFICATION IS NEEDED')
209 FORMAT(15X,'THIS IS A CHARGING PROCESS,ADJUST PROGRAM')
210 FORMAT(1H )
GO TO 777
555 TYPE 202

```

666 GO TO 777
777 TYPE 208
STOP
END
SUBROUTINE FLOW
DOUBLE PRECISION A,BPL,BPT,D,DM,Q,C,PR,P,FNPT
COMMON /SMAY1/AA,BPL,BPT,T0,DM
COMMON /SMAY2/PR,Q
COMMON /SMAY3/C
COMMON /SMAY4/FNPT
CD=0.80
P=BPL
PR=BPT/BPL
D=C
IF(1.-PR) 1,2,2
1 P=BPT
PR=BPL/BPT
D=-C
2 D=D*P*AA*CD/DSQRT(T0)
IF(PR .LE. Q) GO TO 22
IF(PR .GT. Q) CALL FUN
D=D*FNPT
* 22 DM=D
RETURN
END
SUBROUTINE FUN
DOUBLE PRECISION CF1,CF2,F,FNPT,A1,PR,B1
COMMON /SMAY2/PR,Q
COMMON /SMAY4/FNPT
DATA CF1/0.285714286D00/,CF2/3.8639135465D00/
F=0.0
A1=PR**CF1
B1=A1*A1
A1=A1-B1
IF(A1 .GT. 0.0) F=CF2*B1*DSQRT(A1)
FNPT=F
RETURN
END

```

C ****
C * ACTUAL CASE *
C ****
C
DOUBLE PRECISION UA(2,101),AA(2,101)
DOUBLE PRECISION YRL,VRL,URL,ARL,FN,C1,FTL,FC,DT
DOUBLE PRECISION YLI,YRI,VRI,VLI,URI,ARI,ULI,ALI,F1,F2
DOUBLE PRECISION YLR,VLR,ULR,ALR,FTR,C3,PD
DOUBLE PRECISION CC,C,CAVG,EQC,EOCC,EQCAV,DELC
DOUBLE PRECISION C2,A,B#AAA,AREA,G1,G2,G3
DIMENSION ARX(101),ARY(3,101),NP(3)
COMMON /BLK1/C2,A,B
COMMON /BLK2/ARX,ARY
COMMON /BLK3/AMX,AMN
COMMON /BLK4/UA,AA
COMMON /BLK5/T,M,MESH
COMMON /BLK8/KP
COMMON /BLK9/NP
COMMON /BLK10/AAA
COMMON /BLK11/IDP,NC
COMMON /BLK12/Y1,Y2,AREA,C4,C1
DATA KP(1)/1HL/,KP(2)/1HM/,KP(3)/1HR/
DATA AMX/80./
DATA ARX(1)/0./,ARY(1,1)/80./,ARY(2,1)/80./,ARY(3,1)/80./
C ACCEPT THE FOLLOWING DATA
ACCEPT 101,MESH,IDP,NI,AMN
101 FORMAT(I3,I2,I4,F3:0)
N=MESH-1
M=(1+MESH)/3
NC=150
THETA=0.7333333
PL=FLOAT(NC)*50.
FF=0.02
FN=FF*PL*12./2.5
DX=1./FLOAT(N)
DT=THETA*DX
FC=FN*DT
C1=0.578703704D00
C4=94.7-FLOAT(IDP)
AREA=1.22718463D00
AE=0.03984
A=1.2720123456789D00
B=1.3050123456789D00
C INITIAL CONDITIONS
P0=80.
TT=0.0
DO 1 I=1,2
DO 2 J=1,MESH
UA(I,J)=0.0
AA(I,J)=1.304896577D00
2 CONTINUE
1 CONTINUE
UA(1,1)=-C1*AA(1,1)*AE/AREA
UUL=UA(1,1)*1100.

```

```

        UUM=UA(1,M)*1100,
        UUR=UA(1,MESH)*1100,
        TYPE 48
        TYPE 49, IDP, NC
49      FORMAT(35X,'DURING ',I2,'-PSI B.P. REDUCTION.',I3,'-CAR')
        TYPE 48
48      FORMAT(35X,'*****')
        TYPE 50,N
50      FORMAT(1H ,4X,'MESH SIZE=',I2,' ',1X,'L:FIRST CAR',
1'M:ONE-THIRD OF TRAIN, ',R:LAST CAR, ', 'U:VELOCITY OF AIR')
        TYPE 57
        TYPE 55
55      FORMAT(6X,'TIME',18X,'P(L)',11X,'P(M)',11X,'P(R)',11X,
1'U(L)',11X,'U(M)',11X,'U(R)')
        TYPE 56
56      FORMAT(6X,'(SEC.)',23X,'P IN (PSIG)',31X,'U IN (FT/SEC)')
        TYPE 57
57      FORMAT(4X,-----)
1-----'
TYPE 76,TT,P0,P0,P0,UUL,UUM,UUR
76      FORMAT(4X,F6.2,15X,3(F7.4,BX),3(F7.2,BX))
NP=1
C      TIME TAKEN FOR FLOW OF AIR
DO 3 JT=1,NI
T=D*T*PL*FLOAT(JT)/525.
IF(T .LT. 3.1) GO TO 82
C      LEFT BOUNDARY NODAL POINTS
YRL=UA(1,2)*AA(1,1)-UA(1,1)*AA(1,2)
VRL=AA(1,1)-UA(1,1)+UA(1,2)+AA(1,2)
URL=(UA(1,1)+THETA*YRL)/(1.+THETA*VRL)
ARL=(AA(1,1)+THETA*YRL)/(1.+THETA*VRL)
FTL=FC*URL*DABS(URL)
C2=URL-5.*ARL-FTL
PD=14.7*(AA(1,1)**7)-C4
IF(PD .GT. 1.2) AA(2,1)=-C2/(C1*AE/AREA+5.)
IF((PD .LE. 1.2) .AND. (PD .GT. 0.50)) GO TO 120
IF((PD .LE. 0.50) .AND. (PD .GT. 0.40)) GO TO 121
IF((PD .LE. 0.40) .AND. (PD .GT. 0.30)) GO TO 122
IF((PD .LE. 0.30) .AND. (PD .GT. 0.0)) GO TO 123
IF(PD .LE. 0.0) AA(2,1)=(C4/14.7)**(1./7.)
GO TO 112
120  Y1=0.0008
      Y2=0.03885
      GO TO 111
121  Y1=0.005
      Y2=0.03675
      GO TO 111
122  Y1=0.0175
      Y2=0.03175
      GO TO 111
123  Y1=0.1233
      Y2=0.0
111  CALL ROOT
      AA(2,1)=AAA
112  UA(2,1)=+C2+5.*AA(2,1)
C      INTERIOR POINTS
DO 4 MX=2,N
    YLI=UA(1,MX-1)*AA(1,MX)-UA(1,MX)*AA(1,MX-1)
    YRI=UA(1,MX+1)*AA(1,MX)-UA(1,MX)*AA(1,MX+1)

```

```

ALI=(AA(1,MX)-THETA*YLI)/(1.+THETA*VLI)
URI=(UA(1,MX)+THETA*YRI)/(1.+THETA*VRI)
ARI=(AA(1,MX)+THETA*YRI)/(1.+THETA*VRI)
F1=FC*ULI*DABS(ULI)
F2=FC*URI*DABS(URI)
AA(2,MX)=.1*(ULI-URI+5.*(ALI+ARI)+F2-F1)
UA(2,MX)=.5*(ULI+URI+5.*(ALI-ARI)-F2-F1)
4 CONTINUE
IF(14.7*(AA(2,M)**7) .LT. C4) AA(2,M)=(C4/14.7)**(1./7.)
C RIGHT BOUNDARY, NODAL POINTS
UA(2,MESH)=0.0
YLR=UA(1,N)*AA(1,MESH)-UA(1,MESH)*AA(1,N)
VLR=UA(1,MESH)+AA(1,MESH)-UA(1,N)-AA(1,N)
ULR=(UA(1,MESH)+THETA*YLR)/(1.+THETA*VLR)
ALR=(AA(1,MESH)-THETA*YLR)/(1.+THETA*VLR)
FTR=FC*ULR*DABS(ULR)
C3=ULR+5.*ALR-FTR
AA(2,MESH)=C3/5.
IF(14.7*(AA(2,MESH)**7) .LT. C4) AA(2,MESH)=(C4/14.7)**(1./7.)
C PRINT THE RESULTS
82 KT=JT/(NI/100)
IF((NI/100)*KT-JT) 80,81,80
81 NP=NP+1
IF(T .GE. 3.1) GO TO 84
UA(2,1)=-C1*AA(2,1)*AE/AREA
84 CALL OUTP
C TRANSFER OF GRID FROM THE PREVIOUS RESULTS
80 IF(T .LT. 3.1) GO TO 3
DO 5 K=1,MESH
AA(1,K)=AA(2,K)
UA(1,K)=UA(2,K)
AA(2,K)=0.0
UA(2,K)=0.0
5 CONTINUE
3 CONTINUE
TYPE 57
CALL PLOTXY
STOP
END
SUBROUTINE ROOT
DOUBLE PRECISION CC,C,CAVG,EQC,EQCC,EQCAV,DELC
DOUBLE PRECISION C2,A,B,AAA,AREA,G1,G2,G3
COMMON /BLK1/C2,A,B
COMMON /BLK10/AAA
COMMON /BLK12/Y1,Y2,AREA,C4,C1
G1=Y1*14.7*C1/AREA
G2=G1*C4/14.7
G3=Y2*C1/AREA
DELC=1.55555D-02
C=A
EQC=G1*CC**8+(5.-G2+G3)*C+C2
CC=C+DELC
EQCC=G1*CC**8+(5.-G2+G3)*CC+C2
IF(EQC*EQCC) 8,5,7
5 AAA=CC
RETURN
7 IF(CC .GE. B) GO TO 13
IF(CC .LE. A) GO TO 14

```

```
CAVG=(C+CC)/2.0D00
EQCAV=G1*CAVG**8+(5.-G2+G3)*CAVG+C2
IF(EQC*EQCAV) 10,12,9
9
C=CAVG
EQC=EQCAV
GO TO 11
10
CC=CAVG
EQCC=EQCAV
11
CONTINUE
12
AAA=CAVG
RETURN
13
AAA=B
RETURN
14
AAA=A
RETURN
END
SUBROUTINE PLOTXY
DIMENSION ARX(101),ARY(3,101),KP(3),KPT(101)
COMMON /BLK2/ARX,ARY
COMMON /BLK3/AMX,AMN
COMMON /BLK6/KPT
COMMON /BLK7/I,IFLAG
COMMON /BLK8/KP
COMMON /BLK9/NP
COMMON /BLK11/IDP,NC
C
XSCALE=(ARX(NP)-ARX(1))/100.
C
PLOT THE RESULTS
TYPE 93
93
FORMAT(1H ,37X,'BRAKE PIPE PRESSURES VS. TIME')
TYPE 94
94
FORMAT(37X,'-----')
TYPE 92,IDP,NC
92
FORMAT(1H ,37X,'DURING ',I2,'-PSI B.P. REDUCTION,',I3,
1'-CAR TRAIN')
TYPE 95
95
FORMAT(1H ,37X,'L: P(L), M: P(M), R: P(R)')
YMIN=AMN
YSCALE=(AMX-AMN)/100.
DO 10 I=1,3
TYPE 100,AMN,(AMN+YSCALE*L*10.),L=1,9),AMX,KP(I)
100
10
FORMAT(4X,F7.2,10(3X,F7.2),2X,A1)
CONTINUE
MNP=1
DO 20 III=1,101
I=III-1
IFLAG=I/10*10
CALL COOPRT
MXSC=INT((ARX(MNP)-ARX(1))/XSCALE+.5)
IF(I .NE. MXSC) GO TO 21
DO 22 L=1,3
IYPT=INT((ARY(L,MNP)-YMIN)/YSCALE+.5)
KPT(IYPT)=KP(L)
22
CONTINUE
MNP=MNP+1
21
CONTINUE
```

```

IF(IFLAG .EQ. I) GO TO 23
TYPE 101,(KPT(I),I=1,101)
101 FORMAT(8X,101A1)
GO TO 24
23 CONTINUE
XX=ARX(1)+XSCALE*I
TYPE 102,XX,(KPT(I),I=1,101)
102 FORMAT(F8.2,101A1)
24 CONTINUE
20 CONTINUE
RETURN
END
SUBROUTINE COOPRT
DIMENSION KPT(101)
COMMON /BLK6/KPT
COMMON /BLK7/I,IFLAG
DATA K1/1H/,K2/1H./,K3/1H./,K4/1H./,K5/1H./
LFLAG=0
KK=K1
KPT(1)=K2
KPT(101)=K2
IF(IFLAG .NE. I) GO TO 10
KK=K4
IF(I .EQ. 0 .OR. I .EQ. 100) KK=K3
KPT(1)=K5
KPT(101)=K5
LFLAG=1
10 CONTINUE
DO 20 J=2,100
KPT(J)=KK
IF((J-1)/10*10 .EQ. (J-1)) KPT(J)=K4
IF(LFLAG .EQ. 1 .AND. (J-1)/10*10 .EQ. (J-1)) KPT(J)=K5
20 CONTINUE
RETURN
END
SUBROUTINE OUTP
DOUBLE PRECISION UA(2,101),AA(2,101)
DIMENSION ARX(101),ARY(3,101)
COMMON /BLK2/ARX,ARY
COMMON /BLK4/UA,AA
COMMON /BLK5/T,M,MESH
COMMON /BLK9/NP
PPL=(AA(2,1)**7-1)*14.7
PPM=(AA(2,M)**7-1.)*14.7
PPR=(AA(2,MESH)**7-1.)*14.7
UUL=UA(2,1)*1100.
UUM=UA(2,M)*1100.
UUR=UA(2,MESH)*1100.
TYPE 66,T,PPL,PPM,PPR,UUL,UUM,UUR
FORMAT(4X,F6.2,15X,3(F7.4,8X),3(F7.2,8X))
66 ARX(NP)=T
ARY(1,NP)=PPL
ARY(2,NP)=PPM
ARY(3,NP)=PPR
RETURN
END

```

C THIS PROGRAM IS TO CALCULATE THE DYNAMIC CHARACTERISTICS
 C OF A BRAKE PIPE(TRAINLINE) BY USING THE METHOD OF CHARACT-
 C ERISTICS FOR LARGE-AMPLITUDE SIGNALS.

C *****
 C *
 C *MODIFIED APPROACH*
 C *
 C *****

DOUBLE PRECISION UA(2,101),AA(2,101)
 DOUBLE PRECISION YRL,VRL,URL,ARL,FN,C1,FTL,FC,DT,EP,DM
 DOUBLE PRECISION YLI,YRI,VRI,ULI,URI,ARI,ULI,ALI,F1,F2
 DOUBLE PRECISION YLR,VLR,ULR,ALR,FTR,C3,AREA,BPL,BPC
 DOUBLE PRECISION RTIME,C,DPC,VC,VL,C2,Q,B1,B2,B3,B4
 DOUBLE PRECISION B5,BPL1,BPL2,FNLC,AAA,PR,C5
 DIMENSION ARX(101),ARY(3,101),KP(3)
 COMMON /BLK1/CD,AREA,BPL,BPC,TH,DM
 COMMON /BLK2/ARX,ARY
 COMMON /BLK3/AMX,AMN
 COMMON /BLK4/UA,AA
 COMMON /BLK5/T,M,MESH
 COMMON /BLK8/KP
 COMMON /BLK9/NP
 COMMON /BLK10/IDP,NC
 COMMON /BLK11/PR,Q
 COMMON /BLK12/C
 COMMON /BLK13/FNLC
 COMMON /BLK15/PPC
 DATA KP(1)/1HL/,KP(2)/1HM/,KP(3)/1HR/
 DATA AMX/80./
 DATA ARX(1)/0./,ARY(1,1)/80./,ARY(2,1)/80./,ARY(3,1)/80./
 C
 ACCEPT THE FOLLOWING DATA
 ACCEPT 101,MESH,IDL,NI,AMN
 101 FORMAT(I3,I2,I4,F3.0)
 N=MESH-1
 M=(1+MESH)/3
 NC=150
 THETA=0.733333
 PL=FLOAT(NC)*50.
 FF=0.02
 FN=FF*PL*12./2.5
 DX=1./FLOAT(N)
 DT=THETA*DX
 FC=FN*DT
 R=640.104
 Q=0.5282817877D00
 C=0.531797514D00
 EN=1.3
 EP=1./7.
 TH=530.
 AREA=4.908738521D-02
 RTN=EN*R*TH
 BPL=9.47D01
 BPC=1.47D01
 RTIME=DT*PL/1100.

C4=BPL-FLOAT(IDP)
C1=0.578703704D00
CD=0.82
VL=1.104466167D05
VC=VL*FLOAT(IDP)/(C4-14.7)
C5=(C4/14.7)**EP
TYPE 77,CD,VC
77 FORMAT(4X,'CD=',F4.2,5X,'VC=',F7.0,'CU.IN.')
B1=CD*AREA*C/DSQRT(TH)
B2=6.355357469D-06
B3=1.22718463D00
B4=2.15535712D00
B5=B4*B1/(B2*B3*1100.*12.)
C INITIAL CONDITIONS
P0=80.
TT=0.0
DO 1 I=1,2
DO 2 J=1,MESH
UA(I,J)=0.0
AA(I,J)=1.304896577D00
2 CONTINUE
1 CONTINUE
UA(1,1)=-B5*AA(1,1)**2
UUL=UA(1,1)*1100.
UUM=UA(1,M)*1100.
PPC=BPC-14.7
TYPE 48
TYPE 49, IDP, NC
49 FORMAT(35X,'DURING ',I2,'-PSI B.P. REDUCTION ','I3,'-CAR')
TYPE 48
48 FORMAT(35X,'*****')
TYPE 50,N
50 FORMAT(1H ,4X,'MESH SIZE=',I3,',',1X,'L:FIRST CAR, ',
1'M:ONE-THIRD OF TRAIN, ','R:LAST CAR, ','U:VELOCITY,
1'P:BRAKE PIPE PRESSURE')
TYPE 57
TYPE 55
55 FORMAT(6X,'TIME',18X,'P(L)',11X,'P(M)',11X,'P(R)',11X,
1' PPC',11X,'U(L)',11X,'U(M)')
TYPE 56
56 FORMAT(6X,'(SEC.)',35X,'P IN (PSIG)',31X,'U IN (FT/SEC)')
TYPE 57
57 FORMAT(4X,'-----')
1-----
TYPE 76,TT,P0,PO,P0,PPC,UUL,UUM
76 FORMAT(4X,F6.2,15X,3(F7.4,BX),3(F7.2,BX))
NP=1

```

C      TIME TAKEN FOR FLOW OF AIR.
DO 3 JT=1,NI
T=DT*PL*FLOAT(JT)/1100.
IF(T .LT. 3.4) GO TO 82
C      LEFT BOUNDARY NODAL POINTS
YRL=UA(1,2)*AA(1,1)-UA(1,1)*AA(1,2)
VRL=AA(1,1)-UA(1,1)+UA(1,2)-AA(1,2)
URL=(UA(1,1)+THETA*YRL)/(1.+THETA*VRL)
ARL=(AA(1,1)+THETA*YRL)/(1.+THETA*VRL)
FTL=FC*URL*DABS(URL)
C2=URL-5.*ARL-FTL
FNLC=1.0D00
CALL FLOW
DPC=RTN*DM*RTIME/VC
BPC=BPC+DPC
PPC=BPC-14.7
IF (PPC .GT. (80.-FLOAT(IDP))) BPC=C4
PR=BPC/BPL
IF ((1.-PR) .LT. 0.) PR=BPL/BPC
IF (PR .GT. Q) CALL FUN
AAA=(-5.+DSQRT(25.-4.*B5*C2*FNLC))/(2.*B5*FNLC)
BPL1=(AAA**7)*14.7
BPL=BPL1
PR=BPC/BPL
IF ((1.-PR) .LT. 0.) PR=BPL/BPC
IF (PR .LE. Q) GO TO 111
CALL FUN
AAA=(-5.+DSQRT(25.-4.*B5*C2*FNLC))/(2.*B5*FNLC)
BPL2=(AAA**7)*14.7
BPL=DSQRT(BPL1*BPL2)
111 IF (BPL .LT. C4) BPL=C4
AA(2,1)=(BPL/14.7)**EP
UA(2,1)=5.*AA(2,1)+C2
C      INTERIOR POINTS
DO 4 MX=2,N
YLI=UA(1,MX-1)*AA(1,MX)-UA(1,MX)*AA(1,MX-1)
YRI=UA(1,MX+1)*AA(1,MX)-UA(1,MX)*AA(1,MX+1)
VLI=UA(1,MX)+AA(1,MX)-UA(1,MX-1)-AA(1,MX-1)
VRI=AA(1,MX)-UA(1,MX)+UA(1,MX+1)-AA(1,MX+1)
ULI=(UA(1,MX)+THETA*YLI)/(1.+THETA*VLI)
ALI=(AA(1,MX)-THETA*YLI)/(1.+THETA*VLI)
URI=(UA(1,MX)+THETA*YRI)/(1.+THETA*VRI)
ARI=(AA(1,MX)+THETA*YRI)/(1.+THETA*VRI)
F1=FC*ULI*DABS(ULI)
F2=FC*URI*DABS(URI)
AA(2,MX)=.1*(ULI-URI+5.*(ALI+ARI)+F2-F1)
IF (AA(2,MX) .LT. C5) AA(2,MX)=C5
UA(2,MX)=.5*(ULI+URI+5.*(ALI-ARI)-F2-F1)
4      CONTINUE

```

```

C      RIGHT BOUNDARY NODAL POINTS
UA(2,MESH)=0.0
YLR=UA(1,N)*AA(1,MESH)-UA(1,MESH)*AA(1,N)
VLR=UA(1,MESH)+AA(1,MESH)-UA(1,N)-AA(1,N)
ULR=(UA(1,MESH)+THEJAXYLR)/(1.+THETA*VLR)
ALR=(AA(1,MESH)-THETA*YLR)/(1.+THETA*VLR)
FTR=FC*ULR*DABS(ULR)
C3=ULR+5.*ALR-FTR
AA(2,MESH)=C3/5.
IF(AA(2,MESH) .LT. C5) AA(2,MESH)=C5
C      PRINT THE RESULTS
82      KT=JT/(NI/100)
IF((NI/100)*KT-JT) 80,81,80
81      NP=NP+1
IF(T .GE. 3.4) GO TO 84
UA(2,1)=-B5*AA(2,1)**2
84      CALL OUTP
C      TRANSFER OF GRID FROM THE PREVIOUS RESULTS
80      IF(T .LT. 3.4) GO TO 3
DO 5 K=1,MESH
AA(1,K)=AA(2,K)
UA(1,K)=UA(2,K)
AA(2,K)=0.0
UA(2,K)=0.0
5      CONTINUE
3      CONTINUE
TYPE 57
CALL PLOTXY
STOP
END
SUBROUTINE FLOW
DOUBLE PRECISION AREA,BPL,BPC,D,DM,Q,C,PR
COMMON /BLK1/CD,AREA,BPL,BPC,TH,DM
COMMON /BLK11/PR,Q
COMMON /BLK12/C
COMMON /BLK13/FNLC
P=BPL
PR=BPC/BPL
D=C
IF(1.-PR) 1,2,2
1      P=BPC
PR=BPL/BPC
D=-C
2      D=D*P*AREA*CD/DSQRT(TH)
IF(PR .LE. Q) GO TO 22
IF(PR .GT. Q) CALL FUN
D=D*FNLC
22      DM=D
RETURN
END

```

PROGRAM RELAY (INPUT,OUTPUT)

C
C #####
C # 26-C BRAKE VALVE PORTION-- RELAY VALVE DETAILED MODEL--
C # FULLY NONLINEAR SYSTEM ANALYSIS.
C #
C #####

C LUMPED-PARAMETERS

C
C P1-PRESSURE IN OUTER DIAPHRAGM CHAMBER
C P2-PRESSURE IN OUTPUT CHAMBER
C P3-PRESSURE IN INNER DIAPHRAGM CHAMBER
C PA-AMBIENT PRESSURE
C PI-INPUT PRESSURE
C PH-SUPPLY PRESSURE
C A1-EFFECTIVE AREA INPUT ORIFICE
C A2-EFFECTIVE AREA SUPPLY VALVE
C A3-EFFECTIVE AREA FEEDBACK ORIFICE
C A4-EFFECTIVE AREA EXHAUST VALVE
C AE-EFFECTIVE AREA DIAPHRAGM
C V1-VOLUME OUTER DIAPHRAGM CHAMBER
C V2-VOLUME OUTPUT CHAMBER
C V3-VOLUME INNER DIAPHRAGM CHAMBER
C X0-NEUTRAL POSITION OF DIAPHRAGM
C XM-MAXIMUM DIAPHRAGM DISPLACEMENT
C X1-DIAPHRAGM DISPLACEMENT TO OPEN EXHAUST VALVE
C X2-DIAPHRAGM DISPLACEMENT TO OPEN SUPPLY VALVE
C IM-MASS OF DIAPHRAGM ASSEMBLY

C REAL IM,N

DIMENSION AMN(4),AMX(4)
DIMENSION Z(10),DZ(10),PRHT(5),AUX(16,10)
COMMON DP1,DPB,DP2,DRV1,DRV3,DRV2,DV1,DV2,DX,DU
COMMON P1,P2,P3,RV1,RVB,RV2,V1,V2,X,U
COMMON T1,TB,T2,TA,TI,TH,PA,PI,PH,V3
COMMON A1,A2,A3,A4,AE
COMMON CK1,CK2,CK3,IM,FK1,FK2,FK3,FM
COMMON X0,XM,X1,X2,R,N,IT,JT
COMMON FK11,FK21,FK31
COMMON KP(4),ARX(101),ARY(4,101),NP,NV
EQUIVALENCE (Z(1),P1),(DZ(1),D>1).
EXTERNAL FCT,OUTP

C ACCEPT THE FOLLOWING DATA

KP(1)=1HA
KP(2)=1HB
KP(3)=1HC
KP(4)=1HD

X = .155
X0=.155
XM=.358
X1=.137
X2=.185

U = 0.

A1=1.43E-3

A2=0.

A3=9.81E-3

A4=0.

AE=12.83

C SPRING CONSTANTS

CK1=8.6

CK2=19.

CK3=9.8

FK11=5.69

FK21=5.89

FK31=3.293

C VOLUME

V1=13.

VB=5.

V2=10.

C PRESSURE

PA=14.7

PI=70.

PH=114.7

PI=PI+PA

P1=PA

P2=PA

P3=PA

C TEMPERATURE

TA=530.

TI=TA

TM=TA

T1=TA

TB=TA

T2=TA

C MASS OF AIR

R=640.104

RV1=P1*V1/(R*T1)

RVB=P3*VB/(R*TB)

RV2=P2*V2/(R*T2)

N=1,1

NH=2.073E-3

IT=0

JT=0

NP=0

NV=4

NDIM=10

ERWT=1./FLOAT(NDIM)

NSTEPS=300

RTIME=1.25

DO 3 I=1,NDIM:

DZ(I)=ERWT

73/172 OPT=1

```
C PRMT(1)=0.  
C PRMT(2)=ETIME  
C PRMT(3)=1./FLOAT(INSTEPS)  
C PRMT(4)=.1  
C PRINT 7  
T FORMAT(1H1,///)  
C PRINT HEADINGS  
C PRINT 8  
B FORMAT(18X,*RESULTS FOR NEGLECTING TEMPERATURE CHANGE*,/)  
PRINT 4  
4 FORMAT(1HD,T5,*TIME(SEC) PI(PSIG) P1(PSIG) P2(PSIG)  
1 X(INCH) U(IN/SEC)*,/  
C CALL HPCG(PRMT,Z,DZ,NDIM,XHLP,FCT,OUTP,AUX)  
C AMX(1)=100.  
AMX(2)=100.  
AMX(3)=100.  
AMX(4)=.05  
AMN(1)=0.  
AMN(2)=0.  
AMN(3)=0.  
AMN(4)=-.05  
C CALL PLOT1(ARX,ARY,AMN,AMX,KP,NY,np)  
C STOP  
END
```

SUBROUTINE1 FCT(T,Z,DZ)
 COMMON DP1,DP3,DP2,DRY1,DRVB,DRY2,DV1,DV2,DX,DU
 COMMON P1,P8,P2,RV1,RVB,RV2,V1,V2,X,U
 COMMON T1,T8,T2,TA,TI,TH,PA,PI,PH,V3
 COMMON A1,A2,A3,A4,AE
 COMMON CK1,CK2,CK3,IM,FK1,FK2,FK3,FH
 COMMON X0,XM,X1,X2,R,N,IT,JT
 COMMON FK11,FK21,FK31
 COMMON KP(4),ARX(101),ARY(4,101),NP,NV
 REAL IM,N
 DIMENSION Z(1),DZ(1)

C
C SPRING FORCES:
IF(X=.0001) 1,1,2

1 X=0.
U=AMAX1(0.,U).
FK1=FK11+CK1*(X1-X)
FK2=FK21+CK2*(X-X0)
FK3=0.
A2=0.
A4=2.242*(X1-X)

C
C DIAPHRAGM ASSEMBLY
FH=(P1-P2)*AE+FK1+FK2+FK3
FH=AMAX1(0.,FH)
DU=FH/IM
DX=U
GO TO 600

C
2 IF(X=X1) 100,100,200
100 A2=0.
A4=2.242*(X1-X)
FK1=FK11+CK1*(X1-X)
FK2=FK21+CK2*(X-X0)
FK3=0.
FH=(P1-P2)*AE+FK1+FK2+FK3
DU=FH/IM
DX=U
GO TO 600

C
200 IF(X=X2) 300,300,400
300 A2=0.
A4=0.
FK1=0.
FK2=FK21+CK2*(X-X0)
FK3=0.
FH=(P1-P2)*AE+FK1+FK2+FK3
DU=FH/IM
DX=U
GO TO 600

C
400 IF(X=XH) 500,510,510
500 A2=1.734*(X-X2)
A4=0.
FK1=0.
FK2=FK21+CK2*(X-X0)
FK3=FK31+CK3*(X-X2)

73/17E OPT=1

$FH = (P1 - P2) * AE + FK1 - FK2 - FK3$
 $DU = FM / IM$
 $DX = U$
 $GO TO 600$

C

510

$X = XM$
 $A2 = 1.734 * (X - X2)$
 $A4 = 0$
 $FK1 = 0$
 $FK2 = FK21 + CX2 * (X - X0)$
 $FK3 = FK31 + CX3 * (X - X2)$
 $FH = (P1 - P2) * AE + FK1 - FK2 - FK3$
 $FH = AMIN1(0., FH)$
 $U = AMIN1(0., U)$
 $DU = FN / IM$
 $DX = U$

C

600

$DV1 = AE * DX$
 $DV2 = -AE * DX$
 $T1 = P1 * V1 / (R * RV1)$
 $TB = P3 * VB / (R * RVB)$
 $T2 = P2 * V2 / (R * RV2)$

C

C

MASS FLOW RATE
 $DM1 = FLOW(A1, PI, P1, T1, T1)$
 $DM2 = FLOW(A2, PM, P3, T4, TB)$
 $DM3 = FLOW(A3, PB, P2, TB, T2)$
 $DM4 = FLOW(A4, PB, PA, TB, TA)$

C

C

TIME RATE OF CHANGE OF MASS

$DRV1 = DM1$
 $DRV2 = DM2 - DM3 - DM4$
 $DRV3 = DM3$

C

$DP1 = (N * R * T1 * DRV1 - N * P1 * DV1) / V1$
 $DPB = N * R * T3 * DV3 / V3$
 $DP2 = (N * R * T2 * DRV2 - N * P2 * DV2) / V2$
 RETURN
 END

SUBROUTINE HPCG(PRMT,Y,DERY,NDIM,IHLF,FCT,OUTP,AUX)

C DIMENSION PRMT(1),Y(1),DERY(1),AUX(16,1),JTW(13)

N=1

IHLF=0

X=PRMT(1)

H=PRMT(3)

PRMT(5)=0,0

DO 1 I=1,NDIM

AUX(16,I)=0,0

AUX(15,I)=DERY(I)

1 AUX(1,I)=Y(I)

IF(H*(PRMT(2)-X))3,2,4

2 IHLF=12

GO TO 4

3 IHLF=13

4 CALL FCT(X,Y,DERY)

CALL OUTP(X,Y,DERY,IHLF,NDIM,PRMT)

IF(PRMT(5))6,5,6

5 IF(IHLF)7,7,6

6 RETURN

7 DO 8 I=1,NDIM

8 AUX(8,I)=DERY(I)

ISW=1

GO TO 100

9 X=X+H

DO 10 I=1,NDIM

10 AUX(2,I)=Y(I)

11 IHLF=IHLF+1

X=X-H

DO 12 I=1,NDIM

12 AUX(4,I)=AUX(2,I)

H=0,5*H

N=1

ISW=2

GO TO 100

13 X=X+H

CALL FCT(X,Y,DERY)

N=2

DO 14 I=1,NDIM

AUX(2,I)=Y(I)

14 AUX(9,I)=DERY(I)

ISW=3

GO TO 100

15 DELT=0,0

DO 16 I=1,NDIM

POOR COPY
COPIE DE QUALITEE INFERIEURE

```

16 DELT=DELT+AUX(15,I)*ABS(Y(I)+AUX(4,I))
DELT=0.06666667*DELT
IF(DELT-PRMT(4))19,19,17
17 IF(IHLF-10)11,18,18
C
18 IHLF=11
X=X+H
GO TO 4
C
19 X=X+H
CALL FCT(X,Y,DERY)
DO 20 I=1,NDIM
AUX(3,I)=Y(I)
20 AUX(10,I)=DERY(I)
N=3
ISW=4
GO TO 100
C
21 N=1
X=X+H
CALL FCT(X,Y,DERY)
X=PRMT(1)
DO 22 I=1,NDIM
AUX(11,I)=DERY(I)
22 Y(I)=AUX(1,I)+H*(.375*AUX(8,I)+.79166667*AUX(9,I)
1-.20833333*AUX(10,I)+0.04166667*DERY(I))
23 X=X+H
N=N+1
CALL FCT(X,Y,DERY)
CALL OUTP(X,Y,DERY,IHLF,NDIM,PRMT)
IF(PRMT(5))6,24,6
24 IF(N-4)25,200,200
25 DO 26 I=1,NDIM
AUX(N,I)=Y(I)
26 AUX(N+7,I)=DERY(I)
IF(N-3)27,29,200
C
27 DO 28 I=1,NDIM
DELT=AUX(9,I)+AUX(9,I)
DELT=DELT+DELT
28 Y(I)=AUX(1,I)+0.3333333*H*(AUX(8,I)+DELT+AUX(10,I))
GO TO 23
C
29 DO 30 I=1,NDIM
DELT=AUX(9,I)+AUX(10,I)
DELT=DELT+DELT+DELT
30 Y(I)=AUX(1,I)+.375*H*(AUX(8,I)+DELT+AUX(11,I))
GO TO 23
C
100 DO 101 I=1,NDIM
Z=H*AUX(N+7,I)
AUX(5,I)=Z
101 Y(I)=AUX(N,I)+0.4*Z
C
Z=X+0.4*H
CALL FCT(X,Y,DERY)
DO 102 I=1,NDIM

```

POOR COPY
COPIE DE QUALITEE INFERIEURE

```

Z=H*DERY(I)
AUX(6,I)=Z
102 Y(I)=AUX(N,I)+0.2969776*AUX(5,I)+0.1537596*Z
Z=X+0.4557372*H
CALL FCT(Z,Y,DERY)
DO 103 I=1,NDIM
Z=H*DERY(I)
AUX(7,I)=Z
103 Y(I)=AUX(N,I)+0.2181004*AUX(5,I)-3.050965*AUX(6,I)+3.832665*Z
C
Z=X+H
CALL FCT(Z,Y,DERY)
DO 104 I=1,NDIM
104 Y(I)=AUX(N,I)+1.747603*AUX(5,I)-.5514807*AUX(6,I)
+1.205536*AUX(7,I)+0.1711848*H*DERY(I)
GO TO (9,13,15,21),ISW
C
C
200 ISTEP=3
DO 2001 I=1,13
2001 JTW(I)=0
IF (IHLF.GT.0) JTW(IHLF)=-1
201 IF (N-8) 204,202,504
C
202 DO 203 N=2,7
DO 203 I=1,NDIM
AUX(N-1,I)=AUX(N,I)
203 AUX(N+6,I)=AUX(N+7,I)
N=7
C
204 N=N+1
C
DO 205 I=1,NDIM
AUX(N-1,I)=Y(I)
205 AUX(N+6,I)=DERY(I)
X=X+H
206 ISTEP=ISTEP+1
DO 207 I=1,NDIM
DELT=AUX(N-4,I)*1.333333*H*(AUX(N+6,I)+AUX(N+6,I)-AUX(N+5,I)+
IAUX(N+4,I)+AUX(N+4,I))
Y(I)=DELT-0.9256198*AUX(16,I)
207 AUX(16,I)=DELT
C
C
CALL FCT(X,Y,DERY)
C
DO 208 I=1,NDIM
DELT=0.125*(9.*AUX(N-1,I)-AUX(N-3,I)+3.*H*(DERY(I)+AUX(N+6,I)+
IAUX(N+6,I)-AUX(N+5,I)))
AUX(16,I)=AUX(16,I)-DELT
208 Y(I)=DELT+0.07438017*AUX(16,I)
C
DELT=0.0
DO 209 I=1,NDIM
209 DELT=DELT+AUX(15,I)*ABS(AUX(16,I))
IF (DELT-PRMT(4)) 210,222,222
C

```

```

210 CALL FCT(X,Y,DERY)
    CALL OUTP(X,Y,DERY,IHLF,NDIM,PWY)
    IF(IHLF.GT.0) JIW(IHLF)=JTW(IHLF)+1
    IF(PRMT(5)>212,211,212
211 IF(IHLF-11)>213,212,212
212 RETURN
213 IF(H>(X-PRMT(2)))>214,212,212
214 IF(ABS(X-PRMT(2))-0.1*ABS(H))>212,215,215
215 IF(DELT-0.02*PRMT(4))>216,216,201

```

C

C

```

216 IF(IHLF)>201,201,217
217 IF(N-7)>201,218,218
218 IF(ISTEP-4)>201,219,219
219 JMOD=JIW(IHLF)/2
    IF(JTW(IHLF)-JMOD-JMOD)>201,220,201
220 H=H+H

```

```

    JTW(IHLF)=0
    IHLF=IHLF-1
    IF(IHLF.GT.0) JTW(IHLF)=JTW(IHLF)+JMOD
    ISTEP=0

```

```

DO 221 I=1,NDIM
AUX(N-1,I)=AUX(N-2,I)
AUX(N-2,I)=AUX(N-4,I)
AUX(N-3,I)=AUX(N-6,I)
AUX(N+6,I)=AUX(N+5,I)
AUX(N+5,I)=AUX(N+3,I)
AUX(N+4,I)=AUX(N+1,I)
DELT=AUX(N+6,I)*AUX(N+5,I)
DELT=DELT+DELT+DELT

```

```

221 AUX(16,I)=8.962963*(Y(I)-AUX(N-3,I))-3.361111*H*(DERY(I)+DELT
1+AUX(N+4,I))
GO TO 201

```

C

```

222 IHLF=IHLF+1
    IF(IHLF-10)>223,223,210

```

```

223 H=0.5*H
    ISTEP=0

```

```

DO 224 I=1,NDIM
Y(I)=0.00390625*(80.*AUX(N-1,I)+135.*AUX(N-2,I)+40.*AUX(N-3,I)
1AUX(N-4,I))-0.1171875*(AUX(N+6,I)-6.*AUX(N+5,I)-AUX(N+4,I))*H
AUX(N-4,I)=0.00390625*(12.*AUX(N-1,I)+135.*AUX(N-2,I)+
1108.*AUX(N-3,I)+AUX(N-4,I))-0.0234375*(AUX(N+6,I)+18.*AUX(N+5,I)
29.*AUX(N+4,I))*H
AUX(N-3,I)=AUX(N-2,I)

```

```

224 AUX(N+4,I)=AUX(N+5,I)

```

```

X=X-H

```

```

DELT=X-(H+H)

```

```

CALL FCT(DELT,Y,DERY)

```

```

DO 225 I=1,NDIM

```

```

AUX(N-2,I)=Y(I)

```

```

AUX(N+5,I)=DERY(I)

```

```

225 Y(I)=AUX(N-4,I)

```

```

DELT=DELT-(H+H)

```

```

CALL FCT(DELT,Y,DERY)

```

```

DO 226 I=1,NDIM

```

```

DELT=AUX(N+5,I)*AUX(N+4,I)

```

73/172 OPT=1

```

DELT=DELT+DELT
AUX(16,I)=8.952963*(AUX(N-1,I)+Y(I))-3.361111*H*(AUX(N+6,I)
1+DERY(I)+DELT)
226 AUX(N+3,I)=DERY(I)
GO TO 205
END

```

73/172 OPT=1

```

FUNCTION FLOW(A,P1,P2,T1,T2)
C A=EFFECTIVE ORIFICE AREA (IN**2)
C P1=UPSTREAM PRESSURE (PSIA)
C P2=DOWNSTREAM PRESSURE (PSIA)
C T1=UPSTREAM TEMPERATURE (DEG. R)
C T2=DOWNSTREAM TEMPERATURE (DEG. R)
DATA Q/.528281738/,C/.531797514/
C
P=P1
T=T1
R=P2/P1
D=C
IF(1.-R) 1,2,2
1 P=P2
T=T2
R=P1/P2
D=-C
2 D=D*P*A/SQRT(T)
IF(R.GT.Q) D=D*FN12(R)
FLOW=D
RETURN
END

```

73/172 OPT=1

```

FUNCTION FN12(PR)
C PR=PRESSURE RATIO (DIMENSIONLESS)
DATA C1/.285714286/,C2/3.863925465/
C
F=0.0
A=PR**C1
B=A**A
A=A-B
IF(A.GT.0.),E=C2*B*SQRT(A)
FN12=F
RETURN
END

```

73/172 OPT=1

```

SUBROUTINE OUTP(T,Z,DZ,INLF,NDIH,PRNT)
COMMON DP1,DPB,DP2,DRV1,DRV3,DRV2,DV1,DV2,DX,DU
COMMON P1,PB,P2,RV1,RV3,RV2,V1,V2,X,U
COMMON T1,TB,T2,TD,TI,TH,PA,P1,PM,V3
COMMON A1,A2,A3,A4,A5
COMMON CK1,CK2,CK3,IM,FK1,FK2,FK3,FM
COMMON X0,XM,X1,X2,R,N,IT,JT
COMMON FK11,FK21,FK31
COMMON KP(4),ARX(101),ARY(4,101),NP,NV
REAL IM,N
DIMENSION Z(1),DZ(1),PRNT(1)

```

JT=(T+.00001)*80
IF(JT.LT. IT) RETURN

$T = T + 1$

NPANP+1

PRI=PIW

PPJ-EPJ-PA

$$PPB = PB - PA$$

$$P_1 P_2 = P_2 - P_A$$

XXIX-XO

ARX(NP) 87

ARY(1, NP) = PPI

ARY (2, NP) APPB

ARY(3,NP) = PP2.

ARY(4,NP)=XX

PRINT THE RESULTS

PRINT 1,T,PP1,PP1,PPB,PP2,XX,U

```
FORMAT(1H0,T3,F10,4,F10.2,3F10,3,2X,F10,5,F11,4)
```

RETURN

END - -

APPENDIX C

DYNAMIC CHARACTERISTICS OF THE RELAY VALVE

Since we know the static characteristics of the relay valve as described in Section 1.2, we then set-up a mathematical model of this relay valve in a non-dimensional form based on the assumption of polytropic charging and discharging, as follows:-

In the case of the outer diaphragm chamber, the time rate of change of pressure p_1 is due to mass flow rate \dot{m}_1 through the input orifice and the time rate of change of volume v_1 . Thus,

$$\frac{dp_1}{dt} = \frac{n\theta'_1}{v_1} \frac{dm_1}{dt} - nc_2 u \frac{p_1}{v_1} \quad \dots \quad (C.1)$$

Similarly, the time rate of change of pressure p_2 in the inner diaphragm chamber is due to mass flow rate \dot{m}_2 through the feedback orifice and the time rate of change of the time rate of change of volume v_2 . Thus,

$$\frac{dp_2}{dt} = \frac{n\theta'_2}{v_2} \frac{dm_2}{dt} + nc_2 u \frac{p_2}{v_2} \quad \dots \quad (C.2)$$

For the brakepipe chamber, the time rate of change of pressure p_B is due only to the net efflux of air into that volume. Hence,

$$\frac{dp_B}{dt} = \frac{n\theta'_B}{v_B} \frac{dm_B}{dt} \quad \dots \quad (C.3)$$

where $\frac{dm_1}{d\tau'} = f(a_1, p_I, p_1, \theta'_I, \theta'_1)$
 $\frac{dm_2}{d\tau'} = f(a_2, p_B, p_2, \theta'_B, \theta'_2)$
and $\frac{dm_B}{d\tau'} = f(a_3, p_M, p_B, \theta'_M, \theta'_B) - f(a_2, p_B, p_2, \theta'_B, \theta'_2) - f(a_4, p_B, p_f, \theta'_B, \theta'_f)$

The volumes of the outer and inner diaphragm chambers are modulated by the diaphragm assembly. Thus,

$$\frac{dv_1}{d\tau'} = c_2 u \quad \dots \quad (C.4)$$

$$\frac{dv_2}{d\tau'} = -c_2 u \quad \dots \quad (C.5)$$

The equation of motion for the diaphragm assembly is obtained by equating mass I_M times acceleration to the sum of all external forces acting on it. Therefore,

$$\frac{du}{d\tau'} = c_1(p_1 - p_2) + f_{k1} - f_{k2} - f_{k3} \quad \dots \quad (C.6)$$

where $f_{k1} = c_5(x_1 + x_1 - x) ; 0 \leq x \leq x_1$

$$f_{k2} = c_2(x_2 + x - x_0) ; x_0 \leq x \leq 1$$

$$f_{k3} = c_6(x_3 + x - x_2) ; x_2 \leq x \leq 1$$

$$f(a_j, p_i, p_j, \theta'_i, \theta'_j) = \frac{\sqrt{T_i}}{A_e K P_f} S_C (A_j, P_i, P_j, T_i, T_j)$$

$$a_j = \frac{A_j}{A_e}$$

$$p_j = \frac{P_j}{P_f}$$

$$v_j = \frac{V_i}{A_e X M}$$

$$m_i = \frac{M_i R T_f}{A_e X M P_f}$$

$$x_1 = \frac{x_1}{X_M}$$

$$u_1 = \frac{U_1}{X_M \sqrt{C_{k2} I_M}}$$

$$\frac{KR\sqrt{T_f}}{X_M} t$$

$$c_1 = \frac{A_e P_f}{KR\sqrt{T_f C_{k2} I_M}}$$

$$c_2 = \frac{X_M C_{k2}}{KR\sqrt{T_f C_{k2} I_M}}$$

$$c_5 = \frac{X_M C_{k1}}{KR\sqrt{T_f C_{k2} I_M}}$$

$$c_6 = \frac{X_M C_{k3}}{KR\sqrt{T_f C_{k2} I_M}}$$

$$\frac{dx}{dt'} = c_2 u$$

The effective areas a_3 and a_4 of the supply and exhaust valves are given as follows:

$$a_3 = c_3 (x - x_2) \quad \dots \quad (C.7)$$

$$a_4 = c_4 (x_1 - x) ; \quad 0 \leq x \leq x_1 \quad \dots \quad (C.8)$$

where $c_3 = 2.513 d_3 X_M / A_e$

$$c_4 = 2.513 d_4 X_M / A_e$$

Figure C.1 shows a typical set of results obtained from the mathematical model subject to the application of a step increase in input pressure $P_I = 70 \text{ psig}$ (484 kPag) & a constant supply pressure $P_M = 100 \text{ psig}$ (690 kPag). As the

POOR COPY COPIE DE QUALITE IMPERFECTA

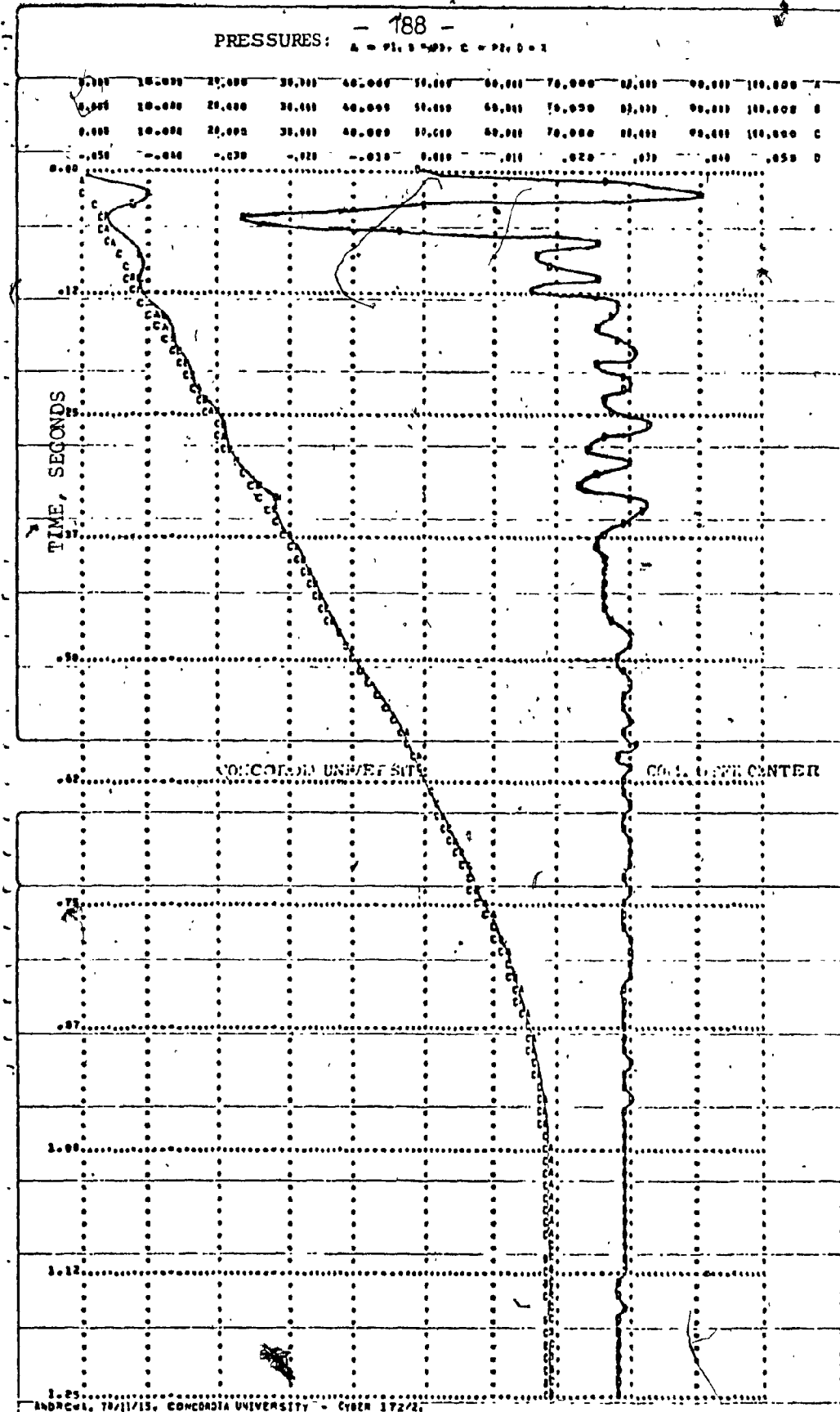


FIG.C] NONLINEAR SYSTEM (Charging Process)

13-23-48, ANDREW,
 13-23-48, ACCOUNT.C778244.,
 13-23-48, C778244.
 13-23-48, 3.3000 C= SECONDS COMPILE TIME
 13-23-48, 0.0000, RELAT.
 13-23-48, 0.0000, LOGICRELAT.
 13-23-48, LGO
 13-24-48, STOP
 13-24-48, 19.987 C= SECONDS EXECUTION.VINIVERSITY
 13-24-48, 0.0000, KUNS.
 13-24-48, 0.0000, KUNS.
 13-24-48, 0.013000, KUNS.
 13-24-48, 0.013000, KUNS.
 T_f = 70° F, $\frac{A_2}{A_1} = 7$, C_{k2} = 19, P_M = 1000 psig
 COMPUTER CENTER

outer diaphragm chamber pressure P_1 increases, time delay $t_d = 0.05\text{sec}$. is reached at which the supply valve opens and the pressure P_B in the brakepipe chamber begins to increase. The rate of increase of P_B is directly proportional to the effective area A_3 of the supply valve and the supply pressure P_M . Since the supply pressure P_M is constant, the initial oscillatory behaviour in P_B can be attributed to the motion of the diaphragm assembly which directly controls the effective area A_3 of the supply valve. It is a fact that the assembly modulates the flow areas of the supply valve and the exhaust valve in response to change in the net pressure force ($F_1 - F_2$). The rate of change of pressure P_2 is directly proportional to the feedback orifice area A_2 and brakepipe pressure P_B . The outer diaphragm chamber pressure response, P_1 , is almost identical to the brakepipe pressure response, P_B , except for the initial time delay. The entire charging process takes approximately 1.15 seconds to reach steady state, with zero load flow. Under these conditions, the delay time is negligible compared to a 10% settling time $t_s = 0.85\text{sec}$. Except for the initial delay time, brakepipe pressure P_B is equal to outer diaphragm chamber pressure P_1 . At the initial stage of charging process, the displacement of the diaphragm assembly has a sudden, negative value

because there is a pressure difference $(P_1 - P_2) = 4.8 \text{ kPa} (0.7 \text{ psi})$ required to overcome the combined force $(F_{k2} + F_{k3})$ which is caused by the diaphragm assembly spring and the supply valve spring.

Figure C2 indicates that the complete discharging process takes approximately 2.2 seconds from steady state pressure to ambient pressure, with no load flow. The rate of pressure drop, dp_B/dt , in the brakepipe chamber has the fastest response than the outer pressures P_1 and P_2 because the rate of decrease of P_B is directly proportional to the effective area A_4 of the exhaust valve and the brakepipe pressure P_B . Before the end of discharging process, amplitude of the displacement of the diaphragm assembly increases as the output pressure decreases. Also, the frequency of the diaphragm assembly decreases as the output pressure decreases.

POOR COPY
COPIE DE QUALITE INFERIEURE

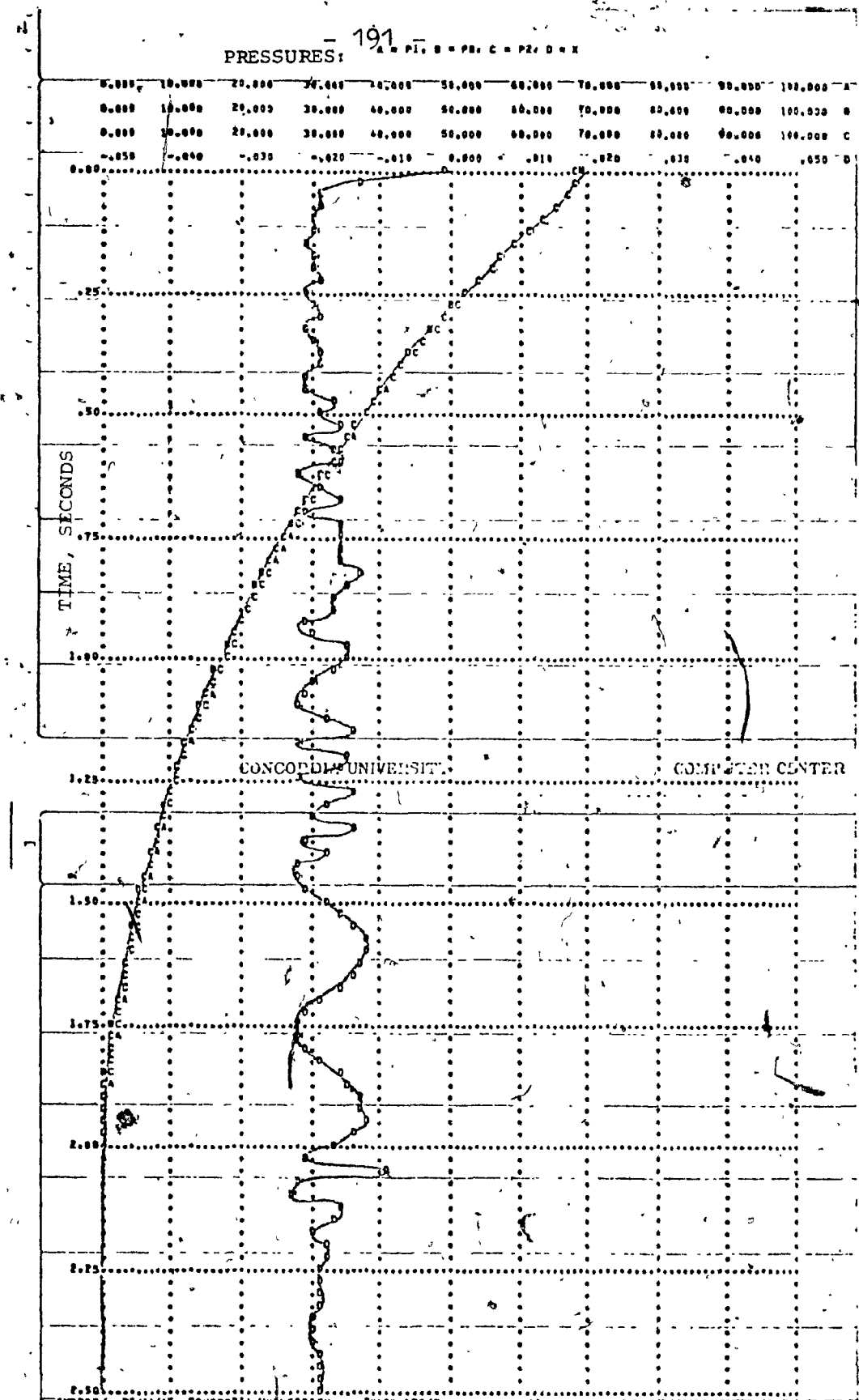


FIG.C2 NONLINEAR SYSTEM (Discharging Process)

14.00,14,ANDRCW,
14.00,14,ACCOUNT,C7782660,
14.00,15,PTN,
14.00,24, 3.331 CP SECONDS COMPILE TIME
14.00,25,828,827,828,
14.00,28,LOST,LIBRARY
14.01,17,LOG
14.10,99, STOP
14.10,99, 50.650 CP SECONDS EXECUTION,CONCUDIA
14.10,99,UEAD0, 0.001KUNS,
14.10,99,UPPF0, 0.013KUNS,

$$T_f = 70^{\circ}\text{F}, \frac{A_2}{A_1} = 7, C_{k2} = 19$$

COMPUTER CENTER

APPENDIX D

PREDICTION OF BRAKEPIPE PERFORMANCE OF A TRAIN

Pressure distribution along the brakepipe in a 150-car train is determined by method of characteristics for large-amplitude signals and lumped modeling. Figures D1 to D4 show a train of 150-car, 15.1m per car, with brakepipe length of 2286m on which a brakepipe reduction of 41kPa and 103kPa with relay valve and with pressure chamber respectively had been performed. We assumed that there was about 2 seconds response time taken for the 1st car to start to apply since it required such a time to equalize the pressure at the outer diaphragm chamber through the equalizing reservoir after the engineman moved the breaking handle to a certain position. It has to be pointed out that although a significant difference in brakepipe pressure existed between Car 1 and Car 150, pressures at Car 50 and Car 150 were slightly different as were the intermediate cars between Car 50 and Car 150. The time for the last car to start was the same for both brakepipe reductions on a train of the same length. The time required was independent of the extent of the reduction since it was related to the quick service function of the control valves on the cars.

When compared with the brakepipe pressure at Car

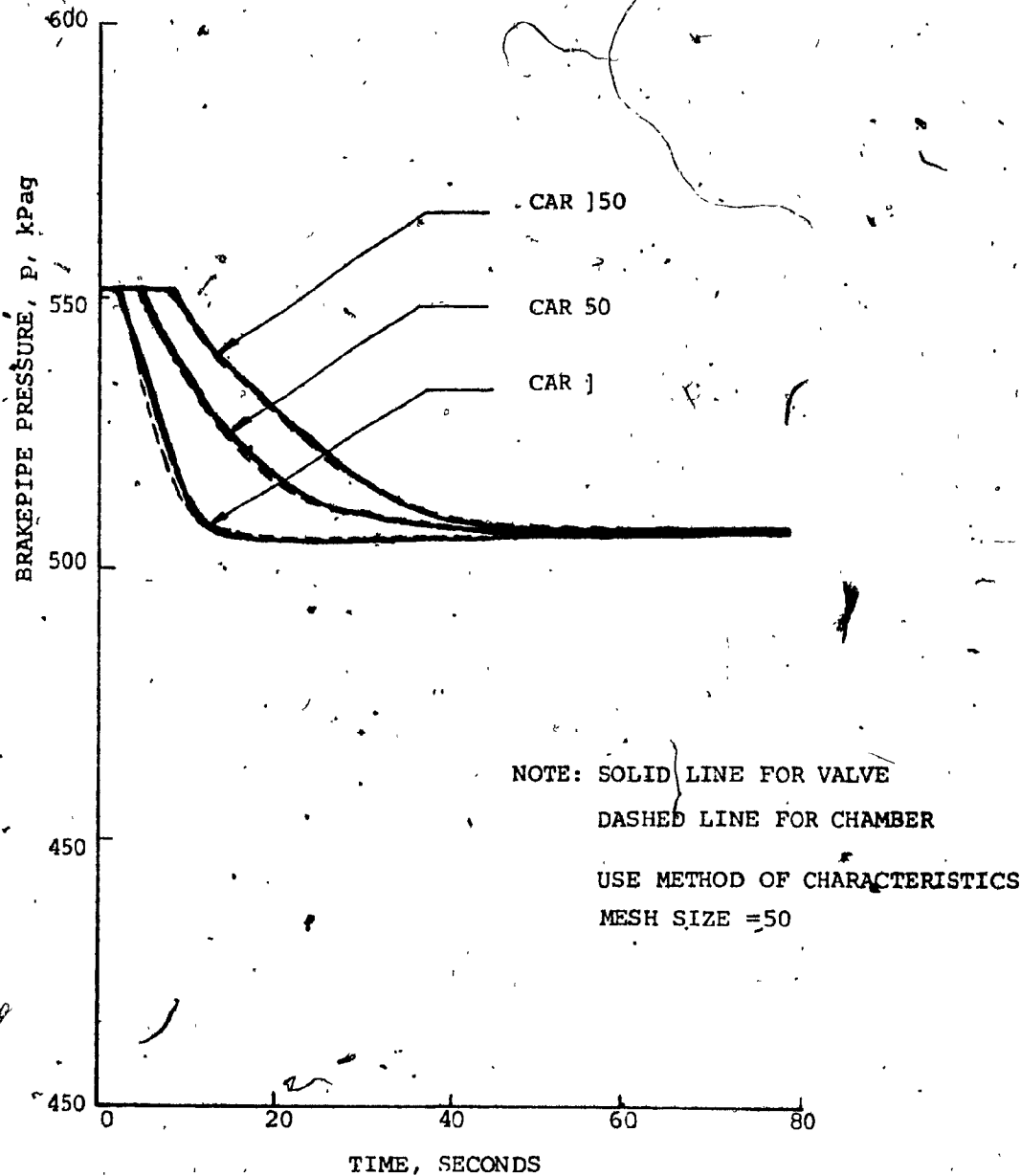


FIG.D] BRAKEPIPE PRESSURE WITH B.P.=552kPag DURING
41kPa B.P. REDUCTION, 150-CAR TRAIN

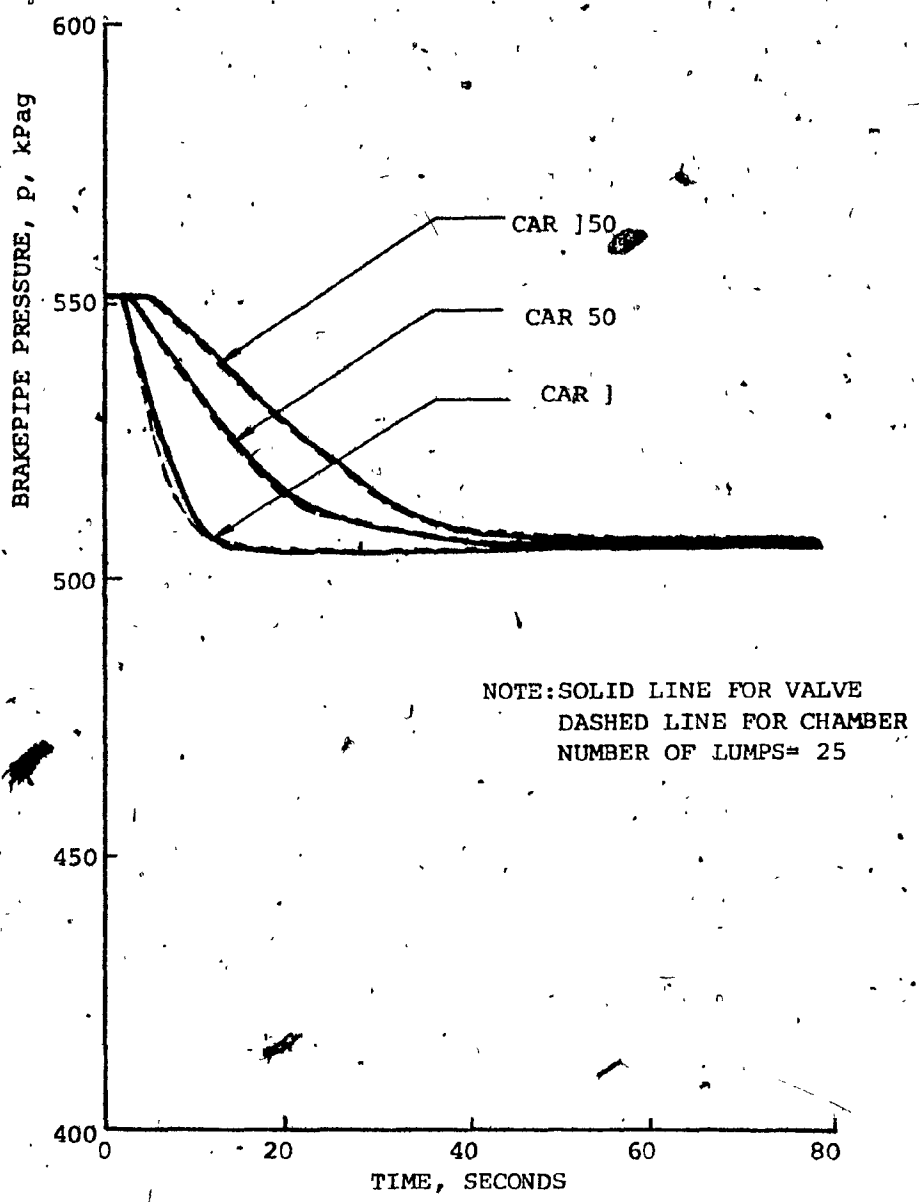


FIG.D2 BRAKEPIPE PRESSURE WITH 552kPag DURING 4]kPa
B.P. PEDUCTION, 150-CAR TRAIN BY LUMPED MODELING

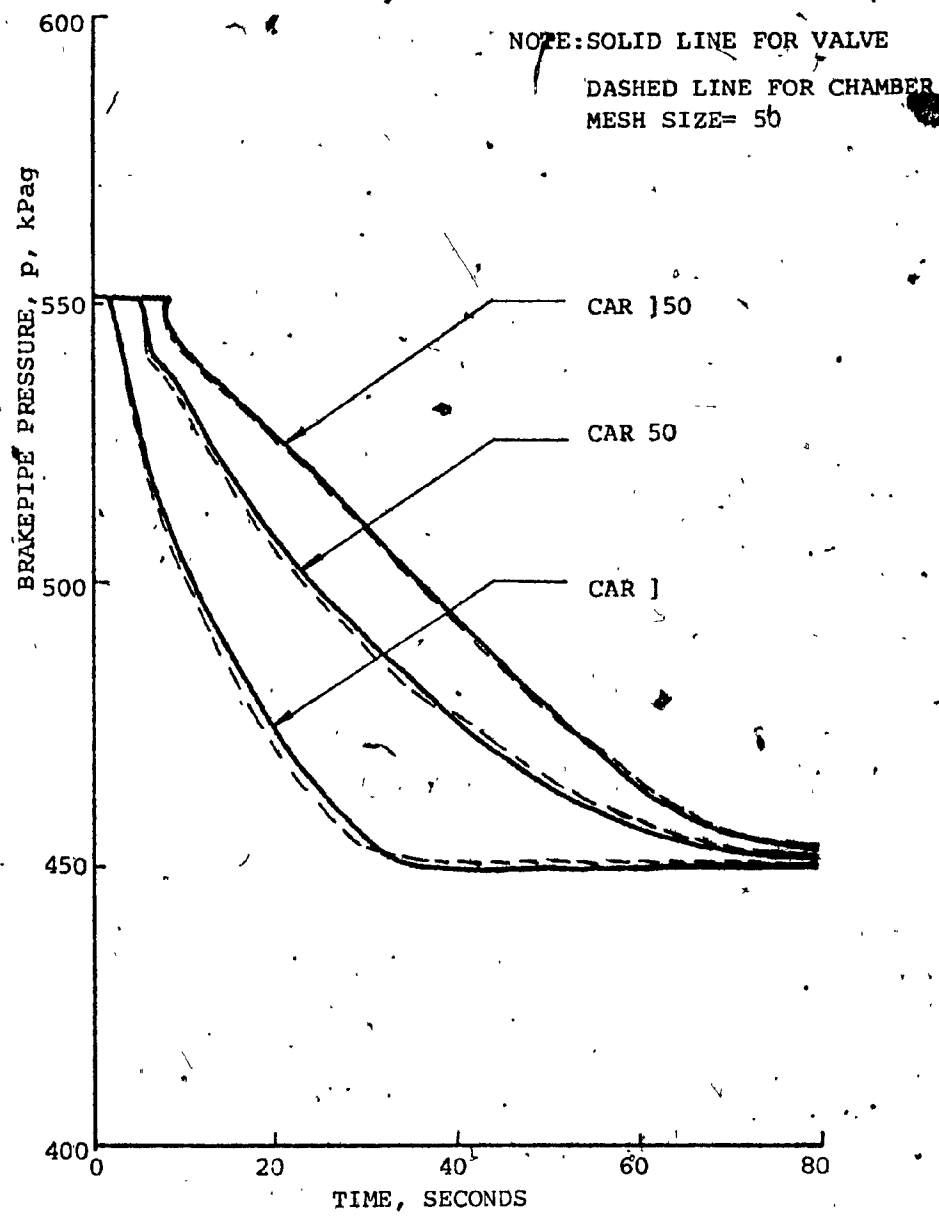


FIG.D3 BRAKEPIPE PRESSURE WITH B.P.=552kPag DURING
303kPa B.P. REDUCTION, 150-CAR TRAIN BY
METHOD OF CHARACTERISTICS

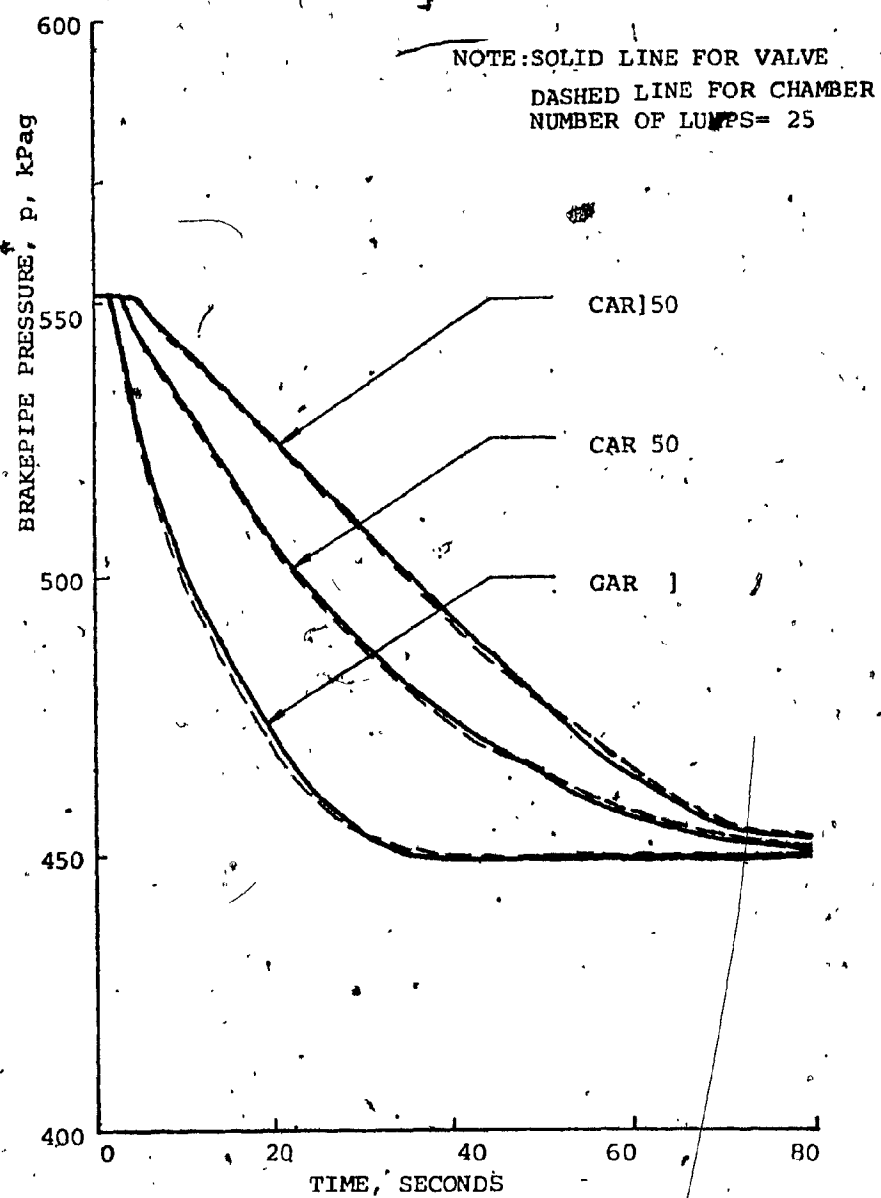


FIG. D4 BRAKEPIPE PRESSURE WITH B.P. = 552kPag DURING 103kPa B.P. REDUCTION, 150-CAR TRAIN : LUMPED MODELING

150 for both pressure reduction between the application of relay valve and pressure chamber, it was found that they were matched closely for both analytical methods. The maximum pressure discrepancy at Car 1 was 1.3kPa and 3.5 kPa respectively for 41kPa and 103kPa reduction. We concluded that the application of the pressure chamber was satisfied.

Referring to figure D5, charging curves of pressure chamber for 41kPa and 103kPa reduction were shown. It took about 25 seconds for the chamber with volume of $14.67(10)^4$ c c charging up to 511 kPag and about 65 seconds for charging up to 449kPag. The results from both analytical methods were in good agreement.

